NOAA Technical Report NESDIS 125

The GOES-13 Science Test: Imager and Sounder Radiance and Product Validations

Washington, D.C.
September 2007

U.S. DEPARTMENT OF COMMERCE
National Oceanic and Atmospheric Administration
National Environmental Satellite, Data, and Information Service

NOAA TECHNICAL REPORTS

National Environmental Satellite, Data, and Information Service

The National Environmental Satellite, Data, and Information Service (NESDIS) manages the Nation's civil Earth-observing satellite systems, as well as global national data bases for meteorology, oceanography, geophysics, and solar-terrestrial sciences. From these sources, it develops and disseminates environmental data and information products critical to the protection of life and property, national defense, the national economy, energy development and distribution, global food supplies, and the development of natural resources.

Publication in the NOAA Technical Report series does not preclude later publication in scientific journals in expanded or modified form. The NESDIS series of NOAA Technical Reports is a continuation of the former NESS and EDIS series of NOAA Technical Reports and the NESC and EDS series of Environmental Science Services Administration (ESSA) Technical Reports.

A limited number of copies are available by contacting Susan Devine, NOAA/NESDIS, E/RA, 5200 Auth Road, Room 701, Camp Springs, Maryland 20746, (301) 763-8127 x136. Copies can also be ordered from the National Technical Information Service (NTIS), U.S. Department of Commerce, Sills Bldg., 5285 Port Royal Road, Springfield, VA 22161, (703) 487-4650 (prices on request for paper copies or microfiche, please refer to PB number when ordering). A partial listing of more recent reports appear below:

NESDIS 96 Hydrography of the Ross Sea Continental Shelf During the Roaverrs, NBP96-06, Cruise December 1996 - January 1997. Michael L. Van Woert, David Pryor, Eric Quiroz, Richard Slonaker, and William Stone, September 2000.

NESDIS 97 Hydrography of the Ross Sea Continental Shelf During the Roaverrs, NBP97-09, Cruise December 1997 - January 1998. Michael L. Van Woert, Lou Gordon, Jackie Grebmeier, Randal Holmbeck, Thomas Henderson, and William F. Van Woert, September 2000.

NESDIS 98 NOAA-L and NOAA-M AMSU-A Antenna Pattern Corrections. Tsan Mo, August 2000.

NESDIS 99 The Use of Water Vapor for Detecting Environments that Lead to Convectively Produced Heavy Precipitation and Flash Floods. Rod Scofield, Gilberto Vicente, and Mike Hodges, September 2000.

NESDIS 100 The Resolving Power of a Single Exact-Repeat Altimetric Satellite or a Coordinated Constellation of Satellites: The Definitive Answer and Data Compression. Chang-Kou Tai, April 2001.

NESDIS 101 Evolution of the Weather Satellite Program in the U.S. Department of Commerce - A Brief Outline. P. Krishna Rao, July 2001.

NESDIS 102 NOAA Operational Sounding Products From Advanced-TOVS Polar Orbiting Environmental Satellites. Anthony L. Reale, August 2001.

NESDIS 103 GOES-11 Imager and Sounder Radiance and Product Validations for the GOES-11 Science Test. Jaime M. Daniels and Timothy J. Schmit, August 2001.

NESDIS 104 Summary of the NOAA/NESDIS Workshop on Development of a Coordinated Coral Reef Research and Monitoring Program. Jill E. Meyer and H. Lee Dantzler, August 2001.

NOAA Technical Report NESDIS 125

The GOES-13 Science Test: Imager and Sounder Radiance and Product Validations

Donald W. Hillger
NOAA/NESDIS/StAR
Colorado State University
Foothills Campus
Fort Collins, CO 80523

Timothy J. Schmit
NOAA/NESDIS/StAR
University of Wisconsin
Space Science and Engineering Center
Madison, WI 53706

Washington, DC
September 2007

U.S. DEPARTMENT OF COMMERCE
Carlos M. Gutierrez, Secretary

National Oceanic and Atmospheric Administration
Vice Admiral Conrad C. Lautenbacher, Jr., U.S. Navy (Ret.), Under Secretary

National Environmental Satellite, Data, and Information Service
Mary Kicza, Assistant Administrator

The GOES-13 Science Test:
Imager and Sounder Radiance and Product Validations

Editors:

Donald W. Hillger[1], and Timothy J. Schmit[3]

Other Contributors:

Americo S. Allegrino[6], A. Scott Bachmeier[4], Jaime M. Daniels[5], Steve Goodman[11], Mathew M. Gunshor[4], Andy Harris[7], Michael P. Hiatt[2], Seiichiro Kigawa[12], John A. Knaff[1], Jun Li[4], Daniel T. Lindsey[1], Eileen M. Maturi[9], Wen Meng[10], Chris Merchant[13], Jon Mittaz[7], James P. Nelson III[4], Walt Petersen[11], Dale G. Reinke[2], Christopher C. Schmidt[4], Anthony J. Schreiner[4], Dave Stettner[4], Chris Velden[4], Gary S. Wade[3], Steve Wanzong[4], Dave Watson[2], and Xiangqian (Fred) Wu[8]

Affiliations:

[1]StAR/RAMMB (SaTellite Applications and Research/Regional and Mesoscale Meteorology Branch)
[2]CIRA (Cooperative Institute for Research in the Atmosphere)
Colorado State University, Fort Collins

[3]StAR/ASPB (SaTellite Applications and Research/Advanced Satellite Products Branch)
[4]CIMSS (Cooperative Institute for Meteorological Satellite Studies)
University of Wisconsin, Madison

[5]StAR/OPDB (SaTellite Applications and Research/Operational Products Development Branch)
[6]Raytheon IIS
Camp Springs MD

[7]CICS (Cooperative Institute for Climate Studies)
University of Maryland, College Park

[8]StAR/SPB (SaTellite Applications and Research/Sensor Physics Branch)
Camp Springs MD

[9]StAR/SOCD (SaTellite Applications and Research/Satellite Oceanography and Climatology Branch)
[10]Perot Systems
Camp Springs MD

[11]NSSTC (National Space Science and Technology Center), Lightning and Thunderstorm Group, NASA (National Aeronautics and Space Administration), MSFC (Marshall Space Flight Center), University of Alabama, Huntsville

[12]Meteorological Satellite Center, Japan Meteorological Agency

[13]University of Edinburgh, Edinburgh, Scotland

TABLE OF CONTENTS

LIST OF TABLES

LIST OF FIGURES

Executive Summary of the GOES-13 NOAA Science Test

The Science Test for GOES-13 produced several results and conclusions:

- GOES-13 Imager and Sounder data were collected during the 5-week NOAA Science Test that began in December of 2006 while the satellite was stationed at 105ºW longitude. Data were also collected during the summer of 2006 and part of the summer of 2007.

Changes were implemented with the GOES-13 compared to previous GOES Imagers:

- Potential to operate the instruments during the eclipse periods.
- Improved image navigation and registration.
- Colder patch (detector) temperatures due to the new spacecraft design.
- In general, Imager and Sounder data from GOES-13 are improved considerably in quality (noise level) to that from GOES-8 through GOES-12.
- GOES-13 Imager data appear to have slightly increased detector-to-detector striping compared to GOES-12. Overall, the Sounder data from GOES-13 exhibited more striping.
- The Imager-to-Imager radiance comparisons show fair agreement, although the GOES-13 Imager band-6 shows a considerable cold bias.
- Retrievals of Total Precipitable Water (TPW) from the GOES-13 Sounder were comparable to those from GOES-12. Derived Product Images (DPIs) of Lifted Index (LI) and cloud-top pressure from the GOES-13 Sounder were similar to those from GOES-12.
- Satellite-derived Sea Surface Temperature (SST) products were generated from GOES-13 data. A high degree of similarity was demonstrated when comparing to the GOES-12 SST to GOES-13. When compared with buoy data, GOES-13 SST shows a slightly smaller bias than GOES-12, but slightly more scatter.
- GOES-12 fire detection capability is about the same as GOES-12, which is much improved over GOES-10.
- Atmospheric Motion Vectors were computed with GOES-13 data for several spectral bands. After applying a radiance bias correction, the quality is similar to GOES-12 data.
- In addition, the image registration with GOES-13 data is much improved, especially in comparison to GOES-12.

1. Introduction

The latest Geostationary Operational Environmental Satellite (GOES), GOES-N, was launched on 24 May 2006, and reached geostationary orbit at 89.5°W on 4 June 2006 to become GOES-13. It was later moved to 105ºW for the Science Test and eventual storage. The National Oceanic and Atmospheric Administration (NOAA)/National Environmental Satellite, Data, and Information Service (NESDIS) conducted a 3-week GOES-13 Science Test that began 7 December 2006 and ended officially on 28 December 2006. The Science Test schedule was integrated within the NESDIS/National Aeronautics and Space Administration (NASA) GOES-13 Post-Launch Test (PLT) schedule. GOES-13 has instruments similar to those on GOES-8/12, but is on a different spacecraft bus (Figure 1.1). The new bus allows improvements both to navigation and registration, as well as the radiometrics. By supplying data through the eclipse periods, the GOES-N/O/P system addresses one of the major limitations which are eclipse and related outages. This is possible due to larger spacecraft batteries. Outages due to Keep Out Zones (KOZ) will be minimized. There are radiometric improvements, since the GOES-13 instruments (Imager and Sounder) are less noisy. A colder patch (detector) temperature is the main reason. In addition, there is a potential reduction in detector-to-detector striping to be achieved through increasing the Imager scan-mirror dwell time on the blackbody from 0.2 sec to 2 sec. There are improvements in both the navigation and registration on GOES-N+. The navigation was improved due to the new spacecraft bus and the use of star trackers (as opposed to the current method of edge-of-earth sensors). In general, the navigation accuracy (at nadir) improves from between 4-6 km with today's Imager to less than 2 km with those on the GOES-N/O/P satellites.

Figure 1.1: GOES-N,O,P series spacecraft

This report describes the NOAA/NESDIS Science Test portion only. This report covers the Imager and Sounder instruments, but not the solar/space instruments. System performance and operational testing of the spacecraft and instrumentation was performed as part of the PLT. During the Science Test, GOES-13 was operated in a special test mode, where the default schedule involved routine emulation of GOES-east or GOES-west operations. Numerous other

scan schedules and sectors were constructed and used for both the Imager and the Sounder. GOES-13 was then placed into storage mode on 5 January 2007. Current plans call for GOES-13 not to become operational until it would most likely replace GOES-12, GOES-12 is currently in the GOES-east position, and GOES-11 is in the GOES-west position.

1.1. Goals for the GOES-13 Science Test

First, the quality of the GOES-13 data was investigated and quantified. This was accomplished by comparison to data from other satellites or by calculating the signal to-noise ratio, as well as detector-to-detector striping analysis.

The second goal was to generate products from the GOES-13 data stream and compare to those produced from other satellites. These products included several Imager and Sounder products: land skin temperatures, temperature/moisture retrievals, total precipitable water, lifted index, cloud-top pressure, atmospheric motion vectors, and sea surface temperatures. Validation of these products was accomplished by comparing these products to products generated from other satellites or by comparing them to radiosondes and ground-based instruments.

The third goal was to investigate the impact of the recent instrument changes. For example, the better navigation, improved calibration and the capabilities of the GOES-N series to operate through eclipse, when the satellite is in the shadow of the earth, as well as to minimize outages due to Keep Out Zones (KOZ), when the sun can potentially contaminate imagery by being within the field of view of the instruments.

In addition, nearly-continuous rapid-scan imagery of significant weather cases will be investigated as part of GOES-R Risk Reduction activities, for improving severe weather forecasts, especially 30-second interval imagery that has not been collected since special scans in 1996.

Finally, the GOES-13 GVAR data stream and ancillary data was archived for use in retrospective studies.

This report documents results from these various activities undertaken by NOAA/NESDIS and its Cooperative Institutes during this test period. Organizations which participated in these GOES-13 Science Test activities included the: NOAA/NESDIS Office of Research and Applications (ORA), now know as SaTellite Applications and Research (StAR); NOAA/NESDIS Office of Satellite Data Processing and Distribution (OSDPD); Cooperative Institute for Meteorological Satellite Studies (CIMSS); Cooperative Institute for Research in the Atmosphere (CIRA); and NOAA/NESDIS Satellite Analysis Branch (SAB).

GOES-13 Imager and Sounder data were received via direct downlink at the following sites: (1) CIRA, Colorado State University, Fort Collins CO; (2) Space Science and Engineering Center (SSEC), University of Wisconsin, Madison WI; and (3) NOAA/NESDIS, Suitland/Camp Springs MD. Each site ingested, archived, and made the data available on its own internal network in McIDAS (Man computer Interactive Data Access System) format, as well as to other sites as needed. The NOAA/NESIDS Regional and Mesoscale Meteorology Branch (RAMMB) at CIRA also made the GOES-13 imagery available over the internet via the RAMSDIS Online homepage. Image and product loops were made available on the CIMSS Web pages. See the

Appendix A for the appropriate URLs for these and many other GOES-13 related web sites. More information on GOES-N can be found at Hillger et al. 2006, Schmit et al. 2006, Daniels et al. 2007, and Hillger et al. 2007).

NOAA Technical Reports similar to this one were produced for both the GOES-11 (Daniels et al. 2001) and GOES-12 (Hillger et al. 2003) Science Tests.

2. Satellite Schedules and Sectors

A total of eight schedules involving numerous predefined Imager and Sounder sectors were constructed for the GOES-13 Science Test. The choice of Imager and Sounder sectors was a result of input from the various research and development groups participating in the Science Test. Some of these schedules are similar to those run during the GOES-12 Science Test (Hillger et al. 2003).

Thanks to dedicated support provided by the NOAA/NESDIS/Satellite Operations Control Center (SOCC) and the Office of Satellite Operations (OSO), a significant amount of flexibility existed with respect to switching and activating the schedules on a daily basis. The ease with which the schedules could be activated was important for capturing significant weather phenomena of varying scales and locations during the Science Test period.

A brief summary of the eight schedules is provided in Table 2.1. The default C5RTN or C4RTN schedules, emulation of GOES-east or GOES-west operations respectively, were pre-determined if no other schedule was called in to Satellite Operations 1 hour before the 1630 UTC daily schedule change time. For the Sounder, the default schedules were also emulation of normal GOES-east and GOES-west operations. The C1CON schedule was mainly for emulation of GOES-R Advanced Baseline Imager data of 5 minute routine scans. The C2SRSO and C3SRSO schedules, with images as 1-minute and 30-second intervals respectively, were prepared to provide the ability to call up Super Rapid Scan Operations (SRSO) during the test period. A C6FD schedule was for continuous 30-minute interval full-disk imaging of the entire earth. And finally, the C7MOON and C8 schedules were for specialized data sets of the moon and for over-sampling of Imager data to emulate the spatial resolution of the GOES-R Advanced Baseline Imager (ABI).

The daily implementation of the various schedules during the entire Science Test is presented in Table 2.2. The GOES-13 daily call-up began on 7 December 2007 and continued through 28 December. At that time the GOES-13 continued to collect imagery for another week, through 5 January 2007, while further tests took place before GOES-13 was put into on-orbit storage mode.

Table 2.1: Summary of Test Schedules for the GOES-13 Science Test

Test Schedule	Imager	Sounder	Purpose
C5RTN	Emulation of GOES-East routine operations	Emulation of GOES-East routine operations	Radiance and product comparisons
C4RTN	Emulation of GOES-West routine operations	Emulation of GOES-West routine operations	Radiance and product comparisons
C1CON	Continuous 5-minute (conus sector)	26-minute sector every 30 minutes (conus sector)	Test navigation, ABI-like (temporal) CONUS scans
C2SRSO	Continuous 1-minute (with center point specified for storm analysis)1	26-minute sector every 30 minutes (with center point same as Imager)	Test navigation, ABI-like (temporal) mesoscale scans
C3SRSO	Continuous 30-second (with center point over either Huntsville AL2 or Washington DC areas)	26-minute sector every 30 minutes (with center same as Imager)	To coordinate with lightning detection arrays in Huntsville AL2 and Washington DC areas
C6FD	Continuous 30-minute Full Disk (including off-earth measurements)	Alternating east and west limb/space views every hour	Noise, striping, fires, etc.
C7MOON	Capture moon off edge of earth (when possible)3	Emulation of GOES-East routine operations	Test ABI lunar calibration concepts
C8	Emulation of 2 km ABI through spatial over-sampling (continuous 19 minutes for same sector per specific line-shifted scan strategy)	Emulation of GOES-East routine operations	ABI-like higher-resolution product development

Table 2.2: Daily Implementation of GOES-13 Science Test Schedules

Starting Date [Julian Day]	Test Schedule Name	Imager	Sounder	Notes
December 7 [341] (Thursday)	C1CON	5-minute CONUS	30-minute CONUS	Great Lakes lake effect snow
December 8 [342] (Friday)	C5RTN	GOES-East routine emulation	GOES-East routine emulation	
December 9 [343] (Saturday)	C6FD	30-minute Full Disk	Alternating east and west limb/space views	Noise, striping, etc.
December 10 [344] (Sunday)	C6FD	30-minute Full Disk	Alternating east and west limb/space views	Noise, striping, etc.
December 11 [345] (Monday)	C5RTN	GOES-East routine emulation	GOES-East routine emulation	
[345] 2350 UTC to [346] 0010 UTC (inserted into schedule above)	C7MOON	Capture moon off edge of earth	GOES-East routine emulation	Test ABI lunar calibration concepts
December 12 [346] (Tuesday)	C3SRSO	30-second Rapid Scan centered at 34.6°N, 86.75°W	30-minute CONUS	Hazardous Weather Testbed, Huntsville AL
December 13 [347] (Wednesday)	C2SRSO	1-minute Rapid Scan centered at 34°S, 66°W	30-minute CONUS	Severe weather over Argentina
December 14 [348] (Thursday)	C4RTN	GOES-West routine emulation	GOES-West routine emulation	
December 15 [349] (Friday)	C4RTN	GOES-West routine emulation	GOES-West routine emulation	
December 16 [350] (Saturday)	C4RTN	GOES-West routine emulation	GOES-West routine emulation	
December 17 [351] (Sunday)	C5RTN	GOES-East routine emulation	GOES-East routine emulation	
December 18 [352] (Monday)	C4RTN	GOES-West routine emulation	GOES-West routine emulation	

December 19 [353] (Tuesday)	C2SRSO	1-minute Rapid Scan centered at 36°N, 108°W	30-minute CONUS	Intense low over SW U.S.
December 20 [354] (Wednesday)	C2SRSO	1-minute Rapid Scan centered at 38°N, 103°W	30-minute CONUS	Intense low over U.S. high plains
December 21 [355] (Thursday)	C2SRSO	1-minute Rapid Scan centered at 34.6°N, 86.75°W	30-minute CONUS	Hazardous Weather Testbed, Huntsville AL
December 22 [356] (Friday)	C3SRSO	30-second Rapid Scan centered at 39°N, 77°W	30-minute CONUS	Washington DC
December 23 [357] (Saturday)	C1CON	5-minute CONUS	30-minute CONUS	
December 24 [358] (Sunday)	C5RTN	GOES-East routine emulation	GOES-East routine emulation	
December 25 [359] (Monday)	C1CON	5-minute CONUS	30-minute CONUS	Florida/Carolina severe weather
December 26 [360] (Tuesday)	C2SRSO	1-minute Rapid Scan centered at 42°N, 122°W	30-minute CONUS	Pacific Northwest strong frontal system
December 27 [361] (Wednesday)	C1CON	5-minute CONUS	30-minute CONUS	Low pressure center in western U.S.
December 28 [362] (Thursday)	C5RTN	GOES-East routine emulation	GOES-East routine emulation	
[362] 1745, 2345, 0545, and 1145 UTC (inserted into schedule above)	C8	Emulation of ABI-like 2 km resolution through spatial over-sampling	GOES-East routine emulation	ABI-like higher-resolution product development
End of Pre-planned Science Test: Following schedule continued until GOES-13 was put into storage mode, on January 5				
December 29 [363] (Friday) through January 5 [005] (Friday)	C5RTN	GOES-East routine emulation	GOES-East routine emulation	

3. Changes to the GOES Imager from GOES-8 through GOES-13

The differences between spectral bands utilized by the two versions of the GOES Imager (Schmit et al. 2002a) are explained in Table 3.1. Each version has five bands. The Imager on GOES-8 through GOES-11 contains bands 1 through 5. The Imagers on GOES-12, 13, O, and P contain bands 1 through 4 and band 6.

Table 3.1: GOES Imager bands

GOES Imager Band	Wavelength Range (μm)	Central Wavelength (μm)	Meteorological Objective
1	0.55 to 0.75	0.65	Cloud cover and surface features during the day
2	3.8 to 4.0	3.9	Low cloud/fog and fire detection
3	6.5 to 7.0 5.8 to 7.3	6.75 (GOES-8/11) 6.48 (GOES-12/13)	Upper-level water vapor
4	10.2 to 11.2	10.7	Surface or cloud top temperature
5	11.5 to 12.5	12.0 (GOES-8/11)	Surface or cloud top temperature and low-level water vapor
6	12.9 to 13.7	13.3 (GOES-12/13)	CO_2 band: Cloud detection

There was no change in the Imager spectral band map between GOES-12 and GOES-13.

4. GOES Data Quality

4.1. First Images

The first step to ensure quality products is to verify the quality of the radiances that are used as inputs to the product generation.

4.1.1. Visible

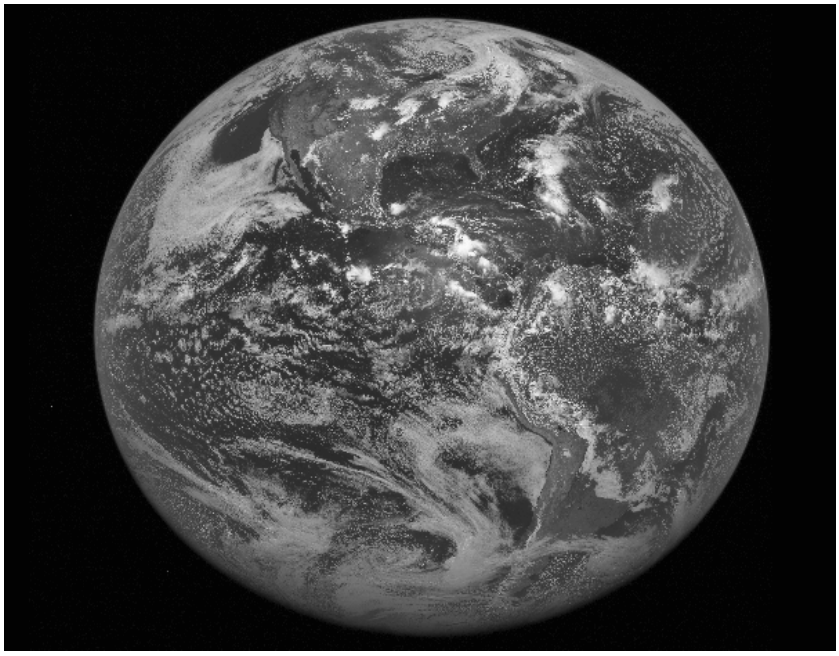

Figure 4.1: The first visible (0.7 μm) image from the GOES-13 Imager occurred on 22 June 2006 at 1720 UTC.

4.1.2. Infrared (IR)

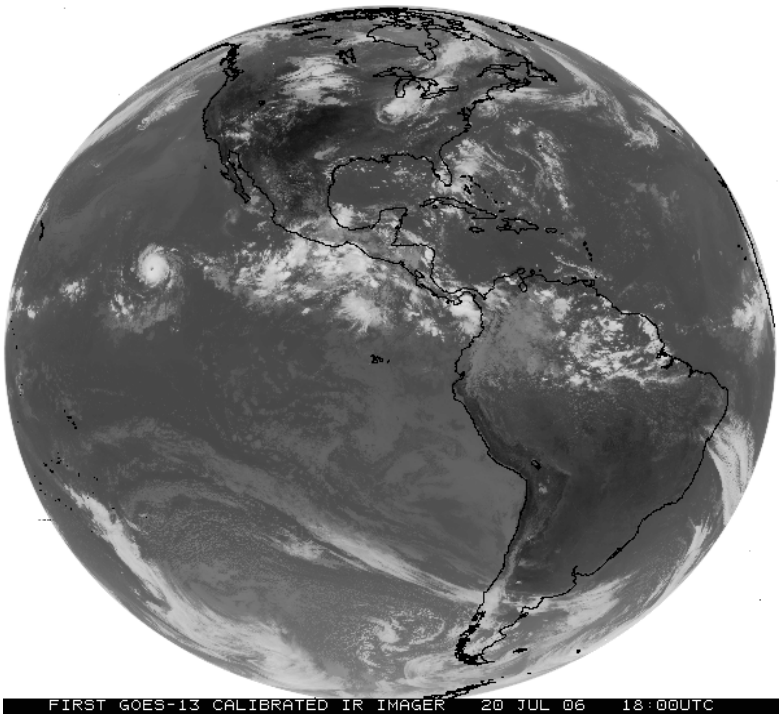

Figure 4.2: GOES-13 full-disk image for the IR window band (band-4, 10.7 μm) from 20 July 2006 at 1800 UTC.

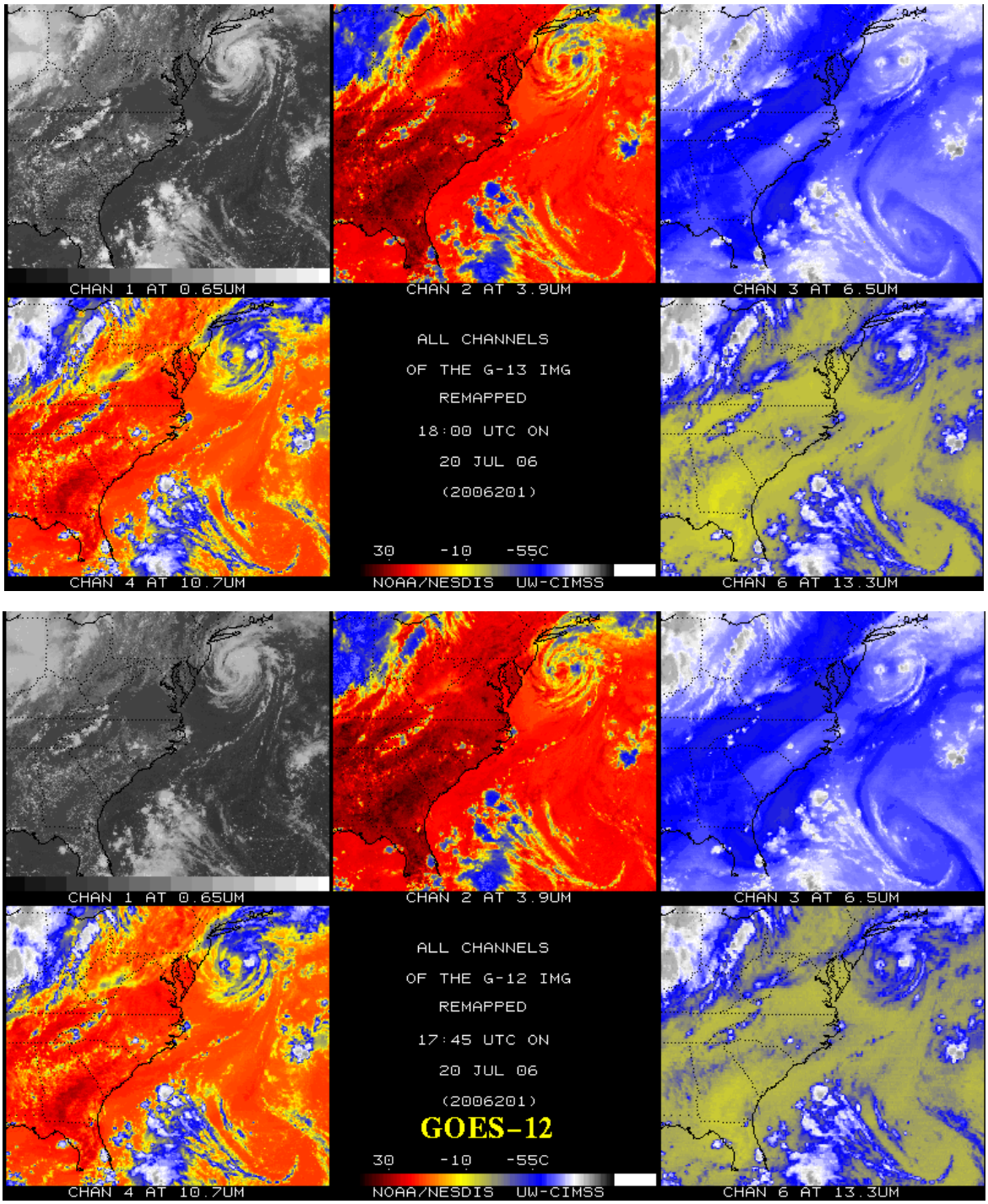

Figure 4.3: GOES-13 Imager bands (top) and the corresponding GOES-12 Imager bands (bottom). Both sets of images have been remapped.

4.1.3. Sounder

Due to an error in the calibration database, the first GOES-13 Sounder visible (band 19) images were unrealistically dark. This was corrected on 6 July 2006.

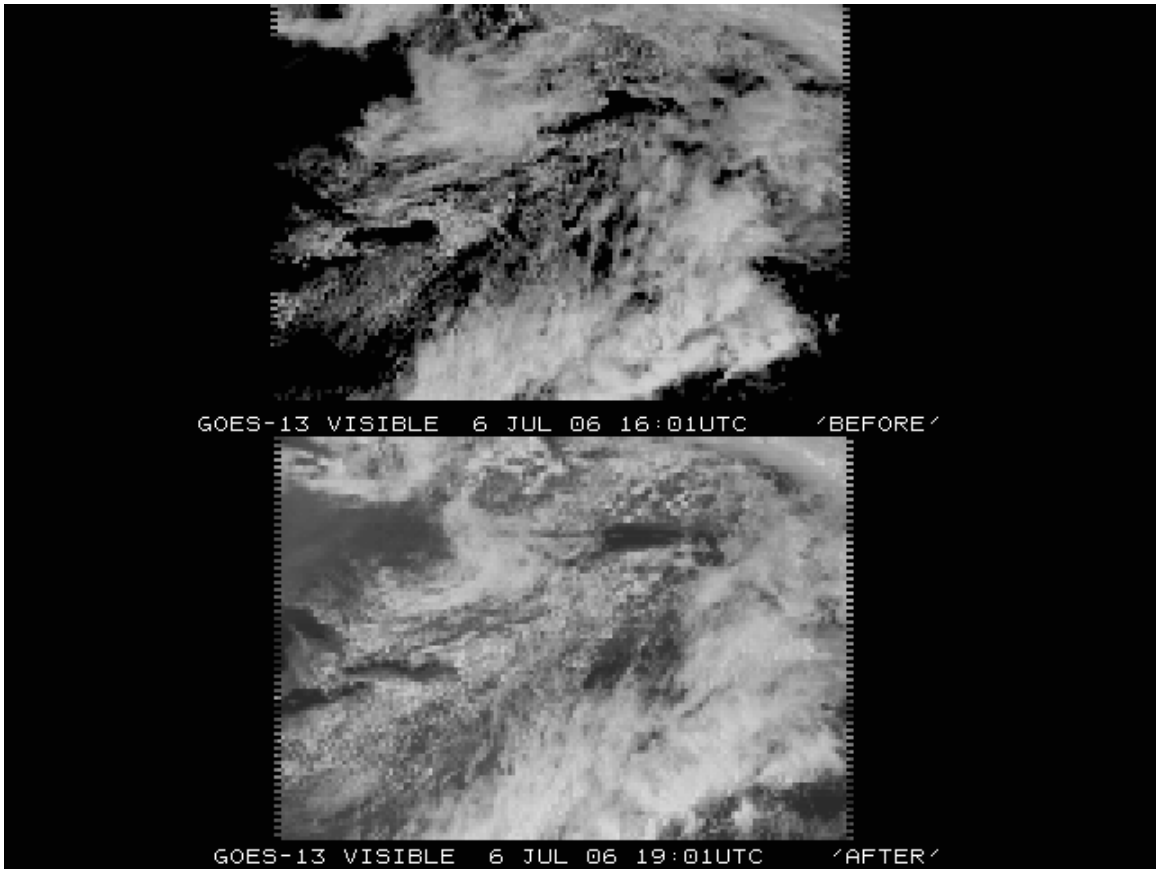

Figure 4.4: The visible (band-19) image from the GOES-13 Sounder shows the database correct on 6 July 2006.

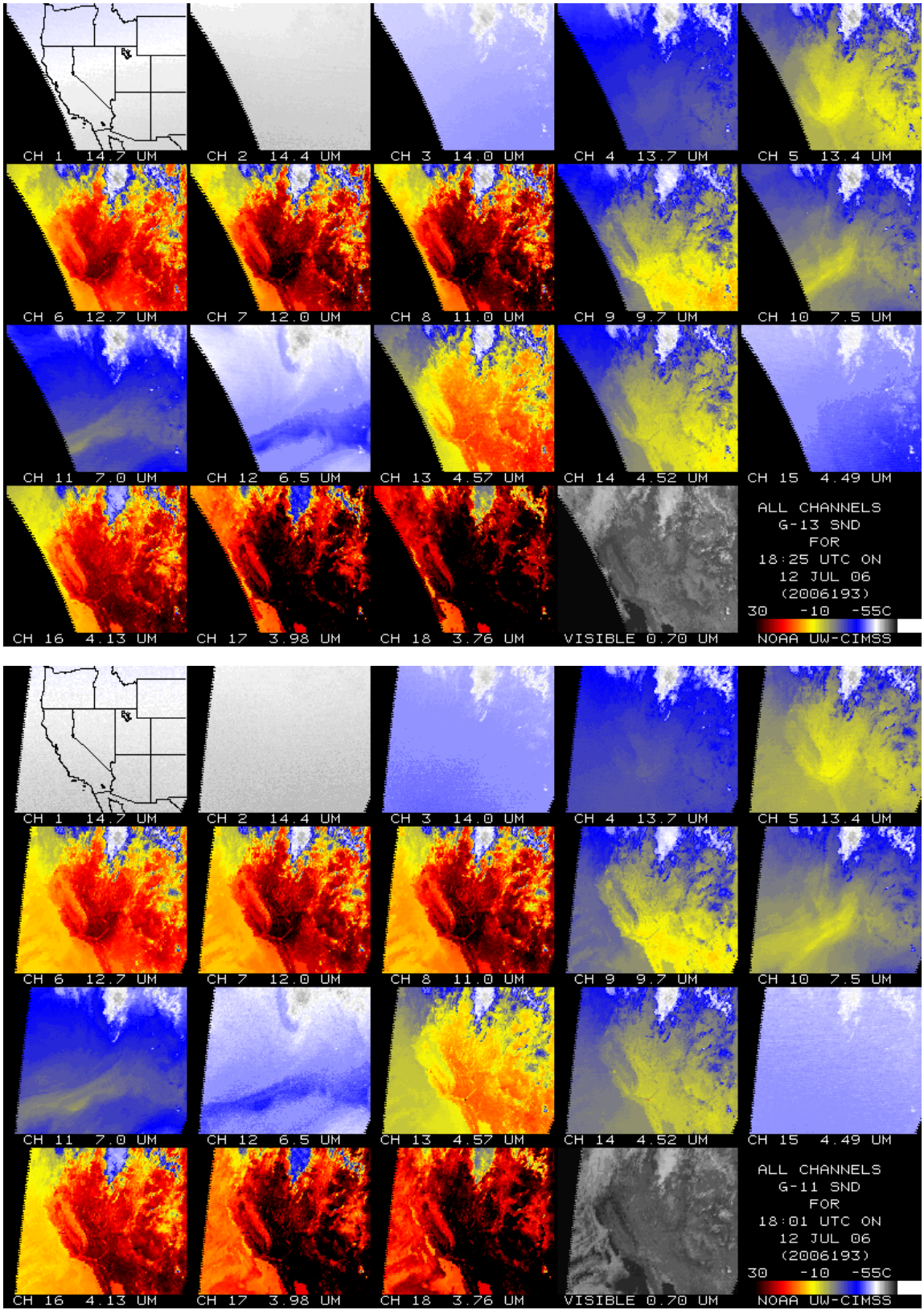

Figure 4.5: The first IR Sounder images for GOES-13 from 12 July 2006 (top) compared to GOES-12 (bottom). Both sets of images have been remapped to a common projection. Note the less noisy Sounder band-15 (4.6 μm).

4.2. Spectral Response Functions (SRFs)

4.2.1. Imager

The GOES spectral response functions (SRFs) for the GOES series Imagers can be found at: http://www.oso.noaa.gov/goes/goes-calibration/goes-imager-srfs.htm and are plotted in Figure 4.6. The GOES-13 Imager is spectrally similar to the GOES-12 Imager, in that it has the spectrally-wide 'water vapor' band. Information about the GOES calibration can be found in Weinreb et al. 1997.

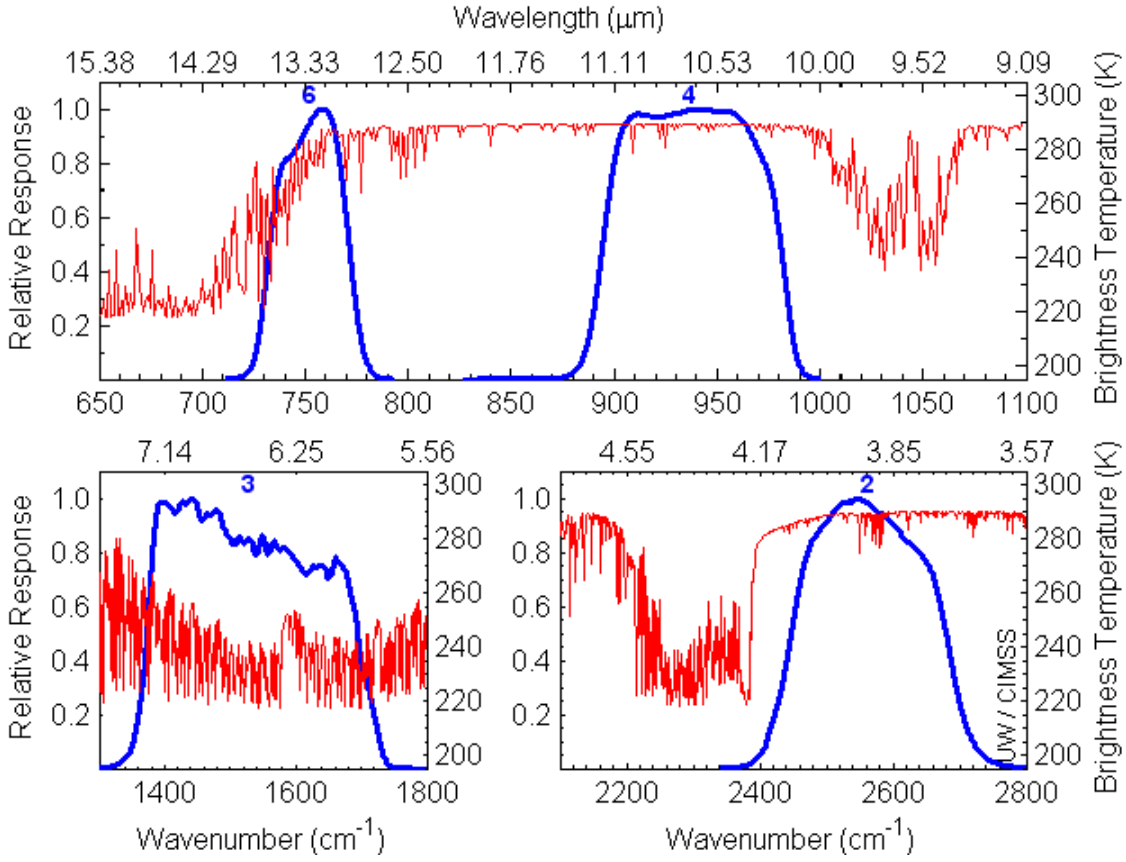

Figure 4.6: The four GOES-13 Imager IR band SRFs super-imposed over the calculated high-resolution earth-emitted U.S. Standard Atmosphere spectrum. Absorption due to carbon dioxide (CO_2), water vapor (H_2O), and other gases are evident in the high-spectral resolution earth-emitted spectrum.

4.2.2. Sounder

The GOES SRFs for the GOES series Sounders can be found at: http://www.oso.noaa.gov/goes/goes-calibration/goes-sounder-srfs.htm and are plotted in Figure 4.7. The band selection is unchanged from previous GOES Sounders (Schmit et al. 2002b). As before, the carbon dioxide (CO_2), ozone (O_3), and water vapor (H_2O) absorption bands are

indicated in the calculated high-spectral resolution earth-emitted U.S. Standard Atmosphere spectrum.

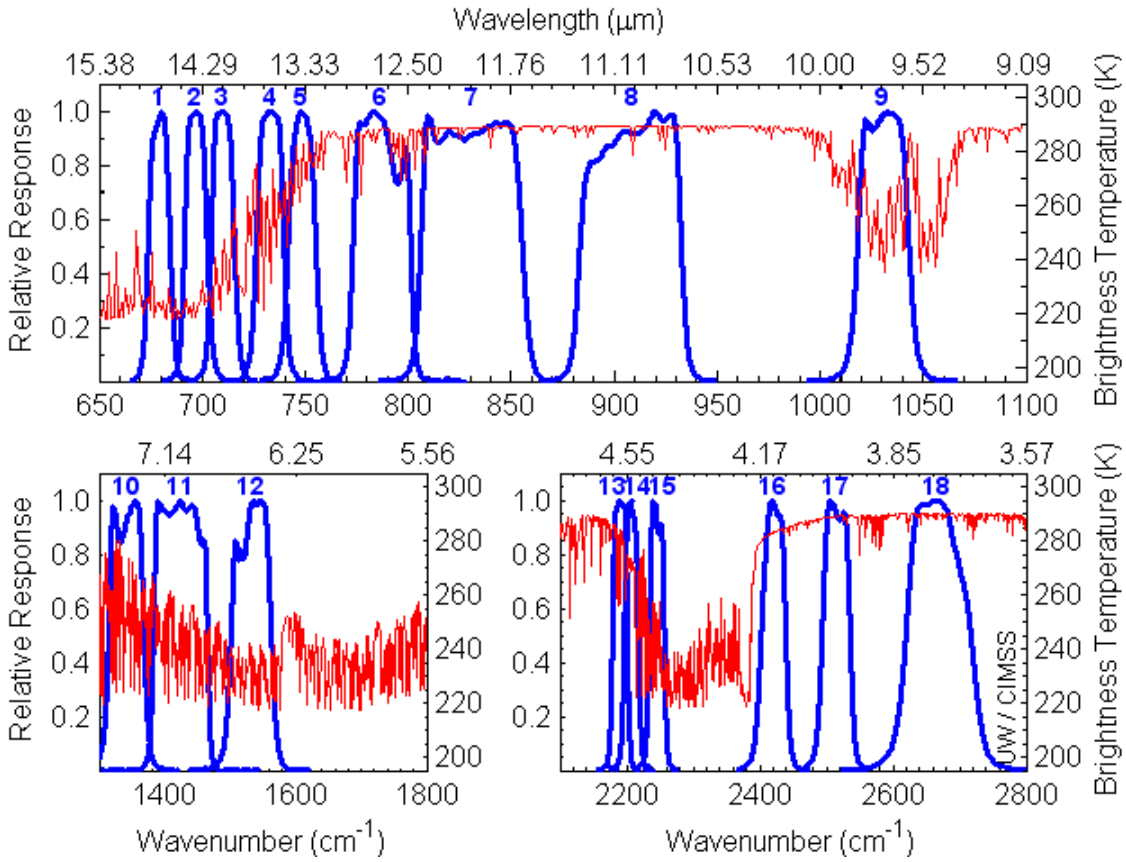

Figure 4.7: The eighteen GOES-13 Sounder IR band SRFs super-imposed over the calculated high-resolution earth-emitted U.S. Standard Atmosphere spectrum. The central wavenumbers (wavelengths) of the spectral bands range from 680 cm^{-1} (14.7 μm) to 2667 cm^{-1} (3.75 μm) (Menzel et al. 1998).

4.3. Random Noise Estimates

Band noise estimates for the GOES-13 Imager and Sounder instruments were computed using two different approaches. In the first approach, the band noise values were determined by calculating the variance of radiance values in a space look scene. The second approach involved performing a spatial structure analysis (Hillger and Vonder Haar, 1988). Both approaches yielded nearly identical band noise estimates and are presented below.

4.3.1. Imager

Full-disk images for the Imager provided space views and allowed noise values to be determined. Estimated noise values for the GOES-13 Imager from 10 December 2006 at 0045 UTC through 11 December 2006 at 1145 UTC were averaged over that time period from both

east and west-limb space views. The noise values were much improved from those for GOES-12 as in Table 4.1. The exception is that the band 3 noise values seem to be comparable.

Table 4.1: Estimated noise for GOES-13 for 10 (0045 UTC) – 11 (1145 UTC) December compared to estimated noise values for GOES-12.

Imager Band	Central Wavelength (μm)	GOES-13	GOES-12
		mW(m^2·sr·cm^{-1})	
2	3.9	0.002	0.008
3	6.5	0.02	0.02
4	10.7	0.09	0.17
6	13.3	0.12	0.32

4.3.1.1. Structure-estimated Noise

Noise was also estimated using spatial structure analysis on a 150-line by 150-element (22,500 pixel) space-view portion of the GOES images. Structure analysis compares adjacent Fields-Of-View (FOVs) to determine the random component of the signal in the images.

Results for GOES-13 are presented in Table 4.2, in both 10-bit GVAR counts and temperature units, with equivalent values for GOES-12 given for comparison (from both the first Science Test images and from images taken at the same time as the preliminary GOES-13 analysis). Variations between preliminary and 5th-year noise levels for all bands of GOES-12, typically values within a factor of two, are as expected.

Table 4.2: GOES-13 Imager noise (in 10-bit GVAR counts and temperature units) compared to GOES-12.

Imager Band	Central Wavelength (μm)	GOES-13	GOES-12 (Preliminary / 5th-year)	GOES-13	GOES-12 (Preliminary / 5th-year)
		(GVAR count, 10-bit, 0-1023)		(K @ 300 K, except band-3 @ 230 K)	
2	3.9	0.45	1.1 / 1.1	0.051	0.13 / 0.12
3	6.5	0.80	0.85 / 0.91	0.14	0.15 / 0.16
4	10.7	0.47	1.0 / 1.6	0.053	0.11 / 0.18
6	13.3	0.59	1.8 / 3.0	0.061	0.19 / 0.32

GOES-13 noise in temperature units is compared to the rest of the GOES series (GOES-8 through GOES-12) in Table 4.3. GOES-13 noise levels in all bands except band-3 appear to be much improved over those from the other GOES satellites.

Table 4.3: Summary of the noise (in temperature units) for GOES-8 through GOES-13 Imager bands. The specification (SPEC) noise levels are also listed.

Imager Band	Central Wavelength (μm)	GOES-13	GOES-12	GOES-11	GOES-10	GOES-9	GOES-8	SPEC
		(K @ 300 K, except band-3 @ 230 K)						
2	3.9	0.051	0.13	0.14	0.17	0.08	0.16	1.40
3	6.5 / 6.7	0.14	0.15	0.22	0.09	0.15	0.27	1.00
4	10.7	0.053	0.11	0.08	0.20	0.07	0.12	0.35
5	12.0	No band	No band	0.20	0.24	0.14	0.20	0.35
6	13.3	0.061	0.19	No band	No band	No band	No band	0.32

4.3.2. Sounder

Special GOES-13 limb-view Sounder sectors allow noise values to be determined by the scatter of radiance values looking at uniform space. Indications from 10 December 2006 at 0045 UTC through 11 December 2006 at 1145 UTC show that GOES-13 appears to be within specification for all bands. Noise values were taken from both west-limb and east-limb and averaged over that time period. The bar plot in Figure 4.8 comparing GOES-11, GOES-12, and GOES-13 to the GOES-I through M specifications illustrates the improvement in most bands GOES-13 represents. The GOES-13 signal to noise values (in radiance units) compare well to those from other satellites. The bar plot in Figure 4.9 shows the ratio of GOES-I through M spec noise to noise measurements comparing GOES-11, GOES-12, and GOES-13.

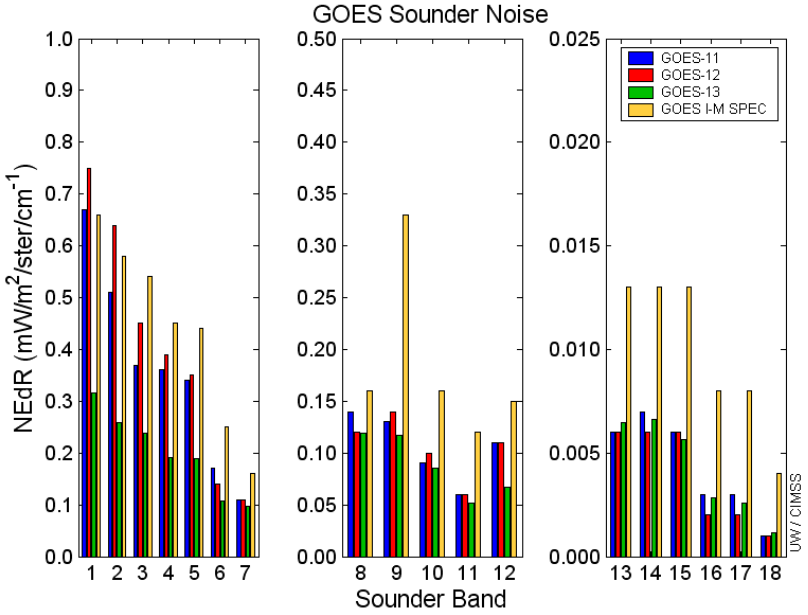

Figure 4.8: GOES-13 Sounder noise values (NEdR) compared to those from GOES-11, GOES-12, and the specification noise values for GOES-I through M.

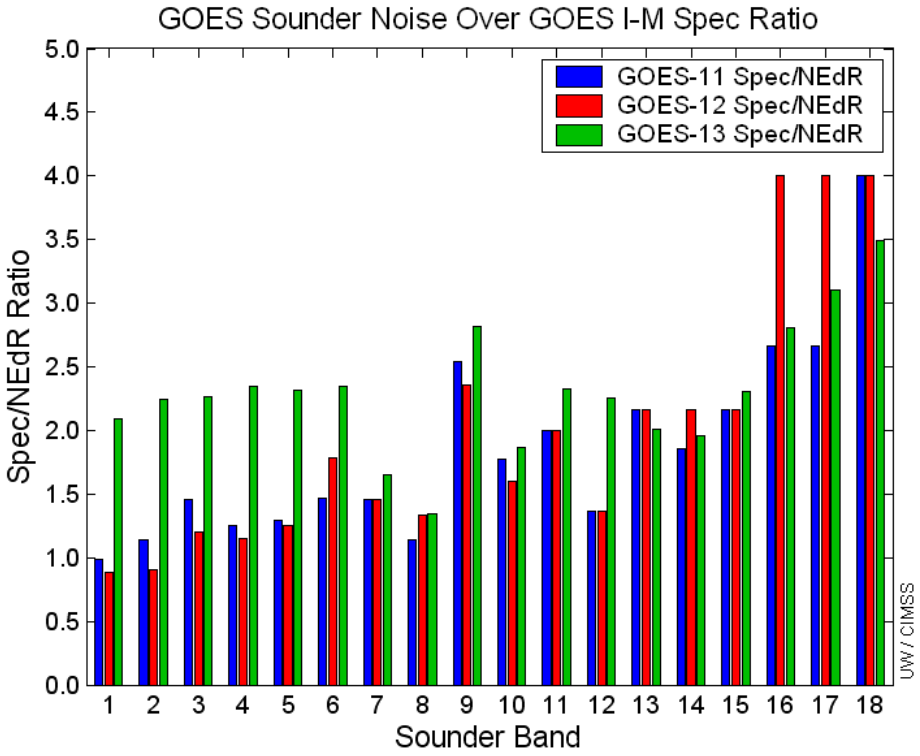

Figure 4.9: The ratio of GOES-I through M specification noise values to the measured noise values for GOES-11, GOES-12, and GOES-13.

4.3.2.1. Structure-estimated Noise

Structure analysis was performed on half-hourly space-view measurements acquired over a 48-h period: 9 December 2006 [Julian day 343] at 1816 UTC through 11 December 2006 [Julian day 345] at 1716 UTC. East-limb, west-limb, and limb-average values are presented and compared to CIMSS analysis values in Table 4.4. The noise estimates from RAMMB/CIRA are very similar to those calculated independently by ASPB/CIMSS.

Table 4.4: GOES-13 Sounder Noise Levels (From 48 hours of limb/space views on Julian days 343-345).

Sounder Band	Central Wavelength (μm)	East Limb	West Limb	Limb Average	Limb Average	CIMSS Analysis
		13-bit GVAR counts (0-8191)			($mW/(m^2 \cdot sr \cdot cm^{-1})$)	
1	14.71	20.8	20.9	20.9	20.8	0.32
2	14.37	17.3	17.0	17.2	17.3	0.26
3	14.06	14.3	13.9	14.1	14.3	0.24
4	13.64	9.17	8.92	9.05	9.17	0.19
5	13.37	8.18	8.05	8.12	8.18	0.19
6	12.66	3.95	4.01	3.98	3.95	0.11
7	12.02	3.14	3.56	3.35	3.14	0.10
8	11.03	4.12	3.99	4.06	4.12	0.12
9	9.71	5.95	5.86	5.91	5.95	0.12
10	7.43	11.5	11.3	11.4	11.5	0.09
11	7.02	11.2	10.8	11.0	11.2	0.05
12	6.51	22.7	22.5	22.6	22.7	0.07
13	4.57	7.51	7.28	7.40	7.51	0.007
14	4.52	11.2	11.1	11.2	11.2	0.007
15	4.46	18.3	17.6	18.0	18.3	0.006
16	4.13	4.01	3.91	3.96	4.01	0.003
17	3.98	3.88	3.90	3.89	3.88	0.003
18	3.74	2.67	2.46	2.57	2.67	0.001

In Table 4.5 GOES-13 Sounder noise appears to be lower than previous GOES in the longwave IR bands in particular. Other bands have noise similar to GOES-12. Noise in all bands is much lower than instrument specifications.

Table 4.5: Summary of the Noise for GOES-8 through GOES-13 Sounder Bands (The Specification (SPEC) values are also listed).

Sounder Band	Central Wavelength (μm)	GOES-13	GOES-12	GOES-11	GOES-10	GOES-9	GOES-8	SPEC
		($mW/(m^2 \cdot sr \cdot cm^{-1})$)						
1	14.70	0.32	0.77	0.67	0.71	1.16	1.76	0.66
2	14.40	0.25	0.61	0.51	0.51	0.80	1.21	0.58
3	14.10	0.23	0.45	0.37	0.41	0.56	0.98	0.54
4	13.90	0.18	0.39	0.36	0.41	0.46	0.74	0.45
5	13.40	0.18	0.34	0.34	0.36	0.45	0.68	0.44
6	12.70	0.095	0.14	0.17	0.16	0.19	0.32	0.25
7	12.00	0.086	0.11	0.11	0.09	0.13	0.20	0.16
8	11.00	0.10	0.11	0.14	0.12	0.09	0.13	0.16
9	9.70	0.11	0.14	0.13	0.10	0.11	0.16	0.33
10	7.40	0.081	0.099	0.09	0.07	0.08	0.08	0.16
11	7.00	0.046	0.059	0.06	0.04	0.05	0.07	0.12
12	6.50	0.063	0.11	0.11	0.07	0.09	0.11	0.15
13	4.57	0.0061	0.0062	0.006	0.007	0.008	0.012	0.013
14	4.52	0.0064	0.0062	0.007	0.005	0.007	0.010	0.013
15	4.45	0.0055	0.0066	0.006	0.005	0.006	0.009	0.013
16	4.13	0.0030	0.0024	0.003	0.003	0.003	0.004	0.008
17	3.98	0.0026	0.0022	0.003	0.002	0.003	0.004	0.008
18	3.70	0.0011	0.00094	0.001	0.001	0.001	0.002	0.004

4.4. Detector-to-Detector Striping

4.4.1. Imager

Full-disk images from the Imager provide off-earth space views, allowing both noise levels and detector-to-detector striping to be determined in an otherwise constant signal situation. Striping estimates for the first calibrated infrared (IR) images from the GOES-13 Imager taken on 20 July 2006 at 1800 UTC were determined to be similar to those for GOES-12 Imager. Table 4.6 gives estimates of GOES-13 Imager detector-to-detector striping (from both-detector mean*) and noise compared to GOES-12. Calculated on ~300,000 earth-view pixels. Comparison is made to striping determined for both the GOES-12 Science Test images and to images from GOES-12 taken at the same time as the preliminary GOES-13 analysis, the 5th year into the life of GOES-12.

Table 4.6: GOES-13 Imager Striping. (20 July 2007 [Julian day 201] 1800 UTC)

Imager Band	Wave-length (μm)	Number of Detectors	GOES-13	GOES-12 (Preliminary / 5th-year)	GOES-13	GOES-12 (Preliminary / 5th-year)
			Striping (GVAR count, 10-bit, 0-1023)		Noise (GVAR count, 10-bit, 0-1023)	
2	3.9	2	0.34	0.35 / 0.22	0.45	1.1 / 1.1
3	6.7	2	0.60	0.30 / 0.077	0.80	0.85 / 0.91
4	10.7	2	0.40	1.0 / 0.29	0.47	1.0 / 1.6
6	13.3	1	One detector only	One detector only	One detector only	One detector only

Striping is defined as the difference between the average value for each detector from the average value in both detectors. Therefore striping between the two detectors is actually twice the value listed, and is often more noticeable than noise. In general, the GOES-13 Imager striping is less than that on GOES-12, possibly due to the longer black-body look.

Striping is also compared to random noise in Table 4.6, to recognize that increased striping may contribute to increased noise. (For example, the increased noise in GOES-13 band-3 compared to the other GOES-13 bands may be the reason the noise in GOES-13 band-3 is higher than the other GOES-13 bands. For GOES-12, noise appears to be equal to or much greater than striping in all bands.)

4.4.2. Sounder

Detector-to-detector striping for the Sounder is documented in Table 4.7 from both earth and space measurements taken from the same limb-view sectors used for the noise analysis for the Sounder. In this case however, the analysis included measurements from the entire Sounder sector, including both the earth and space views. Of significance was the fact that the results from the east-limb and west-limb were significantly different. The last column gives the west-to-east ratio for the striping, indicating that there is significantly more striping in data from the west-limb than from the east-limb.

Table 4.7: GOES-13 Sounder Detector-to-Detector Striping. (From 48 hours of limb (earth and space) measurements on Julian days 343-345)

Sounder Band	Central Wavelength (μm)	Both Earth and Space Measurements		
		East Limb	West Limb	West-to-East Ratio
		13-bit GVAR counts (0-819)		
1	14.71	31.0	48.3	1.6
2	14.37	26.9	45.7	1.7
3	14.06	31.9	52.5	1.6
4	13.64	30.7	56.5	1.8
5	13.37	32.2	58.9	1.8
6	12.66	35.2	71.6	2.0
7	12.02	42.7	72.7	1.7
8	11.03	35.3	63.2	1.8
9	9.71	20.4	27.7	1.4
10	7.43	19.1	40.2	2.1
11	7.02	15.0	38.2	2.5
12	6.51	11.6	17.6	1.5
13	4.57	18.4	28.6	1.6
14	4.52	10.4	17.1	1.6
15	4.46	9.2	11.7	1.3
16	4.13	6.5	12.7	2.0
17	3.98	8.7	16.2	1.9
18	3.74	8.8	16.8	1.9

To determine the source of this difference between the limbs seen in Table 4.7, the limb-view data were split into space-only and earth-only measurements for further analysis. From the results in Table 4.8, the increased west-limb striping is mainly manifested in the earth-only measurements, and to a much lesser extent in the space-only measurements. This implies that the striping is related to the larger signal of the earth-only measurements compared to the low signal of the space-view measurements. Current thought is that this difference might also be related to the east-west correction applied to the measurements due to angular-related emissivity variations of the scan mirror.

Table 4.8: GOES-13 Sounder Detector-to-Detector Striping. (From 48 hours of limb (space-only and earth-only) measurements on Julian days 343-345)

Sounder Band	Central Wavelength (μm)	Space-Only Measurements			Earth-Only Measurements		
		East Limb	West Limb	West-to-East Ratio	East Limb	West Limb	West-to-East Ratio
		13-bit GVAR counts (0-8191)			13-bit GVAR counts (0-8191)		
1	14.71	5.8	5.8	1.00	8.7	12.5	1.44
2	14.37	4.8	4.6	0.96	6.3	6.7	1.06
3	14.06	3.7	3.4	0.92	9.2	13.5	1.47
4	13.64	2.2	1.9	0.86	12.7	30.2	2.38
5	13.37	2.0	1.9	0.95	14.7	35.6	2.42
6	12.66	2.0	2.3	1.15	22.9	51.3	2.24
7	12.02	3.6	4.8	1.33	49.1	64.2	1.31
8	11.03	2.9	3.4	1.17	31.0	37.1	1.20
9	9.71	3.1	3.9	1.34	17.7	24.1	1.36
10	7.43	2.9	3.2	1.10	14.2	30.8	2.17
11	7.02	3.2	3.7	1.16	14.5	39.3	2.71
12	6.51	4.4	4.7	1.07	10.1	11.1	1.10
13	4.57	3.6	4.4	1.22	27.1	38.0	1.40
14	4.52	5.2	6.0	1.15	12.6	20.2	1.60
15	4.46	8.5	10.0	1.18	10.1	11.7	1.16
16	4.13	1.9	2.2	1.16	8.1	14.6	1.80
17	3.98	1.5	2.0	1.33	10.7	17.7	1.65
18	3.74	1.3	1.7	1.31	9.9	15.7	1.59

Finally, Tables 4.9 and 4.10 give the averages and standard deviations, respectively, for each detector for a sample of the space-only measurements in the tables above. These numbers indicate that the signal and noise are similar on both limbs, and the limb effect is probably not due to the scan mirror emissivity correction as first assumed above.

Table 4.9: GOES-13 Sounder Detector Averages. (From limb (space-only) measurements one-time only on Julian day 343 at ~1700 UTC)

Sounder Band	Central Wavelength (μm)	East Limb				West Limb			
		Det #4	Det #3	Det #2	Det #1	Det #4	Det #3	Det #2	Det #1
		13-bit GVAR counts (0-8191)							
1	14.71	215.6	212.9	218.3	216.0	213.0	209.7	214.3	219.1
2	14.37	195.4	191.2	194.6	194.4	189.3	187.2	198.0	191.4
3	14.06	163.1	161.1	161.0	162.0	164.2	159.0	159.6	163.7
4	13.64	110.1	109.2	111.0	110.5	108.1	107.3	109.1	109.3
5	13.37	99.4	96.9	97.9	97.1	97.6	94.1	96.8	97.5
6	12.66	52.3	50.5	51.8	52.0	50.6	46.3	49.6	47.6
7	12.02	30.8	28.4	29.6	29.6	31.2	22.3	25.1	23.9
8	11.03	30.1	30.7	30.8	31.4	33.7	33.3	31.3	35.8
9	9.71	86.0	86.7	85.9	87.8	79.5	79.5	78.5	83.9
10	7.43	108.3	108.7	109.1	110.0	108.6	109.1	107.6	109.6
11	7.02	138.3	138.7	137.5	139.6	135.8	138.2	137.2	140.5
12	6.51	261.0	261.1	261.5	264.5	260.3	263.5	263.6	261.6
13	4.57	72.7	75.4	75.2	75.6	74.9	77.5	76.0	76.7
14	4.52	113.6	114.9	112.9	116..4	114.0	115.3	113.0	113.5
15	4.46	207.9	218.8	213.8	213.8	216.2	216.3	216.3	211.1
16	4.13	52.5	53.1	52.4	52.3	51.7	52.9	52.3	52.8
17	3.98	62.3	61.2	62.5	63.1	61.9	62.3	62.2	61.7
18	3.74	42.9	43.5	42.4	42.8	41.6	42.8	42.2	42.8

Table 4.10: GOES-13 Sounder Detector Standard Deviations (Noise). (From limb (space-only) measurements one-time-only on Julian day 343 at ~1700 UTC)

Sounder Band	Central Wavelength (μm)	East Limb				West Limb			
		Det #4	Det #3	Det #2	Det #1	Det #4	Det #3	Det #2	Det #1
		13-bit GVAR counts (0-8191)							
1	14.71	21.0	20.9	24.2	21.2	20.3	21.1	24.5	19.6
2	14.37	16.0	16.2	19.1	15.9	18.4	15.9	18.9	15.8
3	14.06	15.2	13.4	15.1	13.3	16.4	12.8	15.0	12.1
4	13.64	10.0	8.7	8.5	9.2	9.9	8.4	9.4	8.4
5	13.37	7.7	8.3	7.4	8.6	8.9	8.1	8.3	8.2
6	12.66	3.5	4.2	4.1	4.2	3.4	4.2	4.0	4.3
7	12.02	2.5	2.9	3.0	2.9	2.3	2.7	3.1	2.8
8	11.03	4.0	5.1	3.4	3.6	4.1	4.7	3.0	4.3
9	9.71	5.6	7.3	5.9	5.3	5.4	7.3	5.8	5.3
10	7.43	11.0	14.1	11.0	9.7	11.4	13.6	11.1	9.9
11	7.02	11.6	12.8	9.7	9.6	11.3	13.2	10.0	9.9
12	6.51	22.7	26.4	20.9	19.3	22.4	17.1	20.6	20.1
13	4.57	9.1	5.7	8.0	7.2	8.5	5.3	7.1	7.3
14	4.52	13.1	8.1	10.5	10.5	14.2	8.2	10.4	10.5
15	4.46	21.6	13.4	18.3	17.1	20.4	13.1	18.5	16.9
16	4.13	5.1	3.0	3.8	3.7	4.8	2.9	3.7	3.8
17	3.98	4.9	4.1	3.7	3.9	5.8	3.3	3.9	3.8
18	3.74	3.8	2.1	2.6	2.3	3.0	2.2	2.5	2.4

We found that the GOES-13 Sounder striping noise can be removed by applying a noise filtering technique. Figure 4.10 shows an example of GOES-13 Sounder band 7 radiances, before the de-striping (upper-left), after the de-striping (upper-right), and the differences. The de-striping can help assure the quality of GOES-13 sounding and cloud-top products.

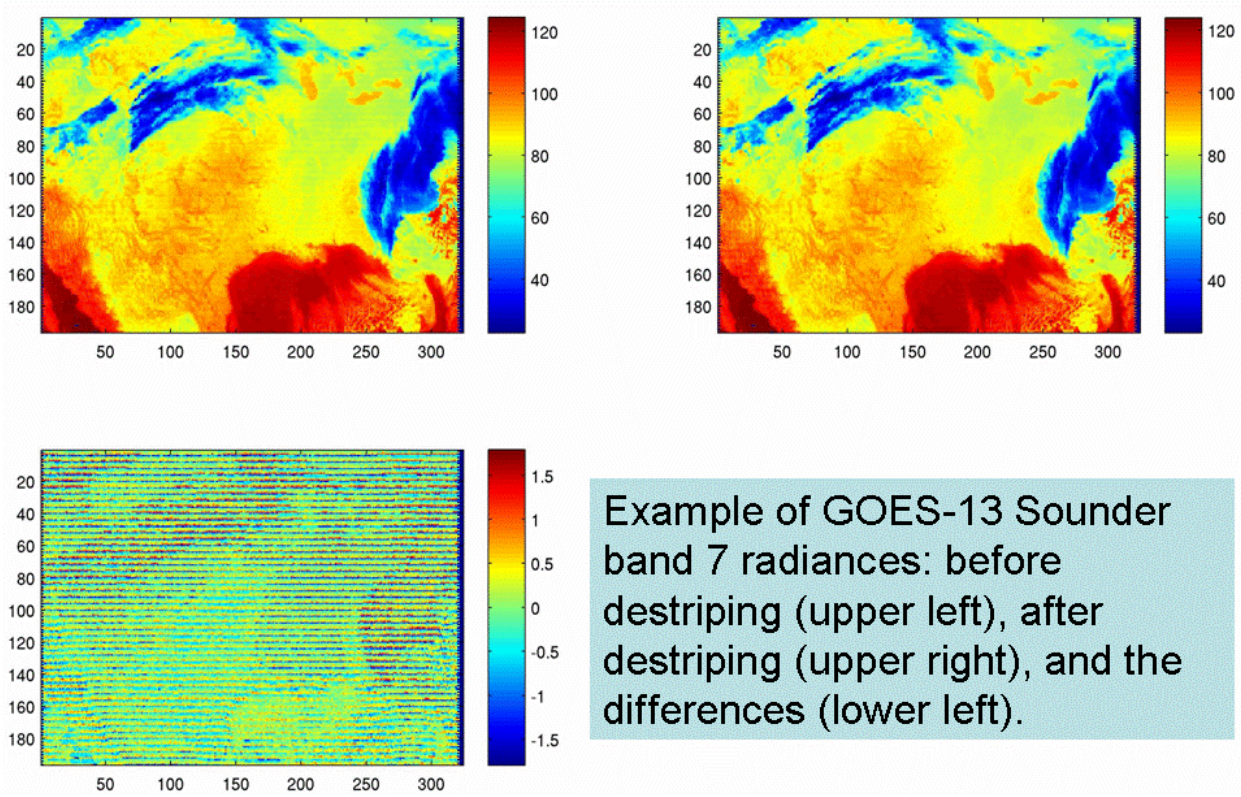

Figure 4.10: GOES-13 Sounder band 7 radiances (mW(m^2·sr·cm^{-1})), before the de-striping (upper-left), after the de-striping (upper-right), and the differences (lower).

4.5. Imager-to-Imager Comparison

On 19 December 2006 GOES-13 was switched to the GOES-11 (GOES-west) schedule. A comparison between the GOES-11 and GOES-13 Imagers at 0600 UTC that day revealed good agreement in brightness temperatures at the mid-point between the two satellites (0°N, 120°W) as shown in Table 4.11. Comparisons were done for a 31 by 31 FOV box, where an average radiance is computed. The band-3 difference of 3.3 K was due mostly to the differing SRFs; the brightness temperatures more closely agree when this is taken into account (to within approximately 0.7 K)

Table 4.11: Imager-to-Imager Comparison Between GOES-11 and GOES-13

Satellite	Imager Band	Radiance ($mW/m^2 \cdot sr \cdot cm^{-1}$)	Temperature (K)
GOES-11	2 (3.9 μm)	0.509	285.7
GOES-13		0.509	285.4
GOES-11	3 (6.7 μm)	6.166	243.6
GOES-13	3 (6.5 μm)	6.021	246.3
GOES-11	4 (10.7 μm)	85.596	283.3
GOES-13		85.782	284.0

On 18 December 2006 GOES-13 was switched to the GOES-12 schedule. A comparison between the GOES-12 and GOES-13 Imagers at 0545 UTC that day revealed mixed results in terms of agreement in brightness temperatures at the mid-point between the two satellites (0°N, 90°W) as shown in Table 4.12. A night-time case was chosen so that the band-2 measurements would not be affected by differing solar reflections. Comparisons were done for a 31 by 31 FOV box, where an average radiance is computed. The most unexpected result is the band-4 (10.7 μm) difference of 1.1 K. It is possible that one of the satellites was not operating optimally during this comparison. The next section discusses comparisons to a polar-orbiting instrument, which will provide another set of measurements to analyze the GOES-13 Imager radiance performance.

Table 4.12: Imager-to-Imager Comparison Between GOES-12 and GOES-13

Satellite	Imager Band	Radiance ($mW/m^2 \cdot sr \cdot cm^{-1}$)	Temperature (K)
GOES-12	2 (3.9 μm)	0.615	290.2
GOES-13		0.618	289.8
GOES-12	3 (6.5 μm)	7.297	252.9
GOES-13		7.249	251.7
GOES-12	4 (10.7 μm)	92.651	288.2
GOES-13		93.693	289.3
GOES-12	6 (13.3 μm)	95.386	271.0
GOES-13		95.474	271.3

4.6. Imager-to-Polar-Orbiter Comparisons

Data were collected during the checkout period near the GOES-13 sub-satellite point from the high spectral resolution Atmospheric InfraRed Sounder (AIRS), polar-orbiting on NASA's Aqua satellite. GOES-13 Imager data were collected within 30 minutes of polar-orbiter overpass time. During the checkout period there were 19 comparisons between GOES-13 and AIRS. The methodology used was identical to that outlined in prior conference reports (Gunshor et al. 2006). The results are presented in Table 4.13. The mean brightness temperature difference for

these comparisons show that GOES-13 is well calibrated based on the accuracy of AIRS measurements and that it compares favorably with similar results to operational GOES-12 and GOES-11. The exception is the 13.3 μm band. The large Imager band-6 bias results, combined with similar results for GOES-12, indicate that there is a significant cold bias in the 13.3um bands on these instruments, greater than 1 K (Gunshor et al. 2006). This issue needs further investigation to see if this due to unknowns in the spectral response measurements or some other factor.

Table 4.13: Comparison of GOES-13 Imager to Atmospheric InfraRed Sounder (AIRS). The Bias is the mean of the absolute values of the differences for n=19.

Imager Band	Mean Difference (K)	Bias (K)	Standard Deviation of Differences (K)
2 (3.9 μm)	0.2	0.4	0.6
3 (6.5 μm)	-0.4	0.4	0.3
4 (10.7 μm)	-0.1	0.4	0.4
6 (13.3 μm)	-2.4	2.4	0.6

4.7. Keep-Out-Zone Analysis

By supplying data through the eclipse periods, the GOES-N/O/P system addresses one of the major current limitations which are eclipse and related outages. This is possible due to larger spacecraft batteries. Outages due to Keep Out Zones (KOZ) will be minimized. See Figure 4.11 for a sequence of 15-minute images from 12 September 2006 comparing GOES-13 to GOES-12 through eclipse. Rather than one long gap while the sun is either within view on each side of the earth or behind the earth, there are two shorter gaps when the sun is within view on each side of the earth.

With the new capability of data during previous outages, comes the risk of allowing images contaminated with energy of the sun to be produced. Of course an image with artificial brightness temperature excursions up to 75 K (e.g. band 2) may affect products. To determine how much good data can be acquired, at the same time minimizing the amount of bad data, many scans were conducted during the eclipse period during the summer of 2006. See Figures 4.12 through 4.16.

It can be seen that all the Imager bands can be affected. Of course the visible and shortwave bands (2) are affected the most. Although to best monitor the affect in the longwave bands (3, 4 and 6), a temporal difference needs to be employed.

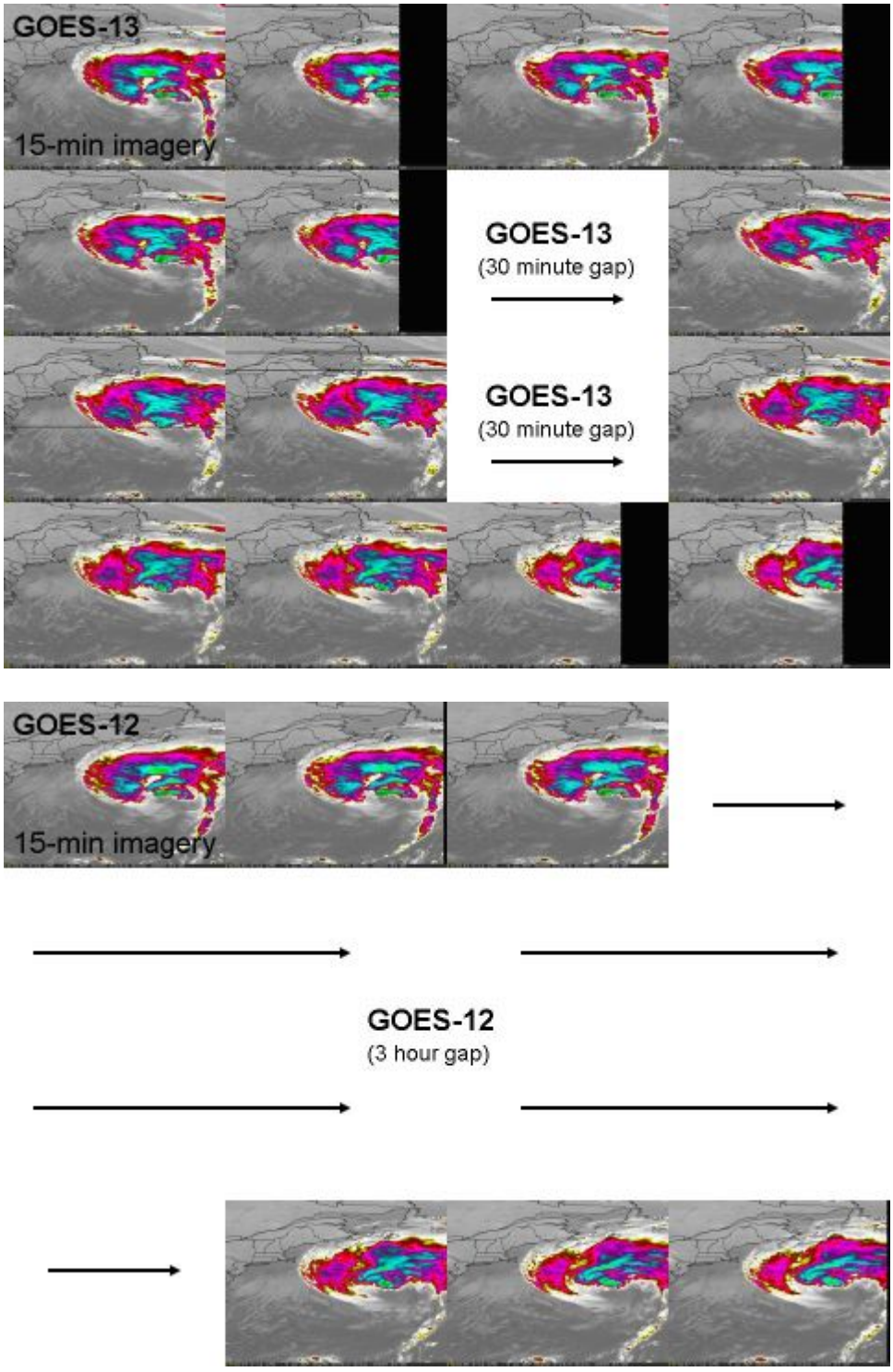

Figure 4.11: Sequences of images from 12 September 2006 comparing GOES-13 (top) to GOES-12 (bottom) through eclipse. Rather than one long gap while the sun is either within view on each side of the earth or behind the earth, there are two shorter gaps when the sun is within view on each side of the earth.

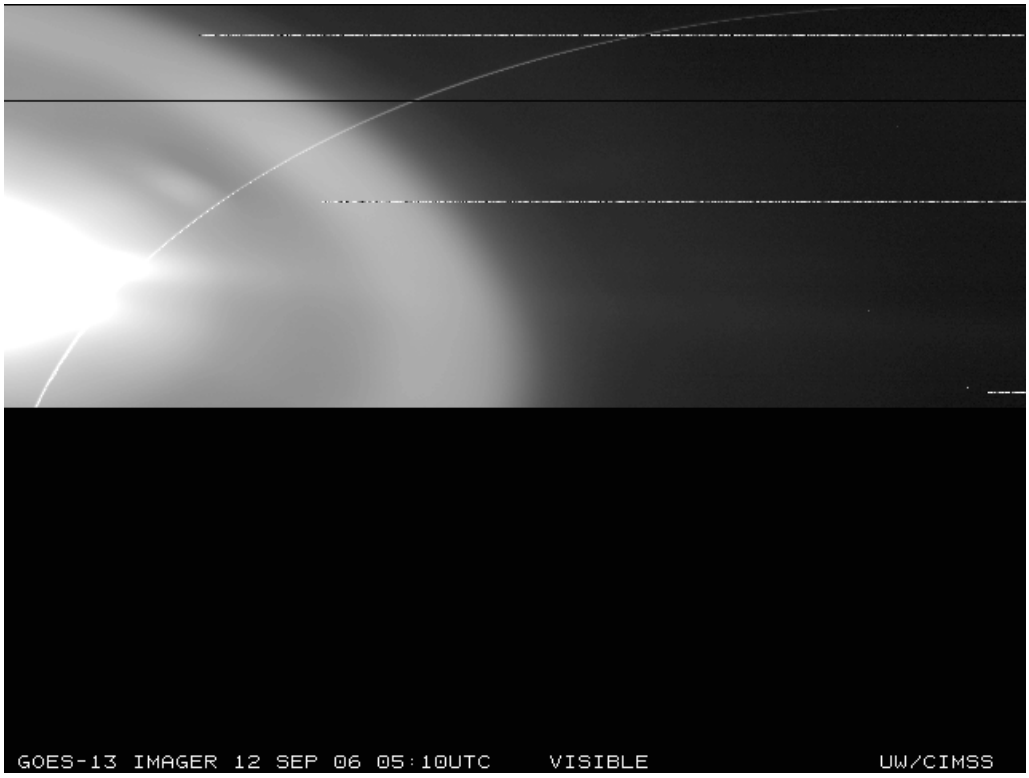

Figure 4.12: GOES-13 Imager visible (0.7 µm) band. The bad lines were due to a noisy data ingest.

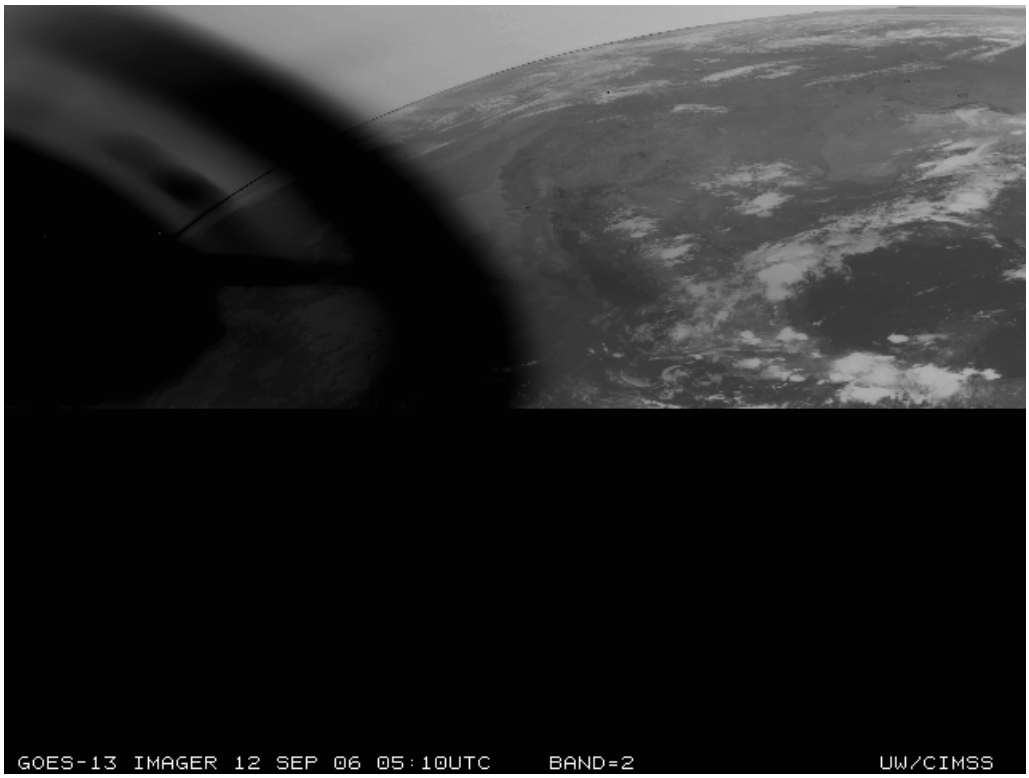

Figure 4.13: GOES-13 Imager shortwave window band.

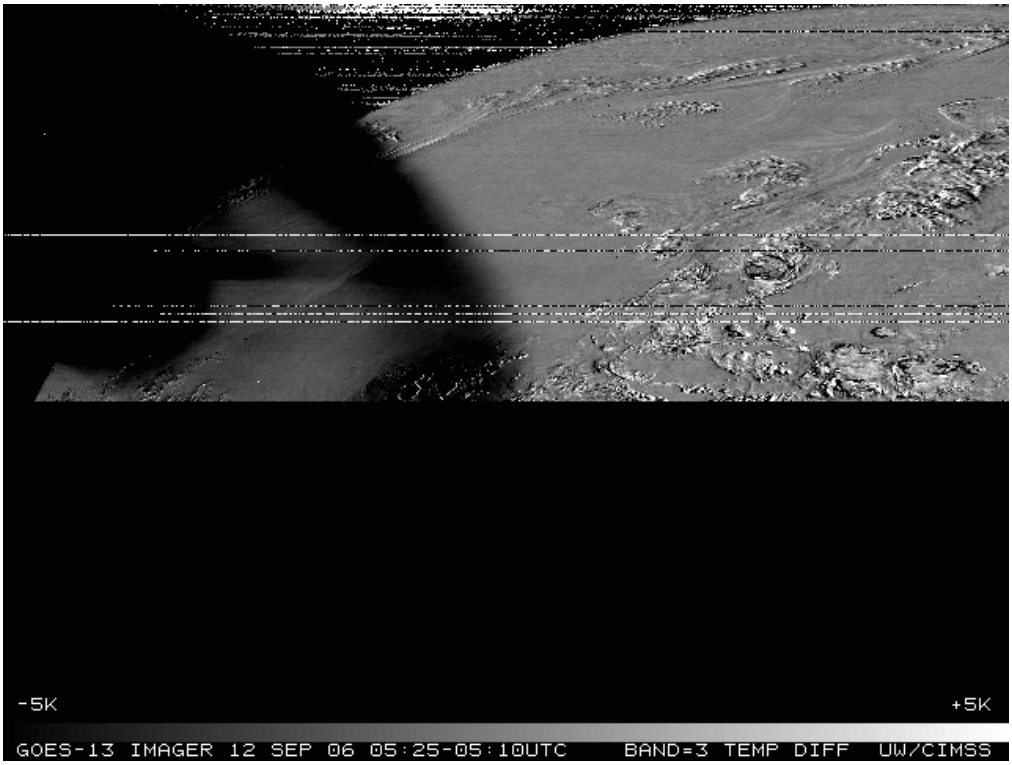

Figure 4.14: GOES-13 Imager temporal difference (0525 – 0510 UTC) of the 'water vapor' band. The bad lines were due to a noisy data ingest.

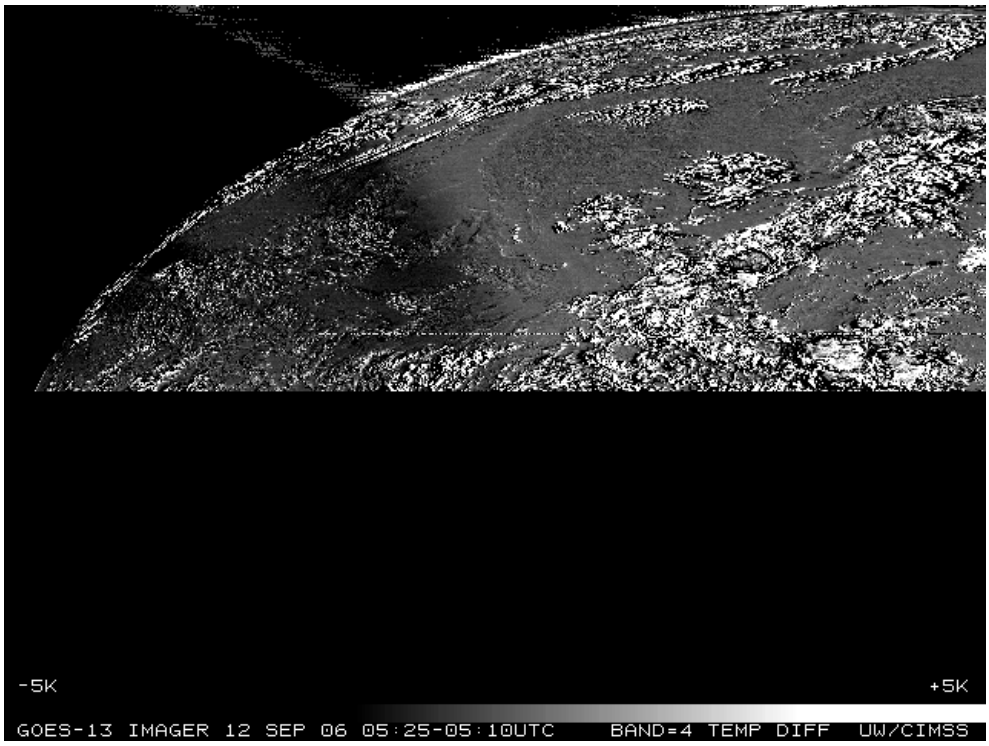

Figure 4.15: GOES-13 Imager temporal difference (0525 – 0510 UTC) of the longwave IR window band.

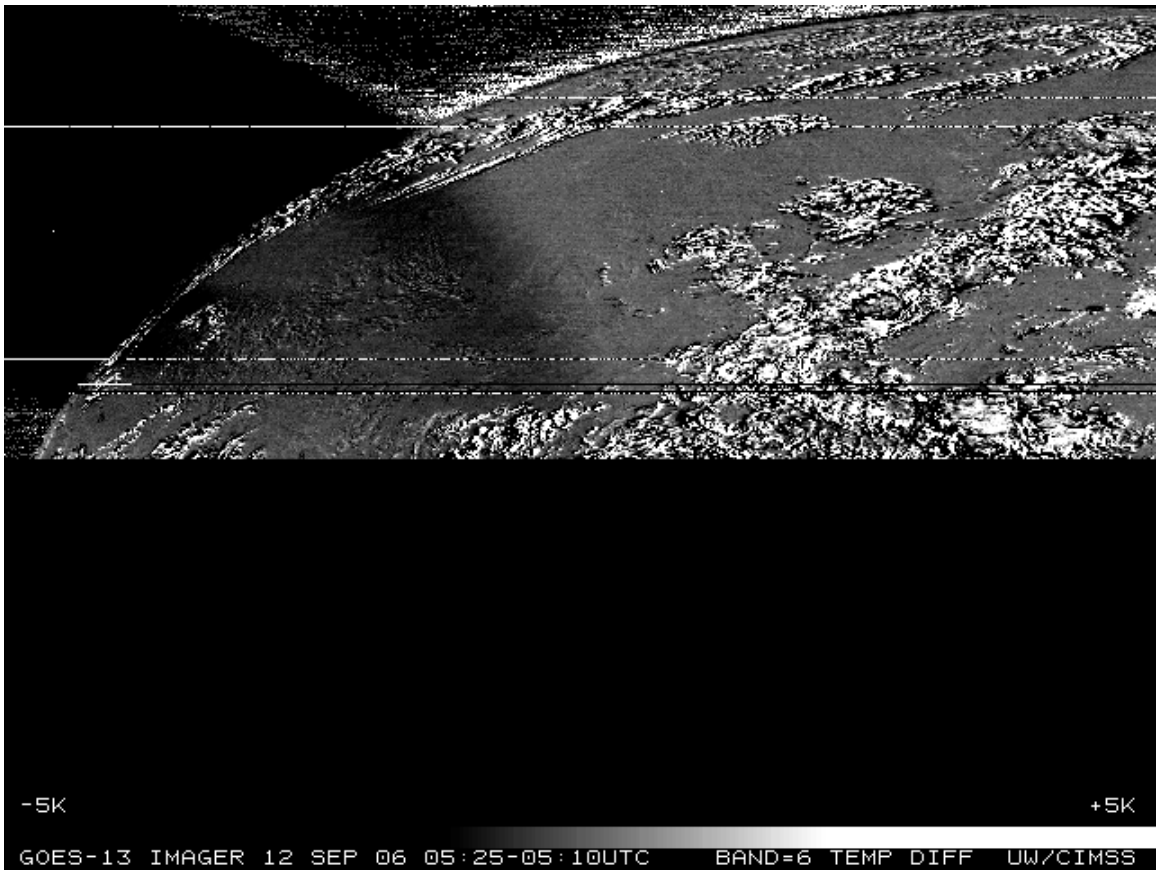

Figure 4.16: GOES-13 Imager temporal difference (0525 – 0510 UTC) of the CO_2 band. The bad lines were due to a noisy data ingest.

In general, the GOES Sounder can be affected even more during the KOZ periods, due to the relatively slow sounder scanning (not shown).

5. Product Validation

A number of products were generated with data from the GOES-13 instruments and then compared to products generated from other satellites or ground-based measurements. Products derived from the Sounder and described below are Total Precipitable Water (TPW), Lifted Index (LI), Clouds products, and Atmospheric Motion Vectors. The products derived from the Imager are Clouds, Atmospheric Motion Vectors, Clear Sky Brightness Temperature (CSBT), Sea Surface Temperature (SST), and Fire Detection.

5.1. Total Precipitable Water (TPW) from Sounder

Total precipitable water retrievals (displayed in the form of an image) for GOES-12 and GOES-13 are presented in Figure 5.1 over the same area at approximately the same time (13 December 2006). These retrievals are generated for each clear radiance Field-Of-View (FOV). Radiosonde

measurements of TPW are plotted on top of the images. Qualitatively, there is good agreement between the GOES-12 and GOES-13 TPW retrievals that, in turn, compare reasonably well with the reported radiosonde measurements of TPW. When comparing measurements from two satellites, one must consider the different satellite orbital locations; even precisely co-located fields-of-view are seen through different atmospheric paths.

There is some striping evident in the GOES-13 TPW image (Figure 5.1). The striping is evident in band 7 (not shown) and was addressed by moving each line's brightness temperature average towards the overall mean. The results after application of this process can be seen in Figure 5.2. Another possible method would be to determine which detector should be used as a reference detector. Ideally, the cause of the striping could be determined and correct farther 'up stream' in the processing chain.

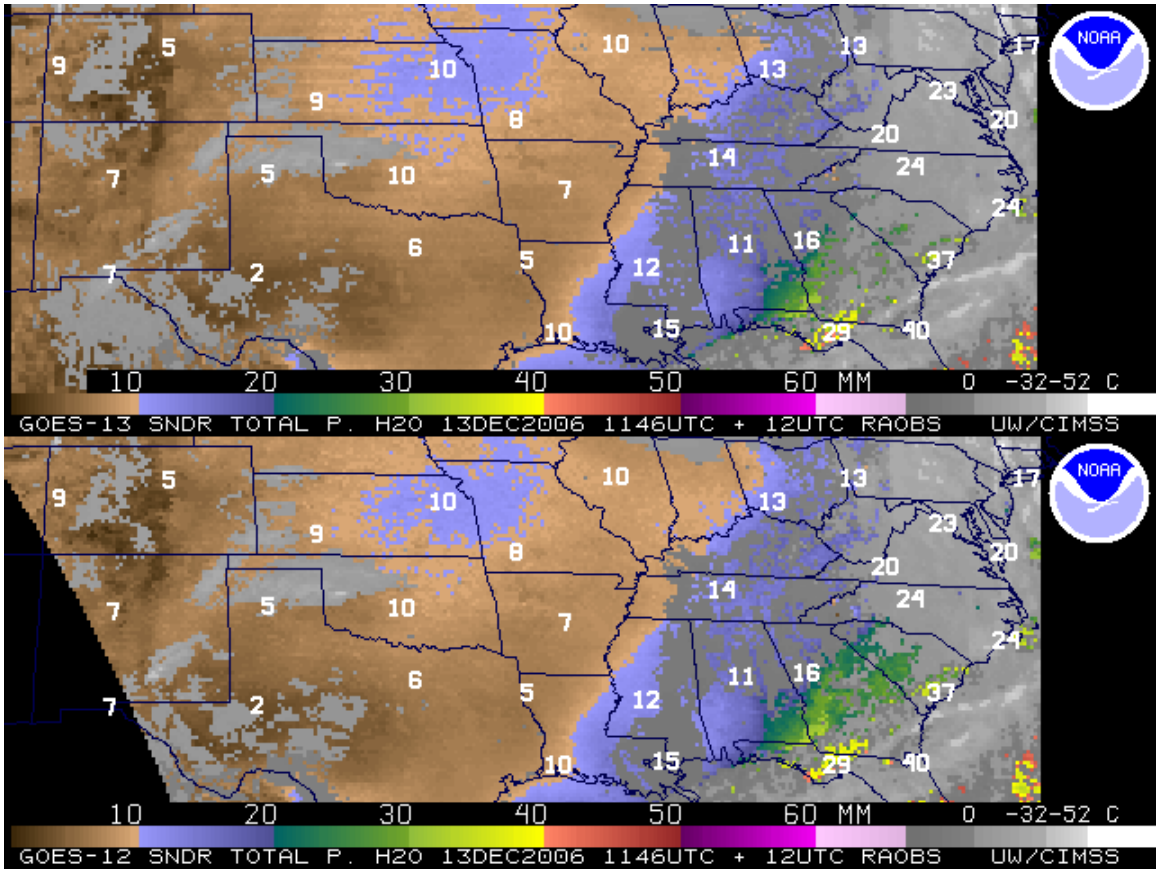

Figure 5.1: GOES-13 (top panel) and GOES-12 (lower panel) retrieved to TPW (mm) from the Sounder displayed as an image. The data are from 1146 UTC on 13 December 2006. Measurements from radiosondes are overlaid as white text; cloudy FOVs are denoted as shades of gray.

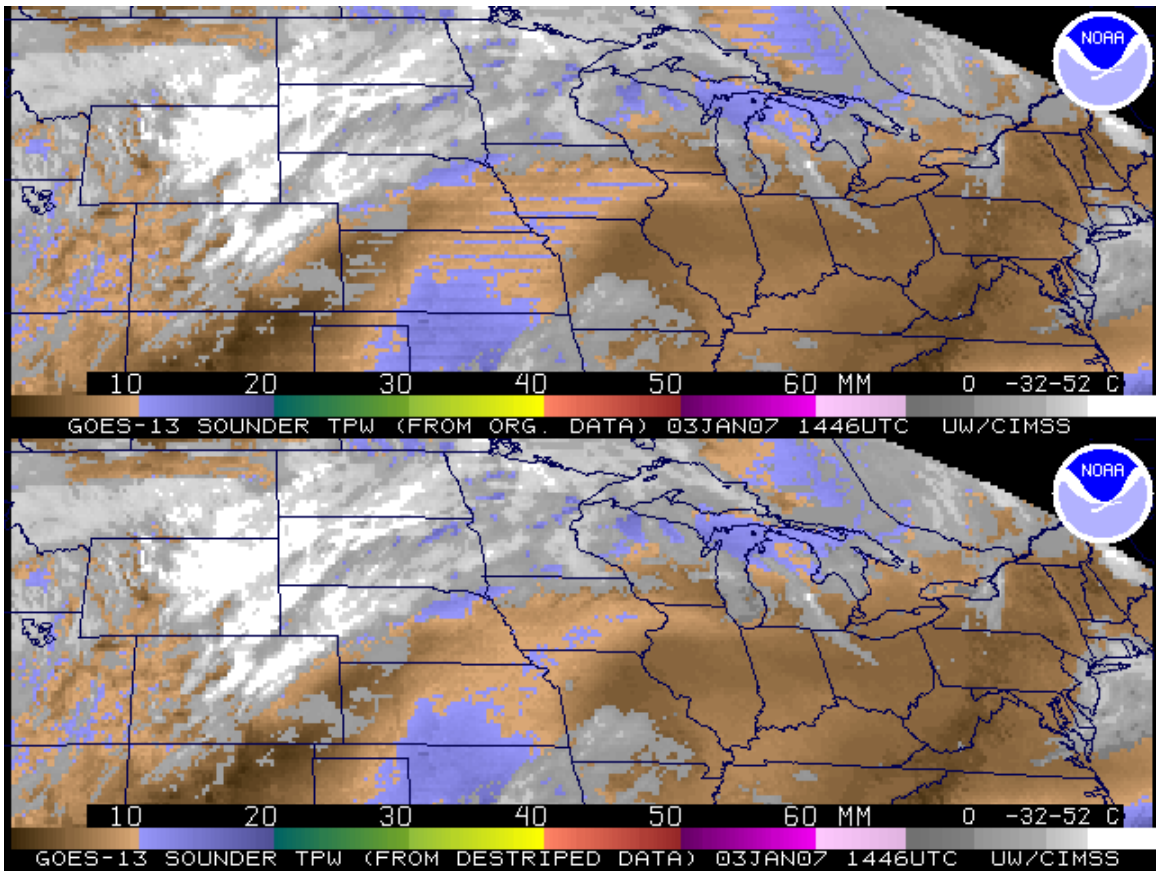

Figure 5.2: GOES-13 Sounder retrieved TPW with the original data (top panel) and after data has been de-striped (lower panel). The data are from 1446 UTC on 3 January 2007. The process to de-stripe the image was generated by D. Hillger; striping is removed via a process that moves each line average toward the mean.

5.1.1. Validation of Precipitable Water (PW) Retrievals from the GOES-13 Sounder

GOES-13 retrievals of precipitable water were validated against radiosonde observations of precipitable water for the period 7 December 2006 to 5 January 2007. To achieve this, GOES-13 retrievals were collocated in space (within 11 km) and time (within 30 minutes) to daily radiosonde observations at 0000 UTC and 1200 UTC. At the same time, these GOES-13 retrievals were collocated in space (within 11 km) and time (within 60 minutes) to GOES-12 retrievals. The relative performance of the GOES-13 PW retrievals, GOES-12 PW retrievals, and first guess PW supplied to the retrieval algorithm could then be compared since all of these PW values were collocated to the same radiosonde observation. Table 5.1 provides a summary of these statistics for the Total Precipitable Water (TPW) and the PW at three layers (Sfc-900 hPa; 900-700 hPa, and 700-300 hPa). The statistics indicate that the quality of the GOES-13 Sounder PW retrievals compare very well to the quality of the operational GOES-12 PW retrievals. It should be remembered that the GOES-13 retrievals used a GOES-12 dataset for the radiance bias adjustment for initial processing.

Table 5.1: Verification statistics between GOES-12 and GOES-13 retrieved precipitable water, first guess (GFS) precipitable water, and radiosonde observations of precipitable water for the period 7 December 2006 to 5 January 2007.

Statistic	GOES-12/RAOB	GOES-13/RAOB	GUESS/RAOB	RAOB
Total Precipitable Water				
RMS (mm)	2.33	2.67	2.56	
Bias (mm)	-0.04	-0.18	0.08	
Correlation	0.98	0.97	0.97	
Mean (mm)	13.63	13.49	13.75	13.67
Sample	2265	2265	2265	2265
Layer Precipitable Water (surface to 900 hPa)				
RMS (mm)	0.89	0.94	0.92	
Bias (mm)	-0.41	-0.38	-0.36	
Correlation	0.98	0.98	0.98	
Mean (mm)	5.09	5.10	5.13	5.49
Sample	2265	2265	2265	2265
Layer Precipitable Water (900 hPa to 700 hPa)				
RMS (mm)	1.45	1.64	1.48	
Bias (mm)	0.12	0.09	0.24	
Correlation	0.96	0.95	0.96	
Mean (mm)	5.87	5.84	5.99	5.75
Sample	2265	2265	2265	2265
Layer Precipitable Water (700 hPa to 300 hPa)				
RMS (mm)	1.09	1.12	1.22	
Bias (mm)	0.23	0.11	0.20	
Correlation	0.87	0.85	0.84	
Mean (mm)	2.38	2.49	2.57	2.38
Sample	2265	2265	2265	2265

Figures 5.3 through Figure 5.6 present time series of various comparison statistics (GOES retrieved TPW vs. radiosonde observed TPW) for GOES-13 (in green with open circles) and GOES-12 (in red with filled circles) for the same time period (7 December 2006 to 5 January 2007) as in Table 5.1. Each tick mark represents a data point (2 points per day) with the calendar day label centered at 0000 UTC of that day. With few exceptions, the GOES-13 data points are very close to, if not on top of, the GOES-12 data points.

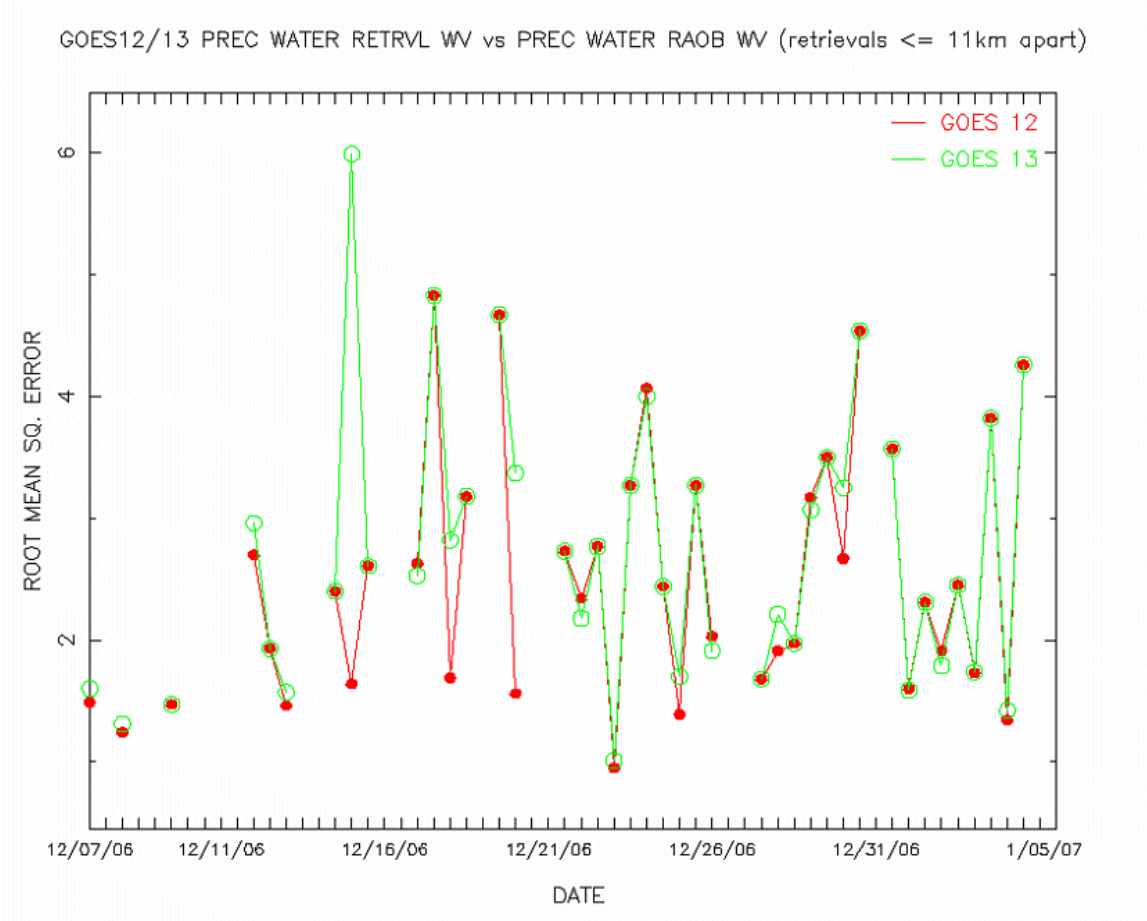

Figure 5.3: Time series of Root Mean Square Error (RMSE) between GOES-12 and GOES-13 retrieved precipitable water and radiosonde observation of precipitable water over the period 7 December 2006 to 5 January 2007.

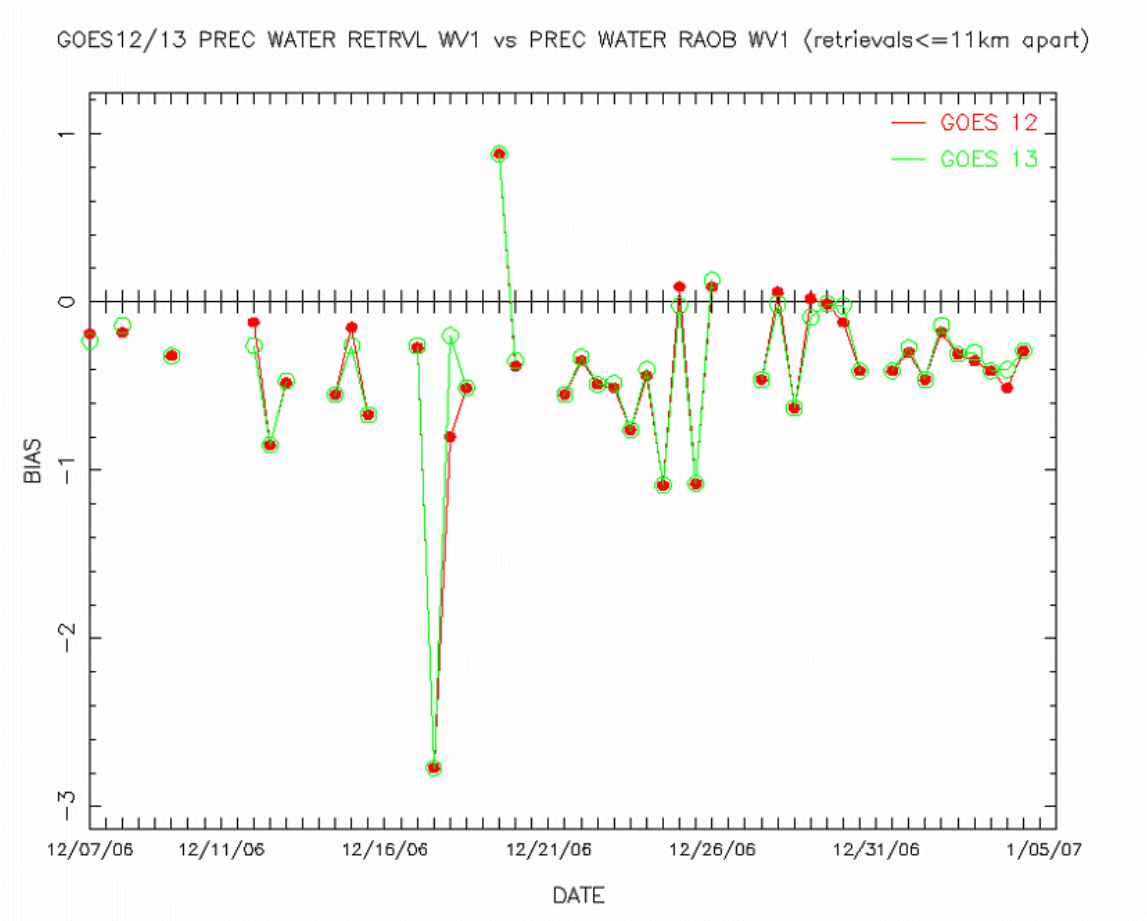

Figure 5.4: Time series of Bias (GOES-radiosonde) between GOES-12 and GOES-13 retrieved precipitable water and radiosonde observation of precipitable water over the period 7 December 2006 to 5 January 2007.

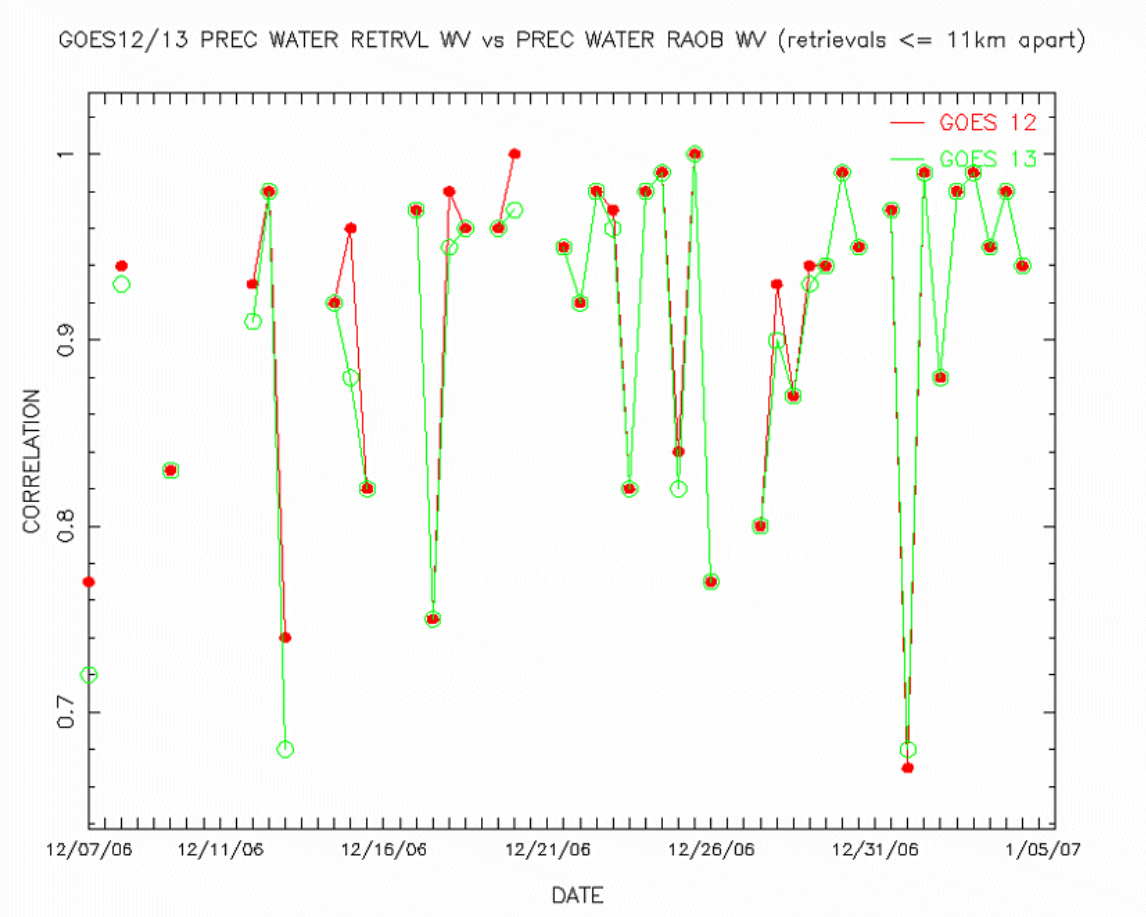

Figure 5.5: Time series of correlation between GOES-12 and GOES-13 retrieved precipitable water and radiosonde observation of precipitable water over the period 7 December 2006 to 5 January 2007.

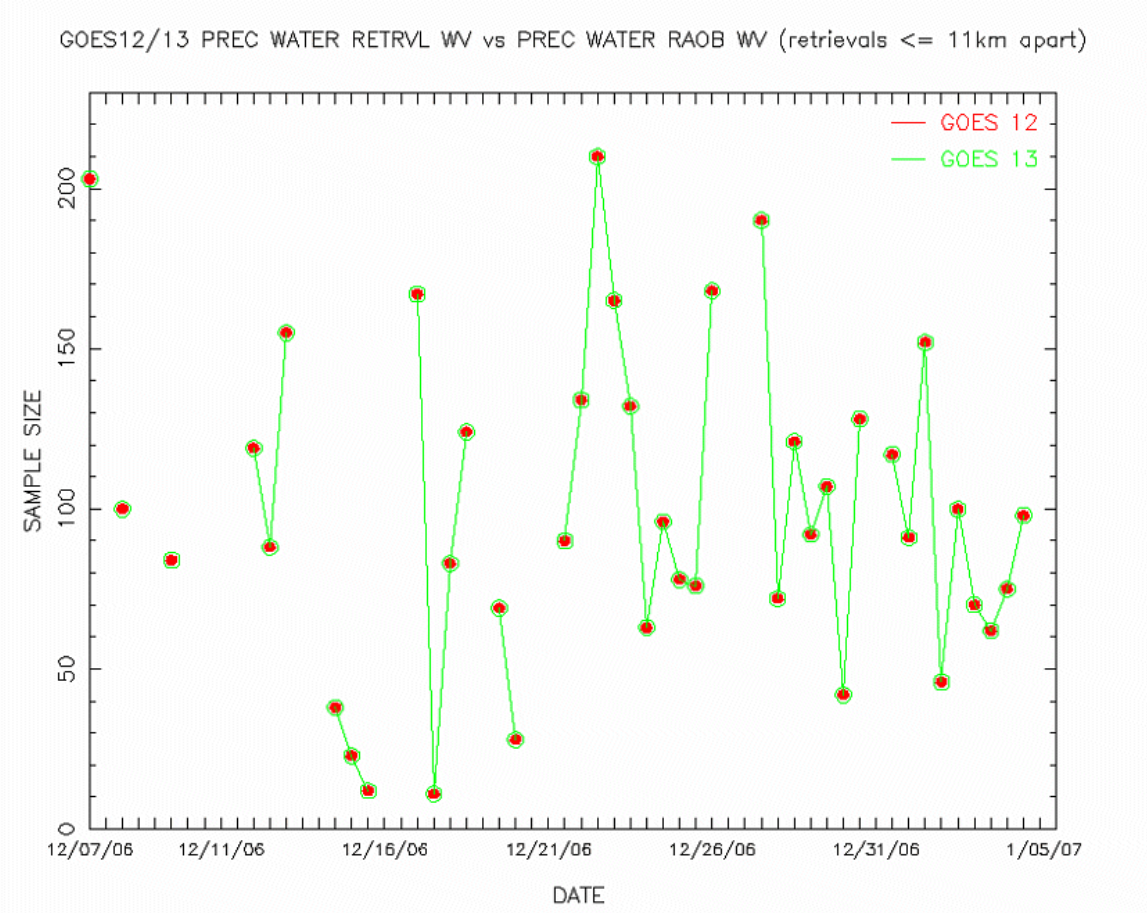

Figure 5.6: Time series of the number of collocations between GOES-12 and GOES-13 retrieved precipitable water and radiosonde observation of precipitable water over the period 7 December 2006 to 5 January 2007.

5.2. Lifted Index (LI) from Sounder

The lifted index (LI) product is generated from the retrieved temperature and water vapor profiles (Ma et al. 1999) that are generated from clear radiances for each FOV. Figure 5.7 shows lifted index retrievals (displayed in the form of an image) for GOES-12 and GOES-13 over the same area at approximately the same time, showing no discernable bias in the LI values. Of course the overall large (stable) LI values also illustrates that ideally satellite post-launch check-outs should be conducted in seasons with more atmospheric moisture/instability.

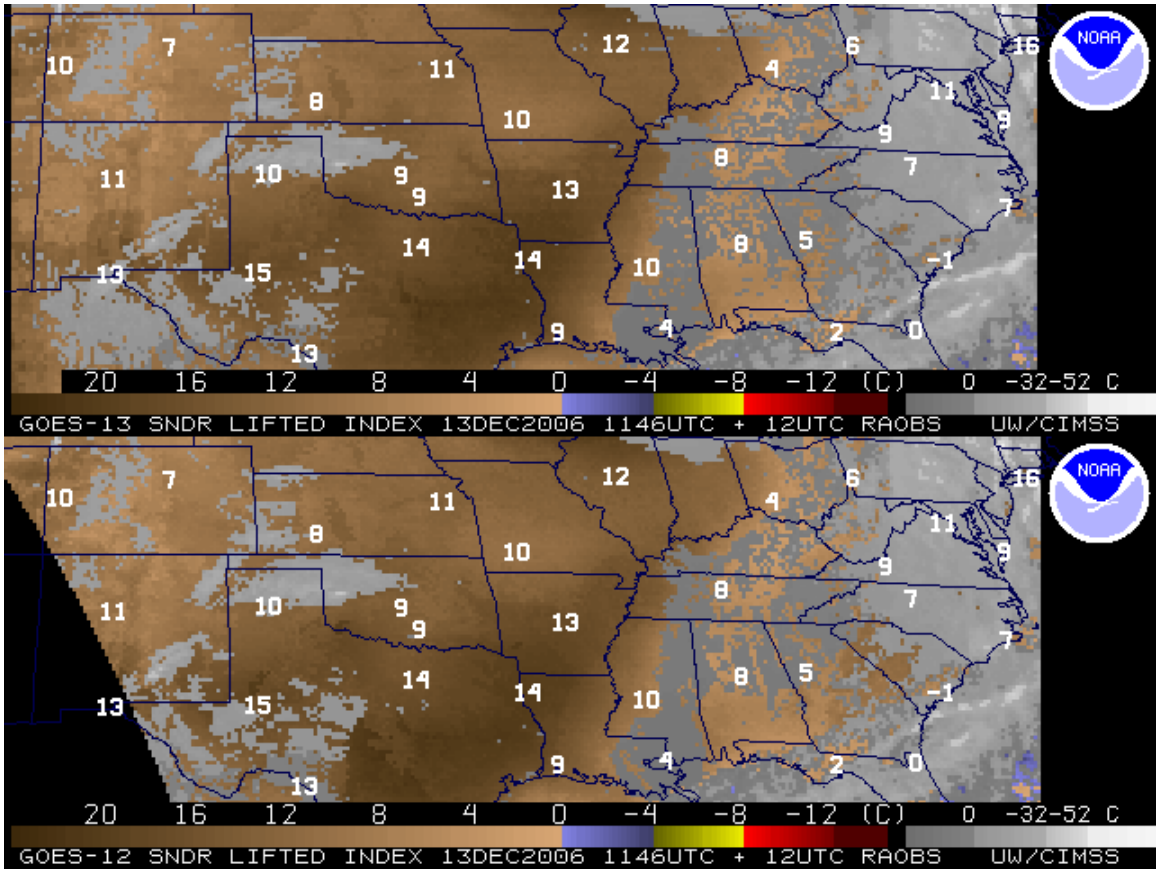

Figure 5.7: GOES-13 (top panel) and GOES-12 (lower panel) retrieved Lifted Index (LI) from the Sounder displayed as an image. The data are from 1146 UTC on 13 December 2006. Radiosonde values are over-plotted.

5.3. Cloud Parameters from Sounder and Imager

The presence of the 13 µm band on the GOES-13 Imager, similar to the GOES-12 Imager, makes near full-disk cloud products possible. This product complements that from the GOES Sounders.

Figure 5.8 shows a comparison of GOES-12 and GOES-13 Sounder cloud-top pressure derived product images from 4 January 2007. Another comparison produced just prior to the GOES-13 Science Test showed good agreement between the GOES-13 Imager and the remapped GOES-13 Sounder cloud top pressure products (or "combined GOES-11 and GOES-12 Sounder cloud-top pressure products") (see Figures 5.9 through 5.11). The comparison displayed show generally good correlations between the Imager-based product and that produced from the full complement of GOES Sounder bands.

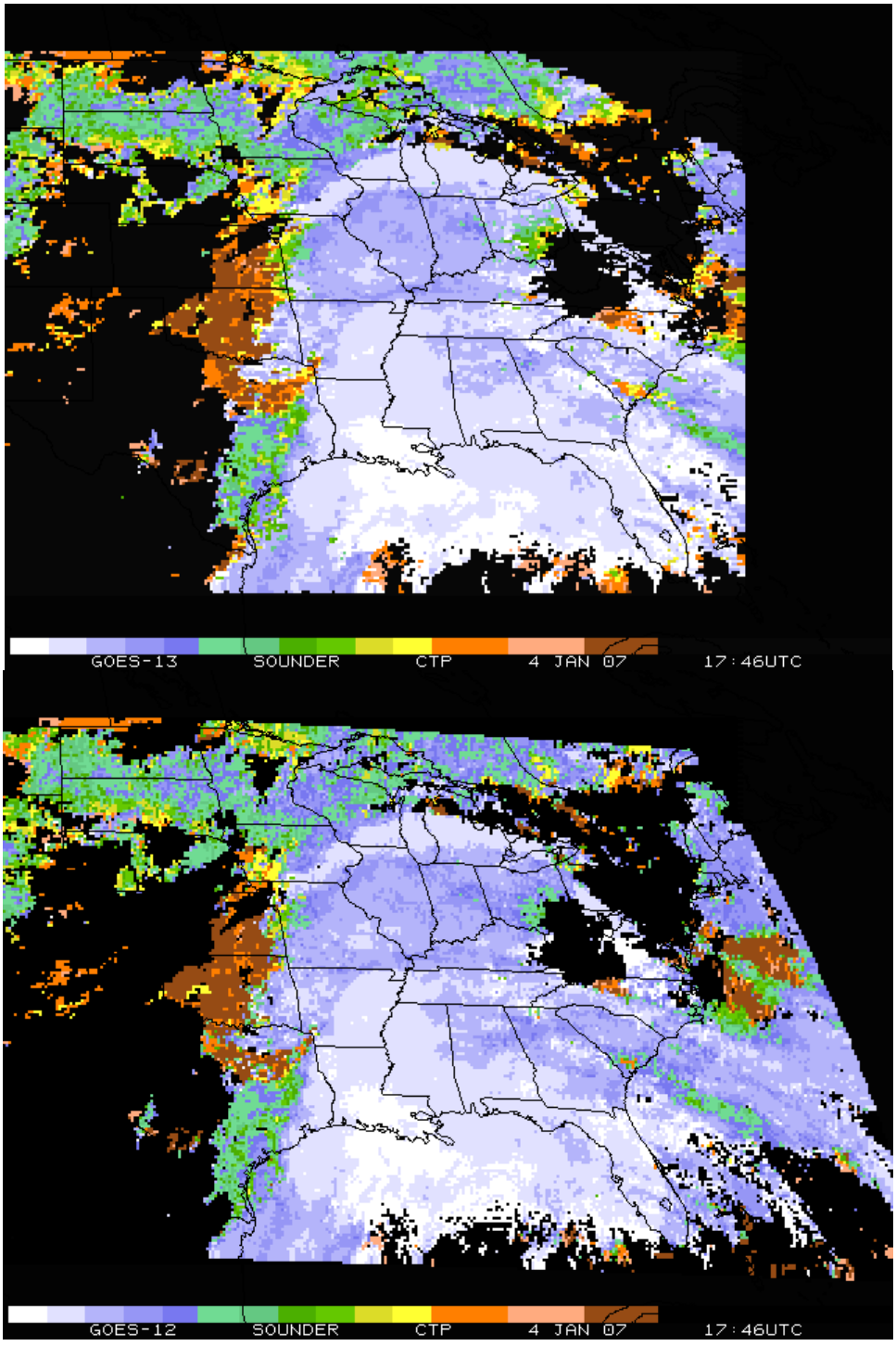

Figure 5.8: GOES-13 (upper panel) and GOES-12 (lower panel) retrieved cloud-top pressure from the Sounder displayed as an image. The data are from 1746 UTC on 4 January 2007 and the GOES-12 is remapped into the GOES-13 Sounder projection.

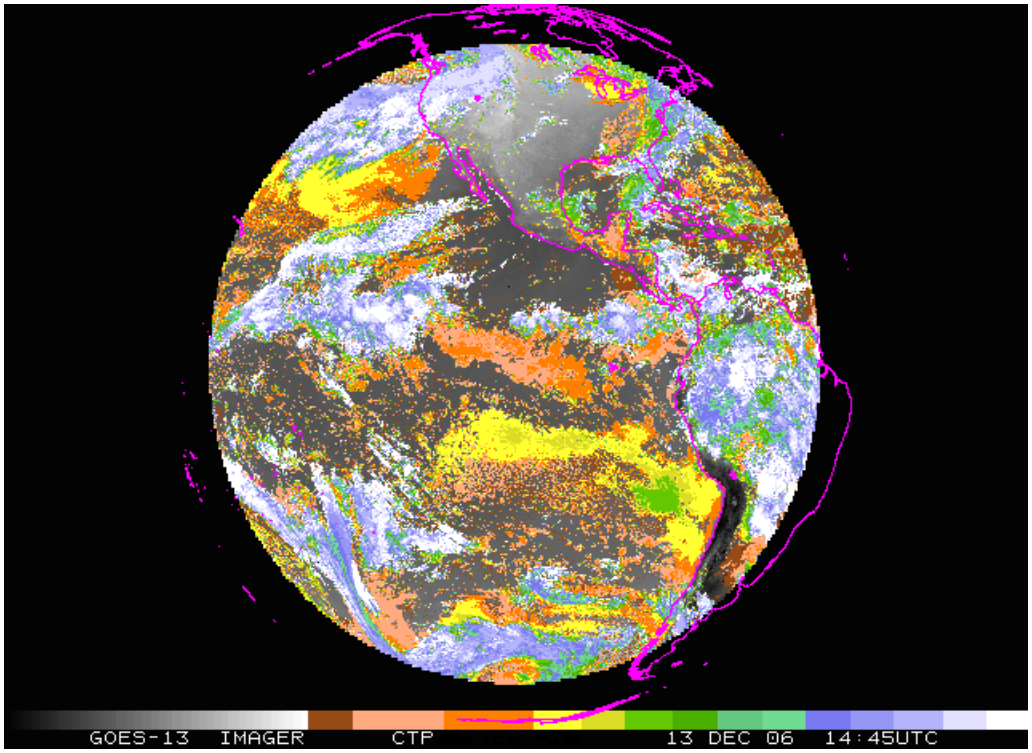

Figure 5.9: GOES-13 cloud-top pressure from the Imager from 1445 UTC on 13 December 2006.

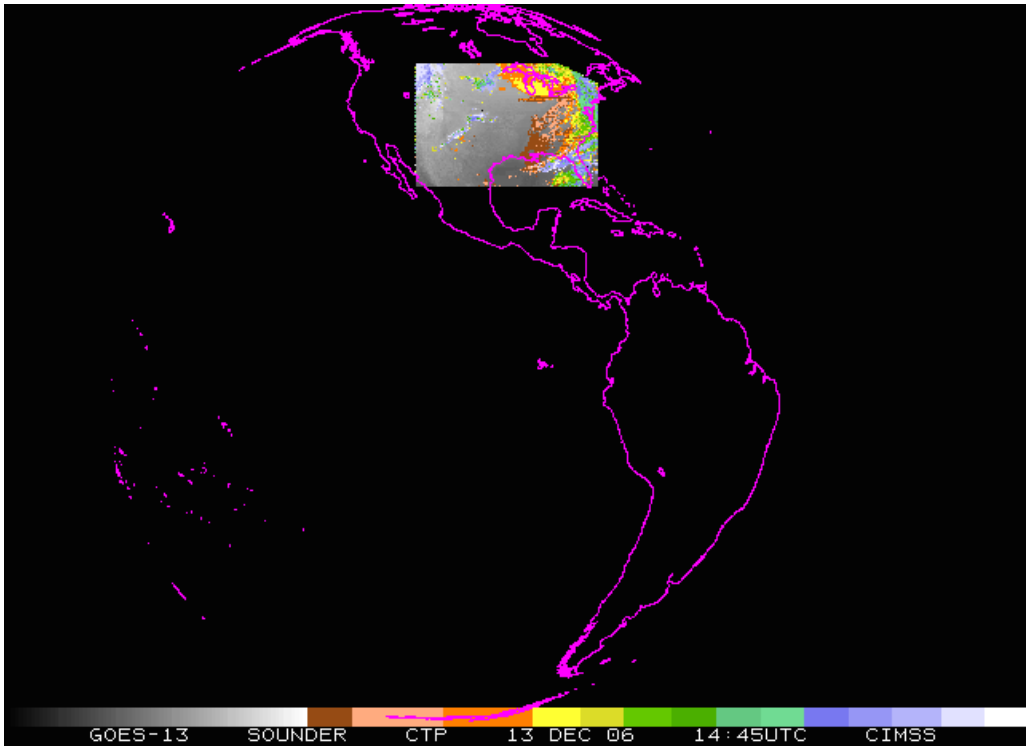

Figure 5.10: GOES-13 cloud top pressure from the Sounder from 1445 UTC on 13 December 2006.

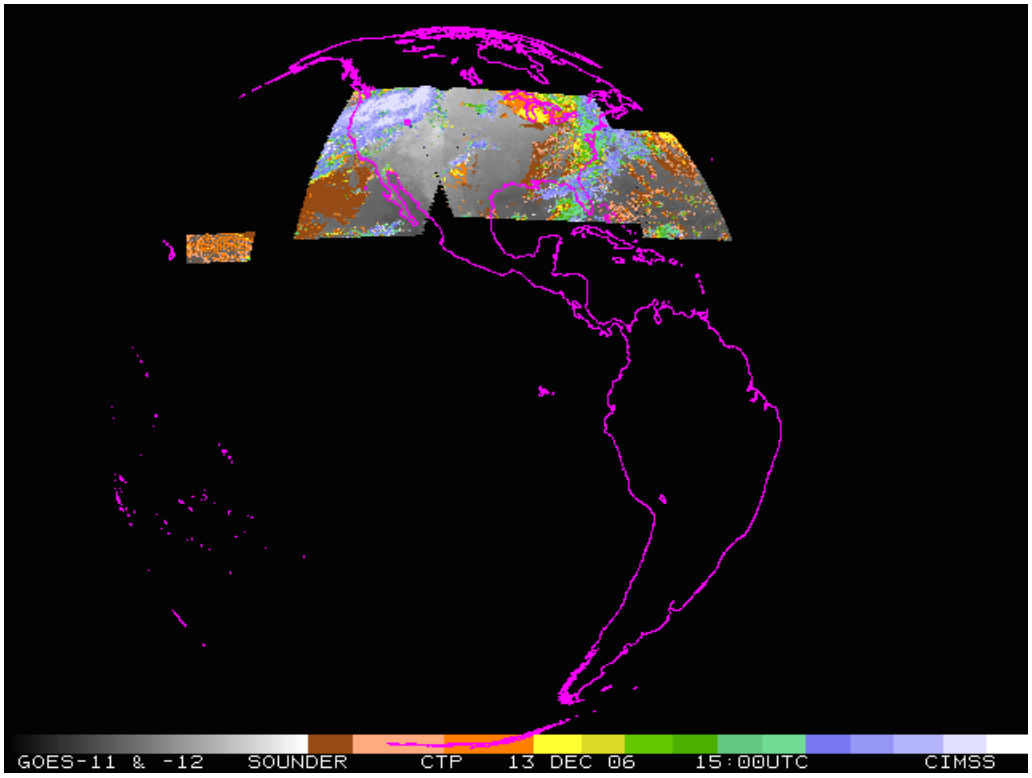

Figure 5.11: GOES-11 and GOES-12 cloud-top pressure from the Sounder from the nominal 1500 UTC on 13 December 2006. The image is reformatted to the GOES-13 Imager projection

5.4. Atmospheric Motion Vectors (AMVs) from Sounder and Imager

Atmospheric Motion Vectors (AMVs) from GOES are derived using a sequence of three images. Features targeted in the middle image (cirrus cloud edges, gradients in water vapor, small cumulus clouds, etc.) are tracked from the middle image back to the first image, and forward to the third image, yielding two displacement vectors. These vectors are averaged to give the final wind vector, or AMV. This report summarizes the quality of AMVs from GOES-13 as part of the special science checkout activation in late 2006.

The varied imaging schedules activated during the GOES-13 Science Test provided an opportunity to run AMV assessments for what are currently considered operational as well as special case scenarios. From the Imager, the GOES-12 emulation periods were used to run collocated GOES-12 and GOES-13 AMV sets. A statistical comparison was conducted with radiosonde wind values (RAOBs) for validation purposes. The one-minute CONUS scan periods provided the opportunity to compare AMVs generated using nested image triplets for various rapid scan intervals. Finally, a comparison of AMVs produced from Sounder WV bands was performed utilizing the current standard sixty-minute interval images and the Science Test special thirty-minute interval images.

Using image triplets near 0000 UTC and 1200 UTC, 18 sets of collocated (both in time and space) GOES-12 and GOES-13 AMVs were compared with RAOBs (assumed to be truth).

There are expected differences between RAOB wind measurements and GOES AMVs since RAOBs do not measure the same volume or take measurements at exactly the same time. In order to minimize the scan angle differences between the two satellites, only the centered coverage overlap region was used for AMV calculation and subsequent evaluation. Therefore, AMVs were processed only over a limited area bounded by 10 to 60 degrees North latitude and 82 to 98 degrees West longitude. Images from five bands, three from the Imager, two from the Sounder, were used as is done operationally (for the quantitative assessment, no 0.65 μm visible image AMVs were included due to daylight limitations at the RAOB comparison times. Spectral bands included from the Imager were the 6.5 μm Water Vapor (WV) at thirty-minute intervals, 10.7 μm Long-Wave InfraRed (LWIR) and 3.9 μm Short-Wave InfraRed (SWIR) at fifteen-minute intervals. Spectral bands included from the Sounder were the 7.0 μm Water Vapor (band-11) and 7.4 μm Water Vapor (band-10) at sixty-minute intervals.

Shown in Figure 5.12 is a thinned (for clarity of display) sample of AMVs from all five of these bands from GOES-12 (left) and GOES-13 (right) for one case. Qualitatively, the results appear quite similar in this example, which is representative of all the cases run. This is supported by the objective statistical comparison with RAOB data shown in Table 5.2. To be considered in the statistical compilation, an AMV had to be within a spatial distance of 100 km from a RAOB. Because the comparisons are not exactly homogeneous, it is not possible to make a definitive statement about the relative quality of the two AMV sets. However, the small differences do confirm that the AMV products from GOES-13 are at least comparable in quality with the existing GOES operational AMVs, which was the intent of the science checkout. Table 5.3 shows the quality of the GOES-12 and GOES-13 AMVs are fairly similar when a radiance bias correction is applied to the 13.3 μm band. In general, the speed bias is reduced when a radiance bias correction is applied.

Table 5.2: Verification statistics for GOES-12 and GOES-13 AMVs vs. radiosonde winds for 18 comparison cases.

	Speed RMS (m/s)	Speed Bias Satellite-RAOB (m/s)	Direction RMS (deg)	Direction Bias Satellite-RAOB (deg)	Total AMVs used
GOES-12	5.26	-0.37	7.07	-2.89	2718
GOES-13	5.44	-0.62	7.45	-3.79	2772

Table 5.3: Verification statistics for GOES-12 and GOES-13 AMVs vs. radiosonde winds, after a fixed bias correction was applied. Only samples that had a radiosonde match in both the GOES-12 and GOES-13 datasets were included.

		Collocated matches (within one tenth of a degree)											
		GOES-12 with CO2 Bias Correction			GOES-12 without CO2 Bias Correction			GOES-13 with CO2 Bias Correction			GOES-13 without CO2 Bias Correction		
		Sat	Guess	RAOB	Sat	Guess	RAOB	Sat	Guess	RAOB	Sat	Guess	RAOB
Overall	**NRMS Difference**	0.36	0.32		0.35	0.3		0.36	0.32		0.35	0.31	
	RMS Difference	7.21	6.23		7.21	6.13		7.47	6.43		7.36	6.47	
	AVG Difference	5.77	4.89		5.85	4.89		5.87	4.96		5.88	5.08	
	STD Deviation	4.33	3.86		4.21	3.7		4.62	4.09		4.42	4.01	
	Speed Bias	-0.27	-0.84		-0.35	-0.97		-0.2	-0.85		-0.51	-1.06	
	Speed	20.29	19.7	20.54	20.81	20.17	21.14	20.58	19.9	20.76	21.23	20.67	21.73
	Sample Size	716			715			716			715		
High	**NRMS Difference**	0.26	0.23		0.27	0.23		0.28	0.25		0.27	0.25	
	RMS Difference	7.06	6.3		7.46	6.42		7.81	6.84		7.72	6.94	
	AVG Difference	5.91	5.32		6.28	5.42		6.38	5.62		6.47	5.81	
	STD Deviation	3.87	3.37		4.03	3.44		4.5	3.9		4.22	3.8	
	Speed Bias	0.08	-0.44		-0.22	-0.86		0.13	-0.64		-0.61	-1.17	
	Speed	27.54	26.99	27.43	28.06	27.38	28.24	28.25	27.45	28.1	28.57	28	29.73
	Sample Size	316			334			322			351		
Middle	**NRMS Difference**	0.52	0.46		0.49	0.44		0.53	0.46		0.53	0.46	
	RMS Difference	8.48	7.26		8.06	6.88		8.34	7		8.26	7.01	
	AVG Difference	6.67	5.41		6.47	5.25		6.46	5.19		6.44	5.24	
	STD Deviation	5.23	4.84		4.81	4.44		5.27	4.7		5.17	4.66	
	Speed Bias	-0.95	-1.6		-0.75	-1.41		-0.99	-1.35		-0.9	-1.26	
	Speed	16.4	15.74	17.34	16.4	15.75	17.15	15.68	15.28	16.63	15.68	15.29	16.55
	Sample Size	233			215			235			206		
Low	**NRMS Difference**	0.44	0.37		0.44	0.37		0.41	0.38		0.4	0.37	
	RMS Difference	5.31	4.25		5.29	4.21		4.99	4.35		4.83	4.25	
	AVG Difference	4.24	3.37		4.22	3.35		3.95	3.29		3.84	3.23	
	STD Deviation	3.21	2.58		3.2	2.55		3.05	2.84		2.94	2.77	
	Speed Bias	0	-0.55		-0.1	-0.62		0.28	-0.54		0.22	-0.54	
	Speed	11.99	11.43	11.97	11.95	11.42	12.04	12.26	11.44	11.98	12.17	11.42	11.96
	Sample Size	167			166			159			158		

In addition, normally an image navigation correction is attempted before the wind generation. Basically, the second and third images are corrected to the first image. As a test, this was needed for GOES-12 in 3 of the 18 cases, yet it was not needed in any of the GOES-13 cases. This is an indication that GOES-13 image registration is improved.

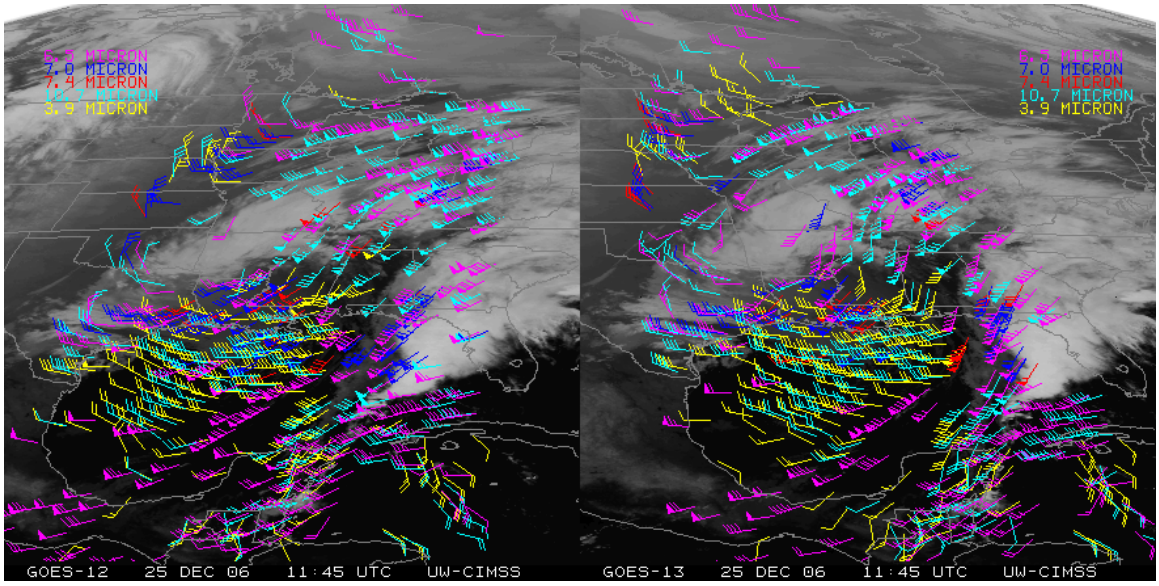

Figure 5.12: GOES-12 (left) and GOES-13 (right) AMVs for 25 December 2006 plotted over band-4 (10.7 µm) images. The color coding differentiates the satellite bands used in AMV derivation. Not all AMVs are shown for clarity of display.

The 20 December 2006 one-minute CONUS scan schedule provided the opportunity to run GOES-13 AMV sets using nested images at 1, 3, 5, 10, and 15-minute intervals. The improved consistency in cloud features over shorter time interval imagery allows for derivation of more AMVs, particularly in the visible (band-1). Since LWIR and WV AMVs provide upper level coverage, visible AMV processing is typically limited to the 600 to 1000 hPa layer. Shown in Figure 5.13 are visible AMVs derived from images at 1, 5, and 15-minute intervals. The increase in AMV quantities makes clear the improved continuity of cloud features available for tracing in the shorter interval imagery (there is no thinning of wind flags in the Figure 5.12 plots, all AMVs are shown). The improved image navigation and image-to-image co-registration for GOES-13 is vital to the successful automated production of AMVs at these smaller image time intervals. Any registration/navigational shifting between images will result in correlation tracking failures and/or significantly reduced vector quality. The improved fidelity of GOES-13 registration/navigation was evident in the case displayed. This is because the objective navigation correctional steps available in the CIMSS/NESDIS AMV automated processing software were not required.

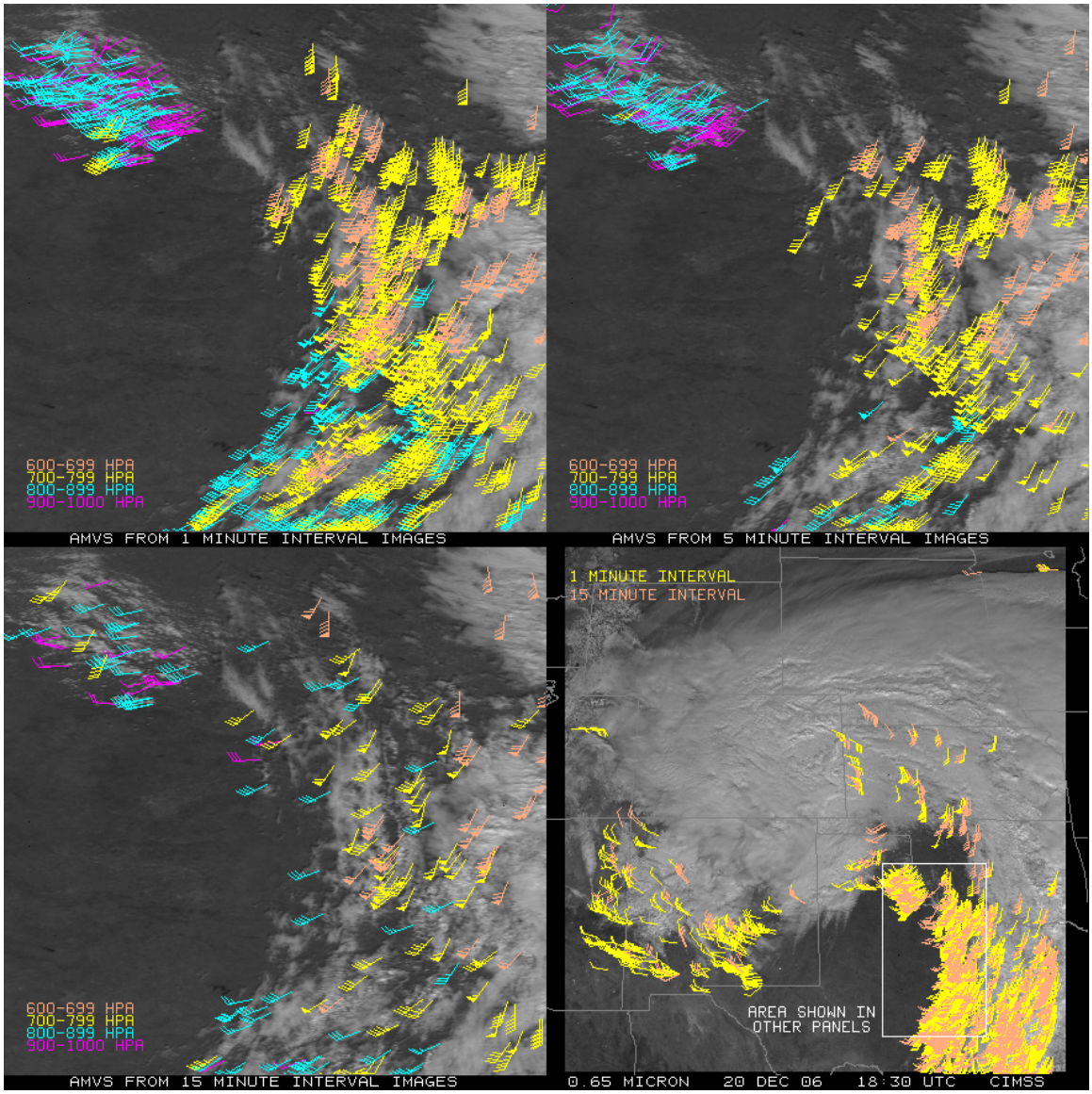

Figure 5.13: GOES-13 Imager (0.65 µm) visible AMVs from 20 December 2006 generated using 1, 5, and 15-minute interval images in upper-left, upper-right, and lower-left panels, respectively. A broader view of the aforementioned 3 panels is shown in the lower-right panel for perspective. Wind flag colors delineate pressure levels, except in the lower-right panel where colors delineate AMVs from different image intervals.

GOES Sounder images have not traditionally been available at better than one-hour time intervals. The thirty-minute interval CONUS images from GOES-13 provided the basis for comparing AMVs generated using the current operational sixty-minute interval images with images at a smaller time step. The results for one such comparison can be seen in Figure 5.14. In this case on 20 December 2006 there was a 50 percent increase in the number of AMVs generated when using 30-minute interval images.

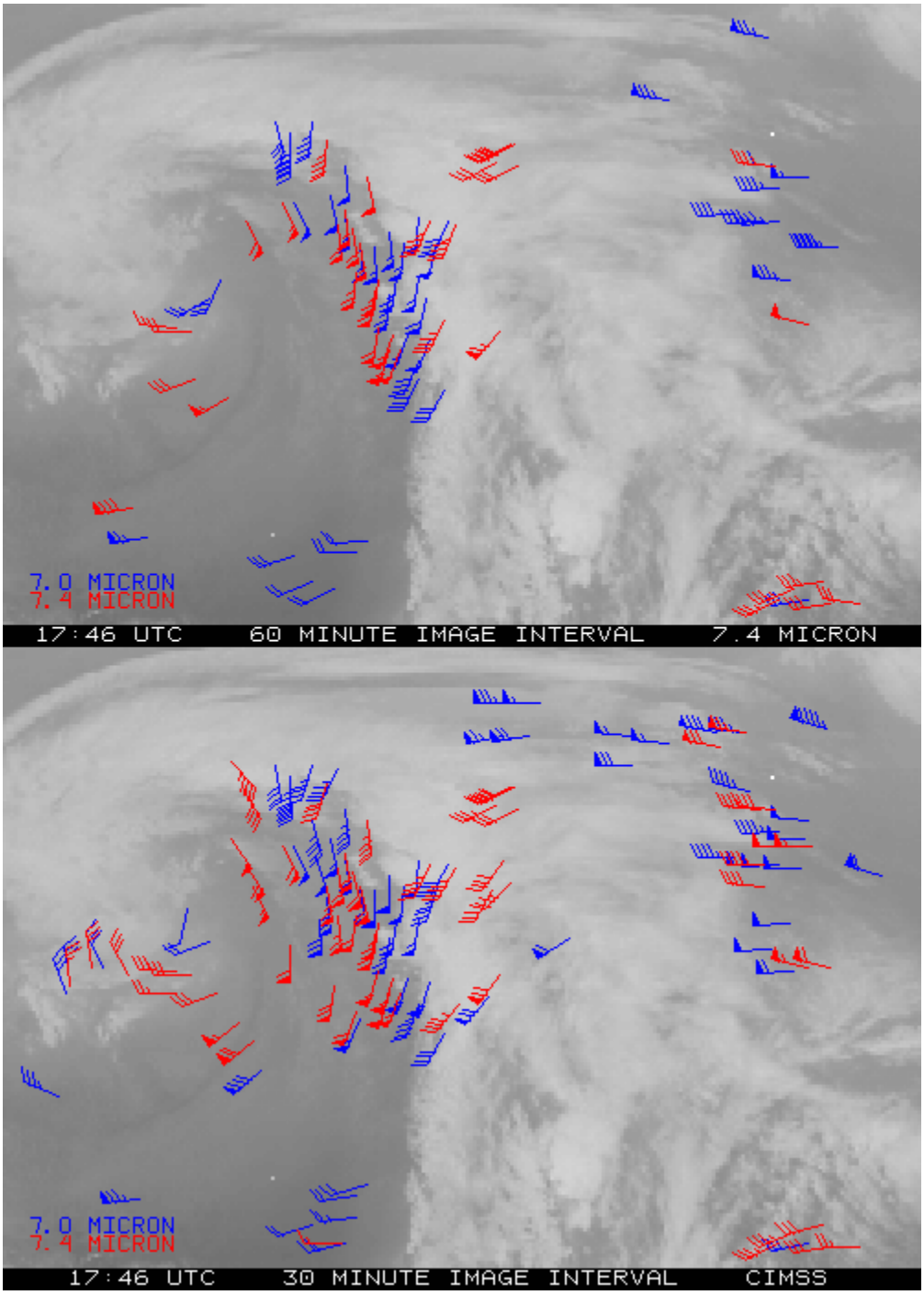

Figure 5.14: AMVs generated using 60-minute interval 7.0 and 7.4 µm images from GOES-13 Sounder are shown in the top panel, while AMVs generated using thirty-minute interval images are shown in the bottom panel, all overlain on GOES-13 Sounder 7.4 µm images from 20 December 2006.

5.5. Clear Sky Brightness Temperature (CSBT) from Imager

The GOES-13 Imager Clear Sky Brightness Temperatures (CSBT) product was generated every 3 hours in near real-time. This product spatially averages the clear fields of view for use in global numerical weather prediction (NWP) applications. In general, there is fair agreement between the GOES-12 and GOES-13, with correlation coefficients between 0.96 and 0.98, varying by band. The CSBT can be used to initialize global numerical models.

A sample GOES-12 Imager Clear Sky Brightness Temperature cloud mask image was generated and is shown in Figure 5.15.

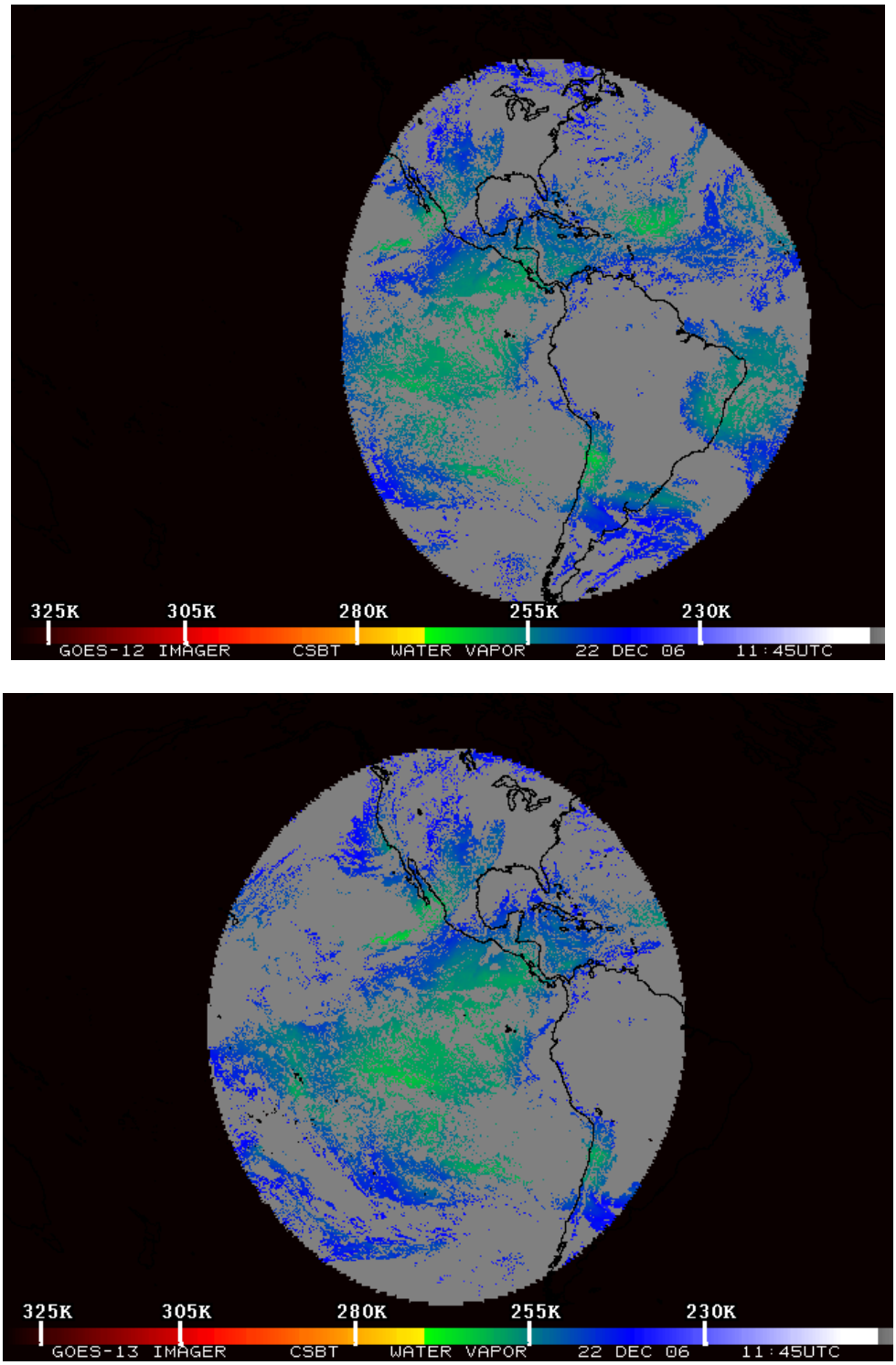

Figure 5.15: GOES-12 (top) and GOES-13 (bottom) Imager Clear-Sky Brightness Temperature cloud mask from 1200 UTC on 22 December 2006.

5.6. Sea Surface Temperature (SST) from Imager

GOES-13 Imager data were collected for both the north and south hemispheric sectors every half hour from 8 December 2006 to 5 January 2007 for use as input for Sea Surface Temperature (SST) retrievals. The north hemispheric sector is centered at latitude 14°19′53″ N, longitude 96°40′17″ W; the south hemispheric sector is centered at latitude 31°55′10″ S, longitude 96°06′36″ W. Pre-processed visible and IR imagery data were used to create multi-spectral imagery files as input of SST retrieval. Examples of the radiance imagery are shown in Figure 5.16.

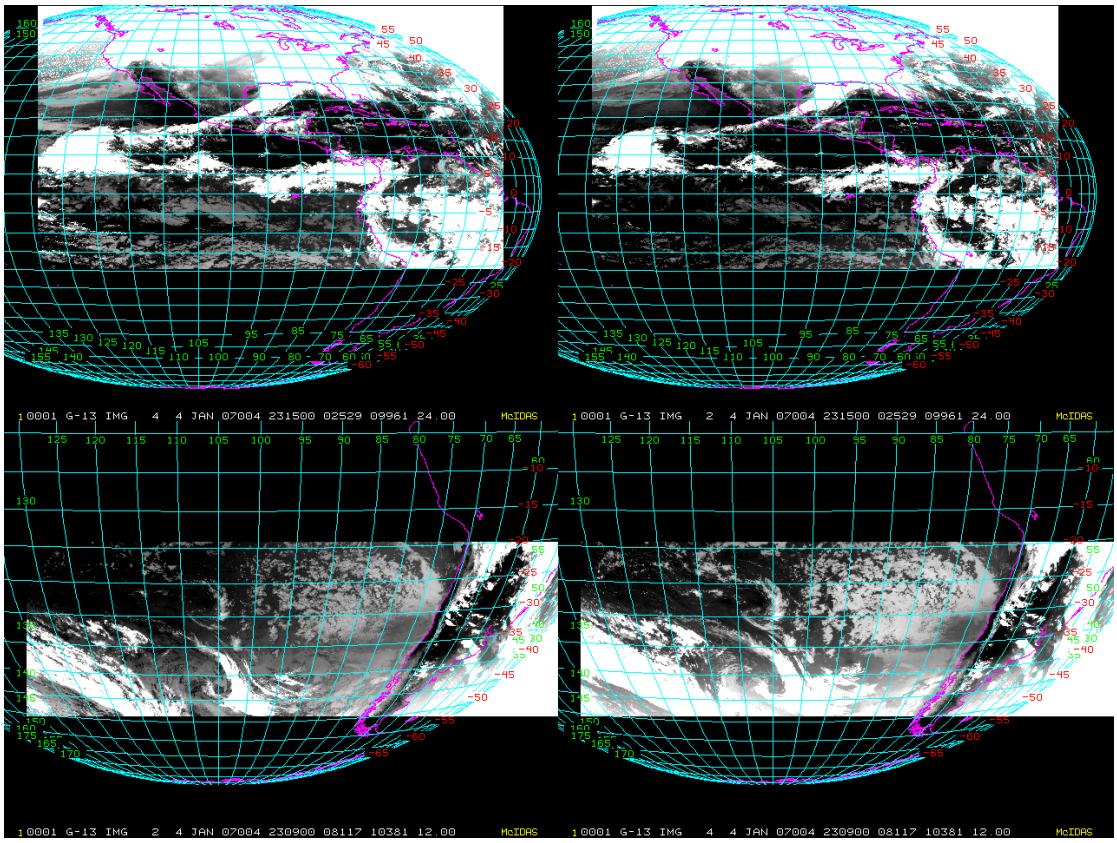

Figure 5.16: Radiance imagery: GOES-13 north sector band-2 (upper-left); GOES-13 north sector band-4 (upper-right); GOES-13 south sector band-2 (lower-left); GOES-13 south sector band-4 (lower-right).

5.6.1. SST Generation

GOES-13 SST coefficients were generated for all possible locations of the GOES-13 satellite (75°W, 105°W, and 135°W). The GOES-13 Community Radiative Transfer Model (CRTM) spectral and transmittance coefficients were acquired. Radiative-transfer-based SST retrieval algorithms are used to generate the GOES-13 SST retrievals. The form of the current GOES operational SST equation is:

$$SST = a_0 + a_0^{'} S + \sum_i \left(a_i + a_i^{'} S\right) T_i$$

where *i* is GOES-Imager band number (2, 4, 6), S = sec (satellite zenith angle) – 1
T_i is band brightness temperature (K).

SST retrievals were generated for dual and triple window. The Radiative Transfer Model (RTM) coefficients for dual window (*3.9 µm and 11 µm*) and triple window *(3.9 µm, 11 µm and 13 µm)* were applied. The GOES-13 SST coefficients for 105°W was used for the algorithm generation. Then a Bayesian Cloud Mask was applied to obtain clear sky pixels. Bayes' theorem applied to estimate the probability of a particular pixel being clear of cloud given the satellite-observed brightness temperatures, a measure of local texture and band brightness temperatures calculated for the given location and view angle using NCEP GFS surface and upper air data and the CRTM fast radiative transfer model. The method is described in detail in a paper by Merchant et al. (2005).

Hourly SST is created by compositing three half hour SST McIDAS Area files with an applied threshold of ≥98% clear sky probability. Satellite retrieval SST was matched with Buoy and NCEP GDAS data to create match-up dataset for validation. Example of the GOES-13 SST imagery is shown in Figure 5.17.

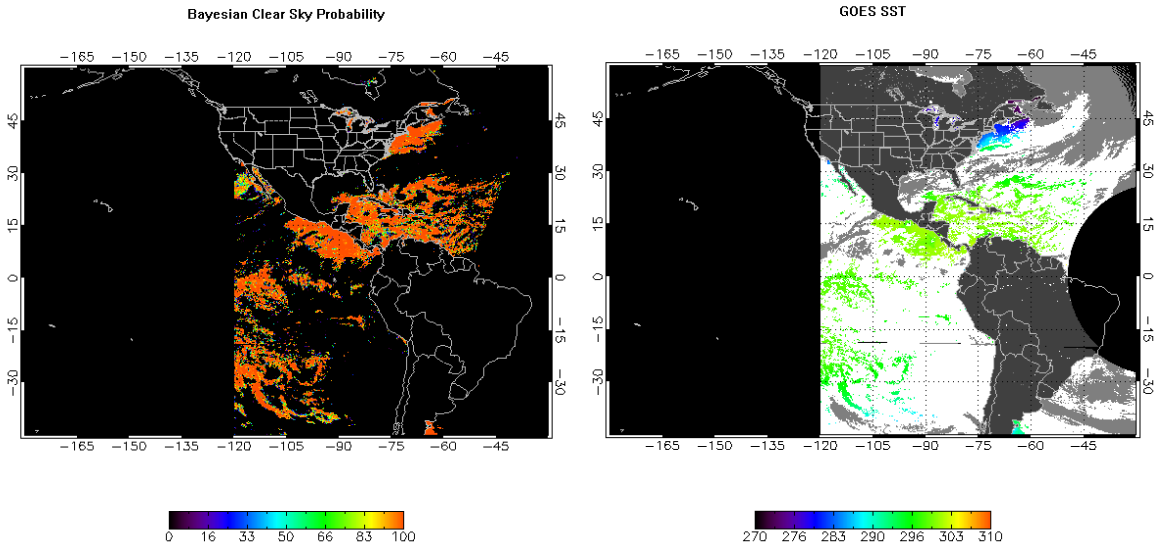

Figure 5.17: GOES-13 SST Imagery (Hourly SST composite with applied 98% clear sky probability (left) and hourly composite clear sky probability)

5.6.2. SST Validation

The comparison of GOES-13 SST with operational GOES-12 SST was performed. Figure 5.18 shows the operational GOES-12 SST validation. Figure 5.19 shows the GOES-13 SST dual-window validation. Figure 5.20 shows the GOES-SST triple-window validation. There are a warm cluster of points where Buoy SST is ~24°C and Satellite SST is ~29°C. Figure 5.21 shows daytime scatter plots. The angular dependence is reduced with triple-window algorithm, also

change in Y-scale for RH plot. Figure 5.22 shows nighttime scatter plots. Since the 13.3 µm band is a lower-tropospheric sounding band, its use at angles above 65° – 70° is inevitably going to be compromised (as shown in the right panel). This increase in warm bias is responsible for the cluster of points noted previously.

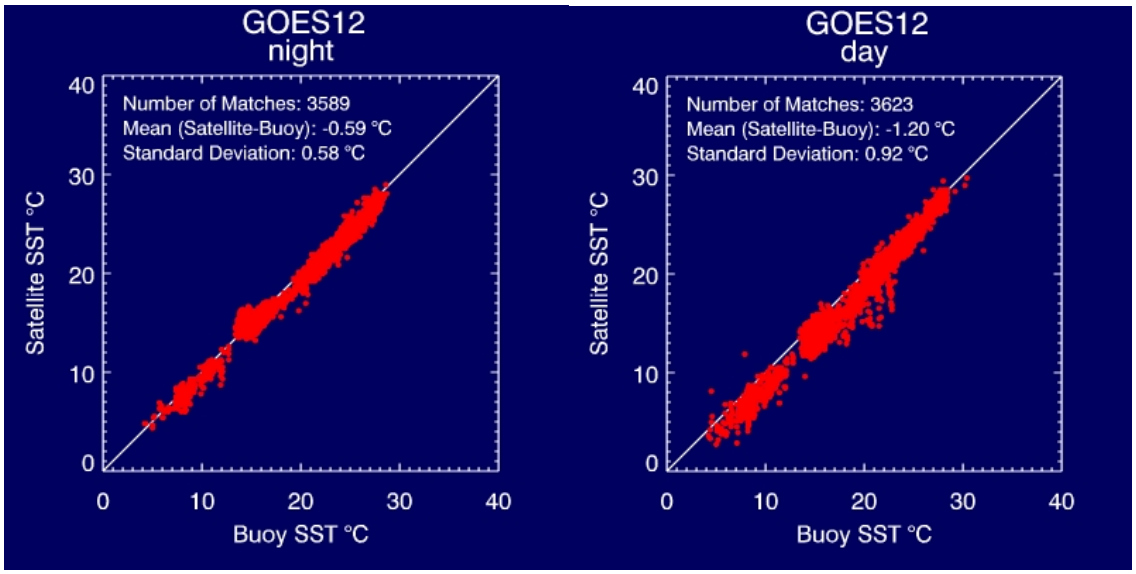

Figure 5.18: GOES-12 SST retrievals vs. Buoys

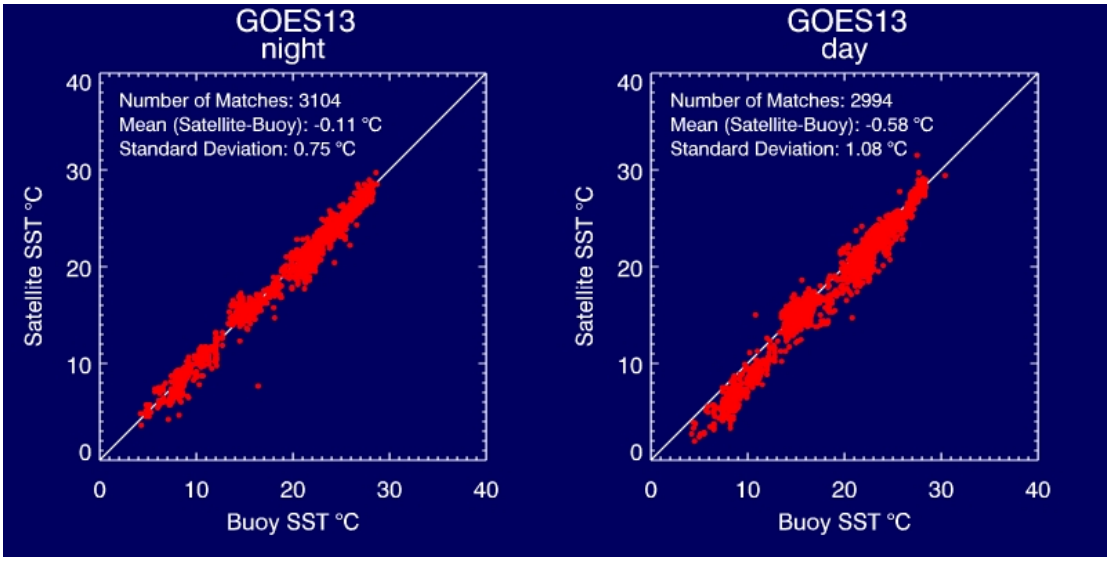

Figure 5.19: GOES-13 SST dual window vs. Buoy SST

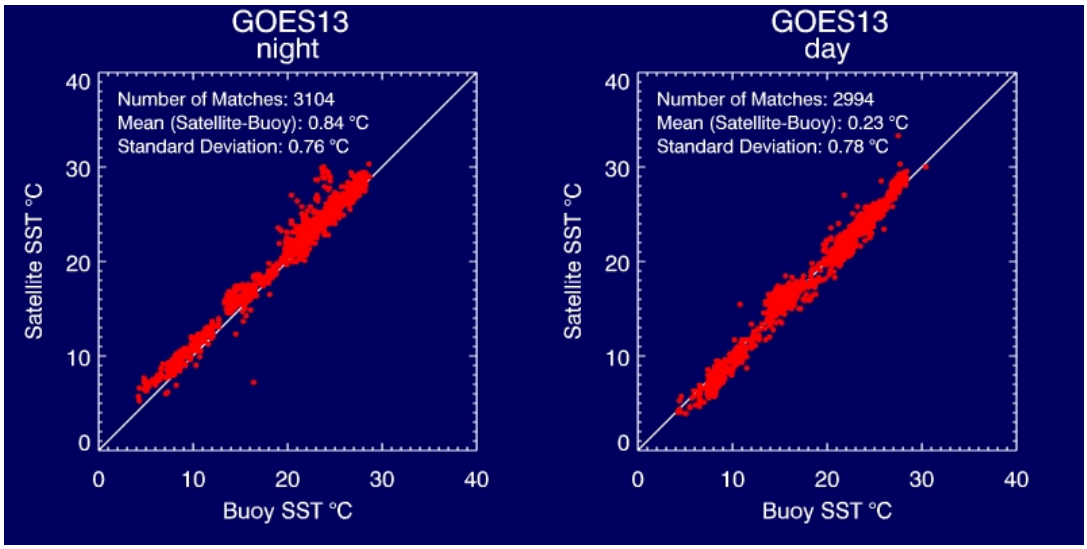

Figure 5.20: GOES-13 SST triple-window vs. Buoy SST.

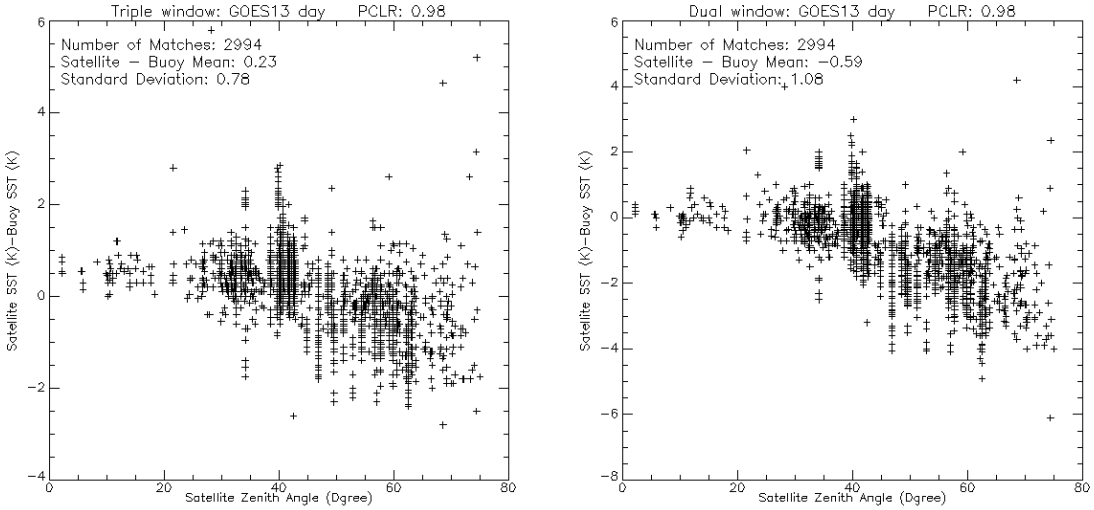

Figure 5.21: GOES-13 Day scatter plots of Satellite – Buoy SST vs. Satellite Zenith Angle for dual window (left) and triple window (right).

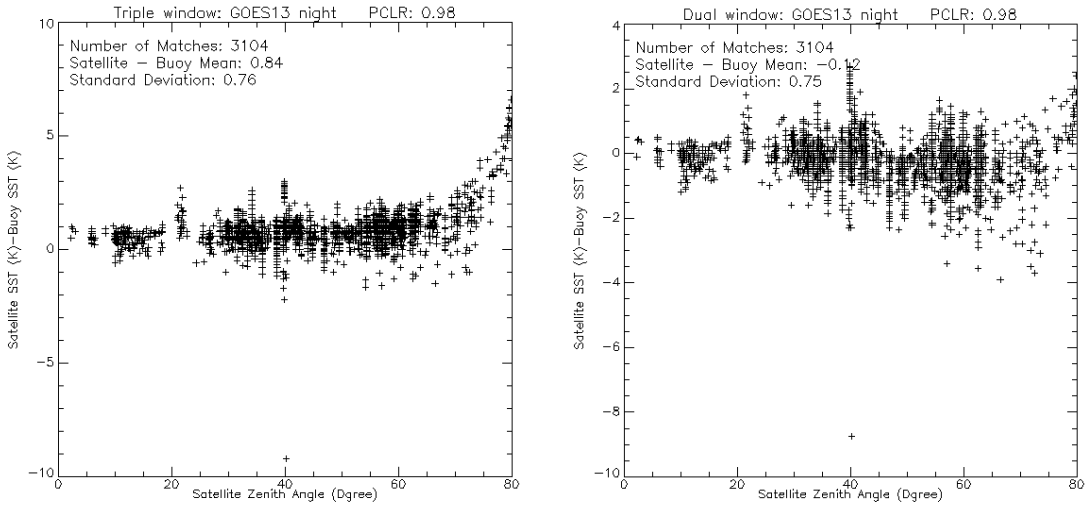

Figure 5.22: GOES-13 Nighttime scatter plots of Satellite – Buoy SST vs. Satellite Zenith Angle for dual window (left) and triple window (right).

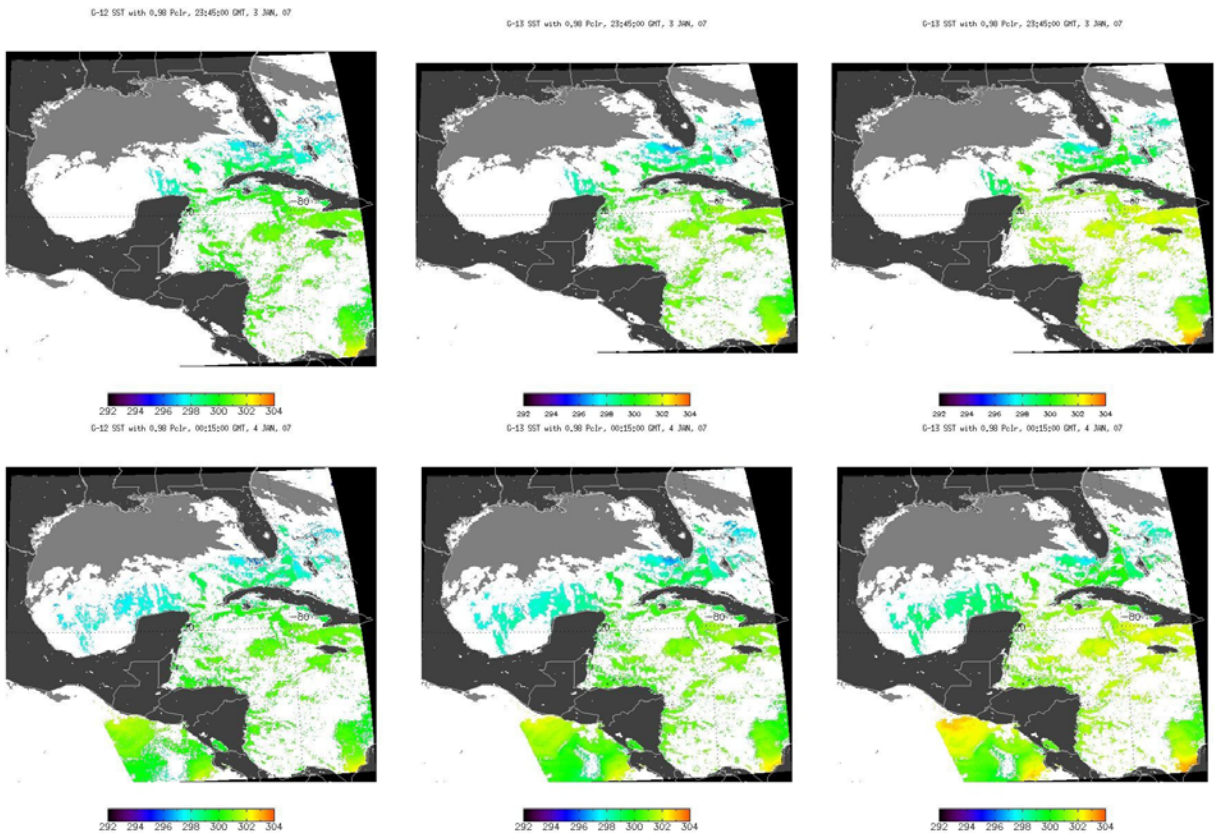

Figure 5.23: Comparisons of GOES-12 SST Imagery with the GOES-13 SST Dual Window and Triple Window for 3 and 4 January 2007.

5.6.3. SST Summary

The GOES-13 SST appears noisier than the GOES-12 SSTs. This may be partially due to the unfavorable view angle conditions for the validation data. The GOES-13 nighttime SST results suggest that 3.9 μm and 11 μm radiances are unbiased compared to the model used to generate the retrieval coefficients. The daytime solar correction appears to be over compensating the 3.9 μm band effects, especially at high satellite angles (colder SSTs). There may be a radiance bias issue in the 13 μm, which happens to compensate for the over-correction of solar contamination – the daytime triple probably looks good because of two opposing biases that occur at high satellite zenith angles. Comparison of the dual window and triple night time plots also suggests that there is some residual cloud that affects the 13 μm band severely but not the 3.9 μm or 11 μm – e.g., thin cirrus. This means that the night-time triple retrieval should not be introduced at night time until the 13 μm is also incorporated into the cloud screening information vector.

In light of the above results, the triple window should be applied in the day. Thin cirrus clouds are more likely to be caught when the visible (band-1) is available.

5.7. Fire Detection

Basic fire detection relies primarily on shortwave window (3.9 μm, band-2) data from the GOES Imager. This band, along with the IR window (11 μm, band-4), provides the basis for locating the fire and other information aids in estimating the sub-pixel fire size and temperature. The number of fires that can be successfully detected and characterized is related to the saturation temperature, or upper limit of the observed brightness temperatures, in the 3.9 μm band. A higher saturation temperature is preferable as it affords a greater opportunity to identify and estimate sub-pixel fire size and temperature. That said, the maximum saturation temperature should still be low enough to the transmitted via the GVAR data stream. Low saturation temperatures can result in the inability to distinguish fires from a hot background in places where the observed brightness temperature meets or exceeds the saturation temperature.

On 08 December 2006 (Day 2 of the GOES-13 post-launch NOAA Science Test), 3.9 μm shortwave IR images from GOES-13 and GOES-12 (Figure 5.24) revealed several “hot spots” (black enhancement) due to fire activity across parts of Arkansas. The performance of the GOES-13 3.9 μm IR band was comparable to that of GOES-12 for this particular group of relatively small and short-lived fires — a plot of the GOES-13 vs. GOES-12 shortwave IR brightness temperatures (Figure 5.25) for the fire that was located between Russellville (KRUE) and Hot Springs (KHOT) Arkansas showed similar values as that particular fire was reaching maximum size and intensity.

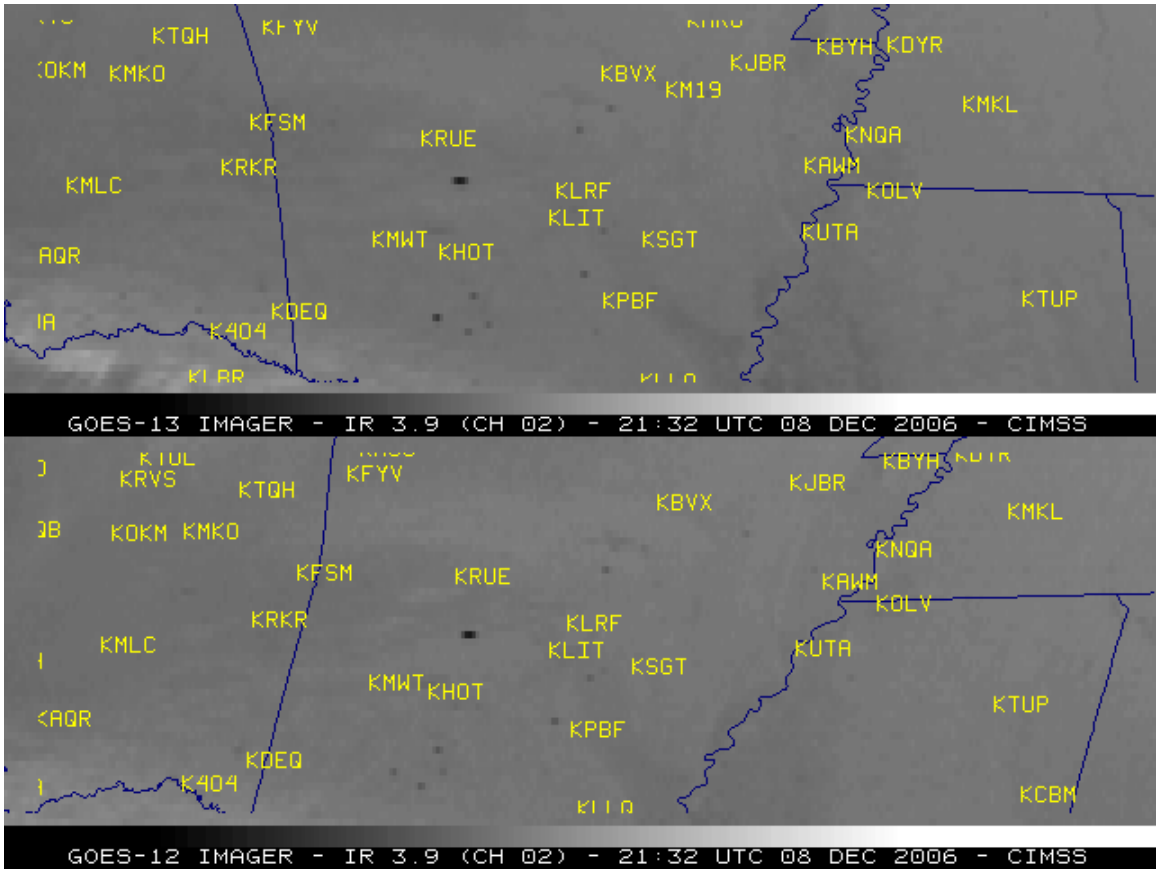

Figure 5.24: GOES Imager 3.9 μm images from GOES-13 (top panel) and GOES-12 (lower panel).

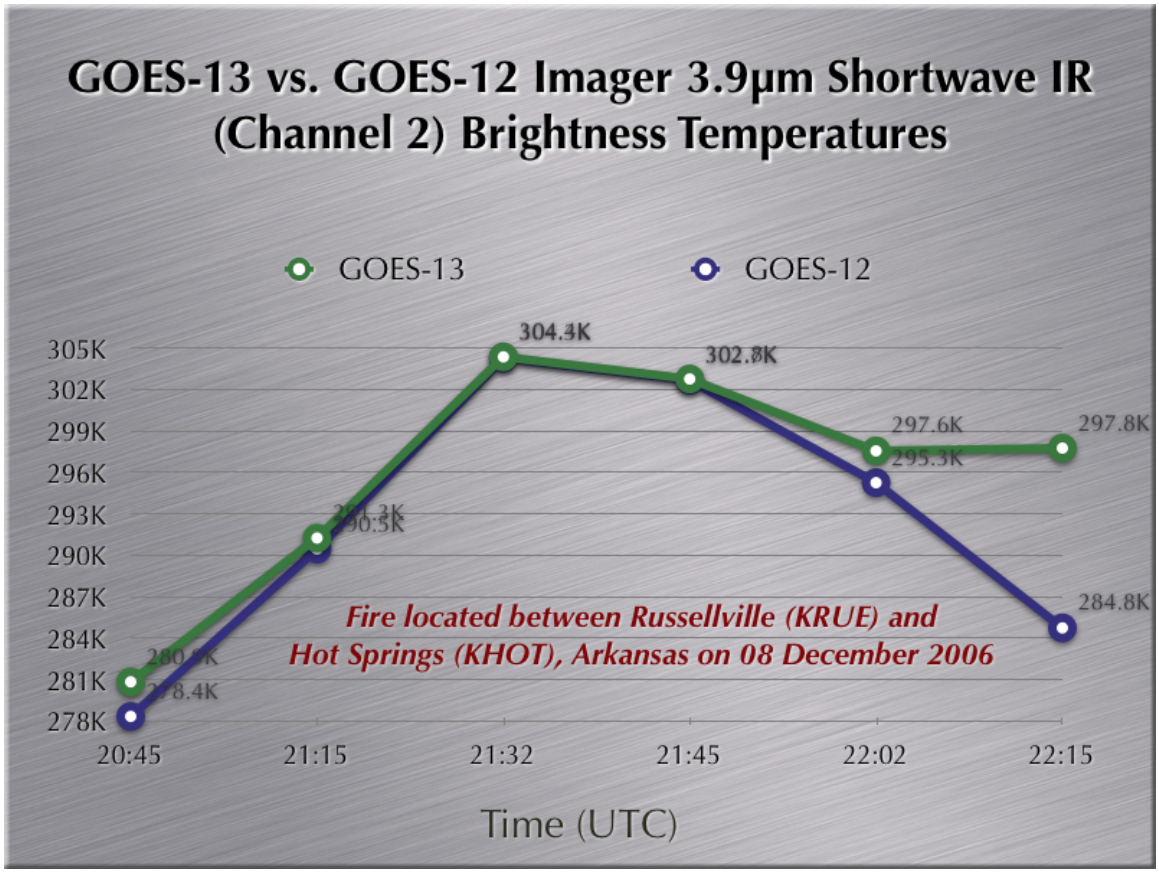

Figure 5.25: GOES Imager 3.9 µm time series from GOES-13 and GOES-12.

The GOES-13 Imager 3.9 µm band has a saturation temperature of approximately 338.5 K. For reference, the GOES-12 Imager 3.9 µm band has a saturation temperature of approximately 336 K, although this value has changed over time, peaking at approximately 342K.

Preliminary indications are that GOES-13 is performing comparably to GOES-12 and much better than GOES-10 insofar as fire detection is concerned.

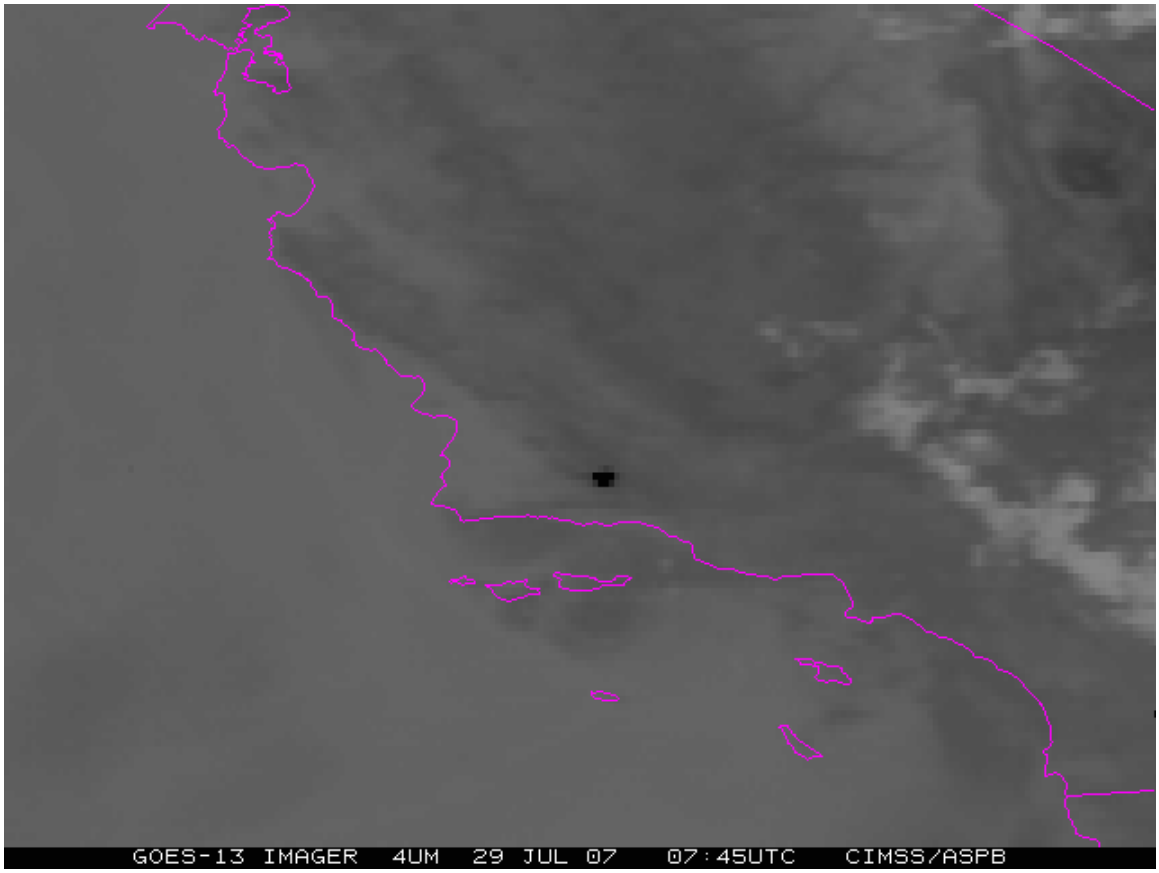

Figure 5.26: Example of GOES-13 Imager 3.9 µm band data while GOES-13 was out of storage during July of 2007.

The Biomass Burning team at CIMSS currently produces fire products for GOES-11/12 covering North and South America. These data can be viewed at the Wildfire Automated Biomass Burning Algorithm page (http://cimss.ssec.wisc.edu/goes/burn/wfabba.html).

5.8. Volcanic Ash Detection

No volcanic ash cases were studied with the GOES-13 during the NOAA Science test. That said, volcanic ash detection from GOES-13 should be comparable or slightly improved (due to the improved SNR) compared to GOES-12. With operations through the eclipse periods, there is the potential for capturing additional events.

5.9. Total Column Ozone

Total Column Ozone (TCO) is an experimental product produced from the GOES Sounder. It is expected to be of similar quality as derived from GOES-13, as GOES-12.

6. Other accomplishments with GOES-13

6.1. GOES-13 Imager Visible (Band-1) Spectral Response

With GOES-13 data (brought out of on-orbit storage for a few weeks of testing and evaluation in July 2007), a comparison of 1 km resolution visible (band-1) imagery from GOES-13 and GOES-12 demonstrates how certain features are more evident with the GOES-13 visible data. For example, the network of cities, towns and highways can be seen in the GOES-13 visible (band-1) image, especially across northwestern Iowa and southwestern Minnesota — these towns and roads show up due to the contrast between the higher albedo of the towns and road surfaces (and the adjacent ditches/medians) and the lower albedo of the surrounding fields of dense, mature corn crops. These features were less apparent in the GOES-12 visible image, in part to the on-orbit visible degradation and in part to the differing SRFs (more reflection from the vegetated surfaces). For example, note that the GOES-12 will acquire more energy from vegetated surfaces, this will tend to reduce the image contrast between vegetation and the already brighter non-vegetated surfaces.

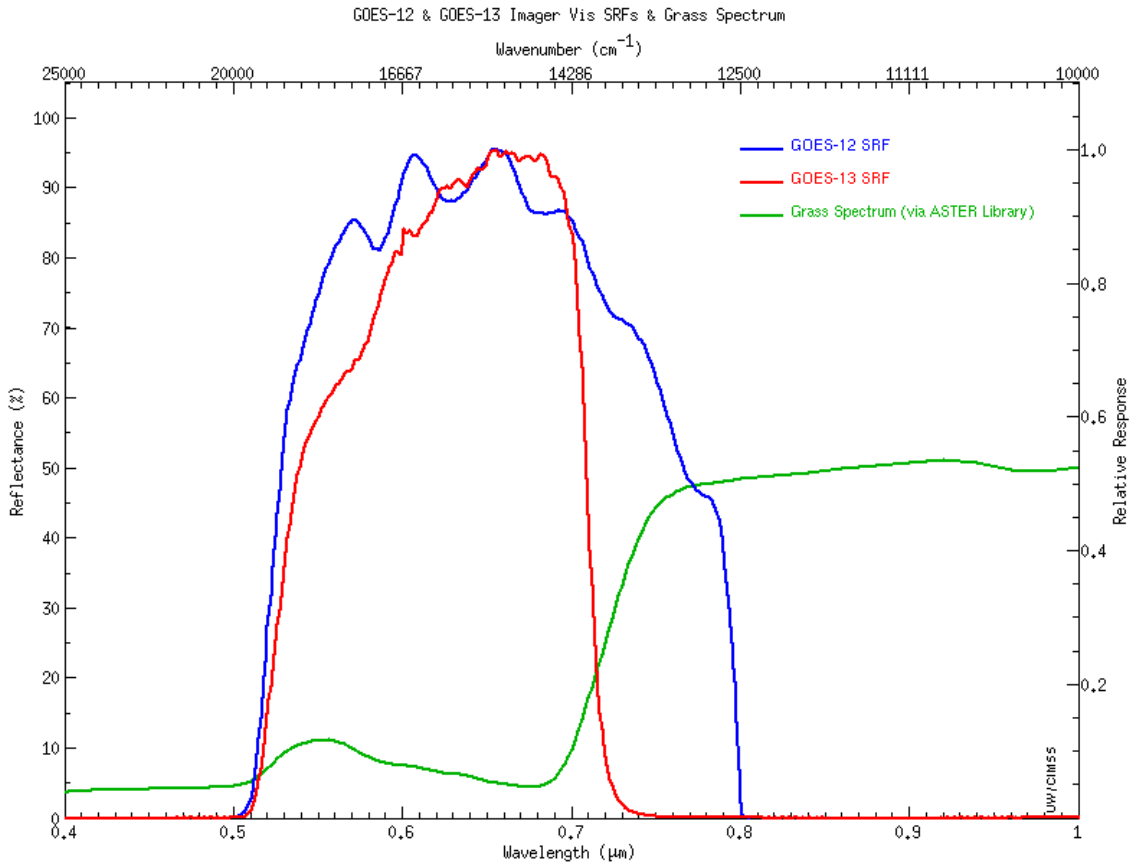

Figure 6.1: GOES-12 (blue) and GOES-13 (red) Imager visible (0.7 µm) band SRFs, with a representative spectrum for grass over-plotted (green).

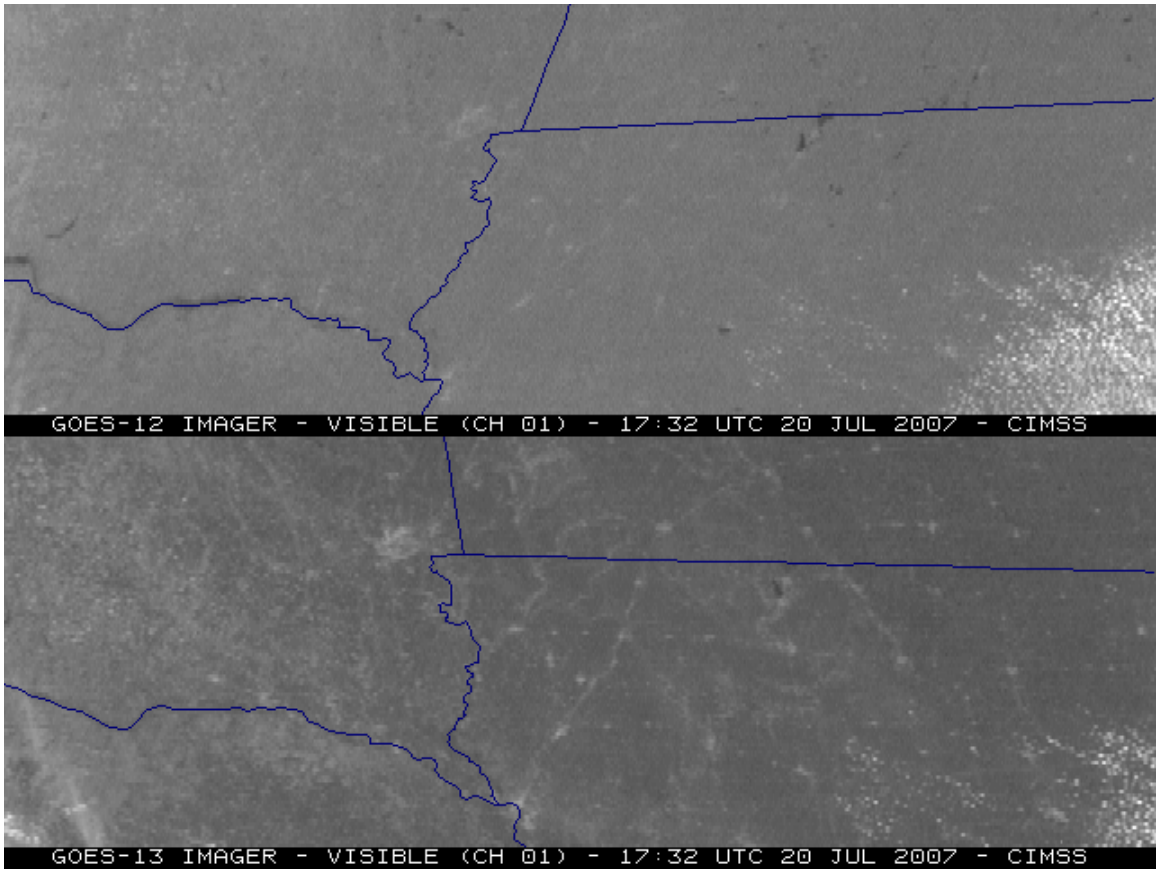

Figure 6.2: Comparison of the visible (0.7 µm) imagery from GOES-12 and GOES-13 (20 July 2007) demonstrates how certain features are more evident with the GOES-13 visible data. For example, the network of cities, towns and highways can be seen in the GOES-13 visible image, especially across northwestern Iowa and southwestern Minnesota.

More information on this case can be found at:
http://cimss.ssec.wisc.edu/goes/blog/2007/07/20/goes-13-vs-goes-12-visible-channel/

6.2. Lunar calibration

Several GEOS-13 Imager datasets were acquired during the PLT. The main objective of these tests was to observe the lunar images as soon as possible in order to establish a baseline for future study of instrument degradation. While not intended, lunar images may allow an attempt on absolute calibration, although this has not been researched.

Figure 6.3: GOES-13 Imager visible (0.7 µm) band image of the moon from 14 July 2006 for a scan that started at 20:41 UTC.

6.3. Over-sampling Test

One of the Science Tests was intended to simulate GOES-R ABI-like (2 km) spatial resolution data. Data for this test were gathered from four different sectors at different times during the day. For each sector thee successive images were taken in rapid succession, in order to minimize any changes between the images, but with the scan lines offset by a half of the normal (4 km) distance between image lines. It was then hoped that this over-sampled data could be de-convolved to produce imagery at 2 km resolution similar to that to be available from ABI.

Unfortunately, the data collector for this test failed to be line shifted between successive images, a fact that was not discovered until the Science Test had concluded and there was not time for redoing the test. The result was no usable data for simulating ABI spatial resolution at 2 km spatial resolution. A similar test was undertaken with GOES-12, but failed for other reasons. Therefore, this test will hopefully be repeated during the Science Test for either GOES-O or GOES-P or both.

6.4. The Effect of Satellite Temporal Resolution on IR Cooling Rate

During the GOES-13 Science Test, Super-Rapid Scan Operation (SRSO) was called on several different days. On 12 December 2006, 30-second data was collected over the southeast U.S., and on 13 December 2006, 1-minute data was collected over central Argentina. This high temporal resolution allows the calculation of 10.7 µm brightness temperature cooling rates and compare them to rates with lower sampling frequency.

6.4.1. Non-severe convection over southern Mississippi

Figure 6.4 shows four band-4 (10.7 µm) images from 12 December 2007. Between 1639 - 1740 UTC, a storm in southern Mississippi was growing (shown by the black box in each of the 4 panels), and its brightness temperatures were cooling.

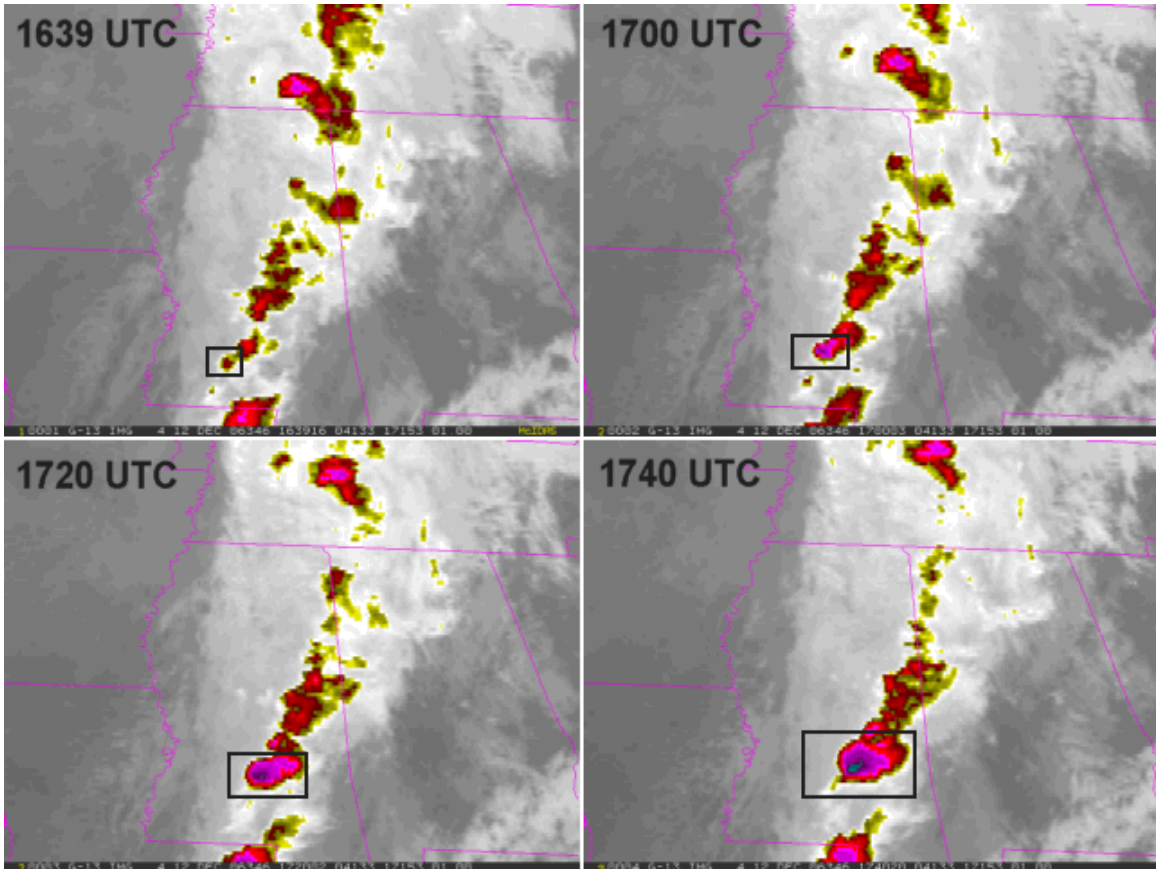

Figure 6.4: Band-4 (10.7 µm) images at 4 different times from GOES-13 on 12 December 2007. The black box in each image shows the storm which is analyzed in Figure 6.5.

Thirty-second imagery was collected nearly continuously during the period shown in Figure 6.4. Figure 6.5 shows the time evolution of the 10.7 µm brightness temperature rate of change, for 3 different sampling rates: 30-seconds, 5-minutes, and 15-minutes. As the storm was undergoing its most rapid growth (1639 - 1700 UTC), the 30-second data was able to capture a cooling rate

of 2.25 K per minute, while the maximum 5-minute data cooling rate was 1.4 K per minute, and the maximum 15-minute data cooling rate was about 0.2 K per minute.

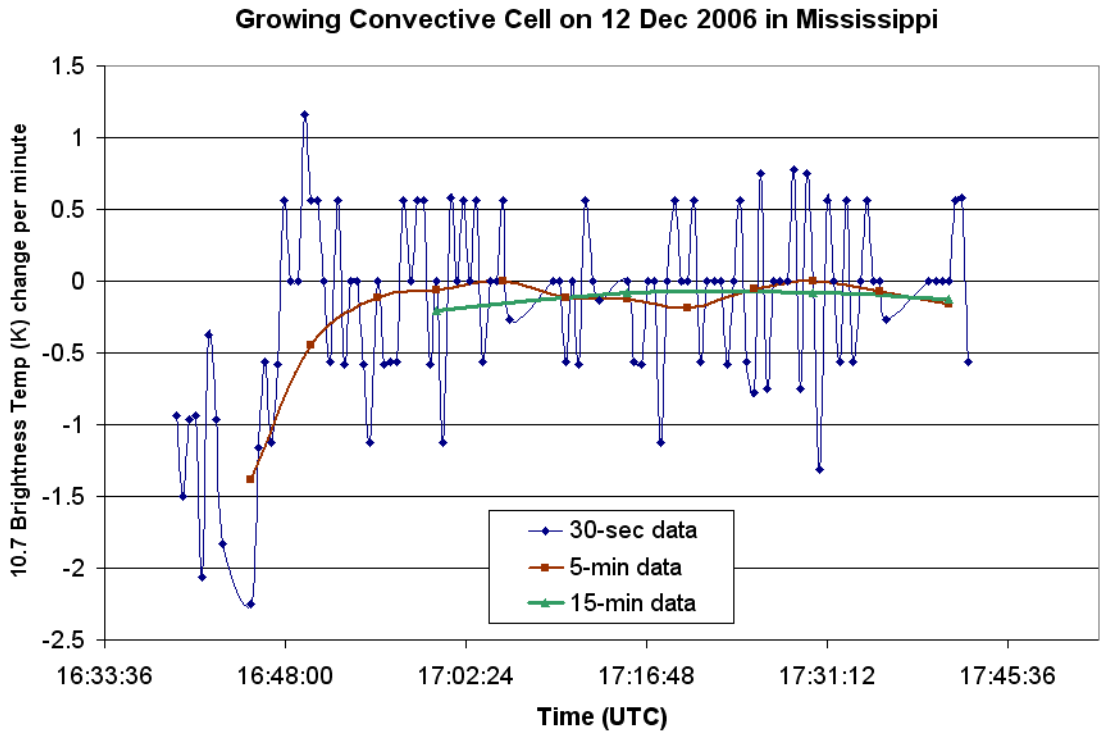

Figure 6.5: 10.7 µm brightness temperature (K) change per minute for the storm identified in Figure 6.4, for 3 different satellite sampling rates: 30-seconds, 5-minutes, and 15-minutes. The plotted value shows the rate for the previous 30-seconds, 5-minutes, or 15-minutes, so the first 15-minute value was not available until 1655 UTC.

6.4.2. Strong convection over central Argentina

A similar analysis was performed on 13 December 2006 over central Argentina, except we captured 1-minute data instead of 30-second data. Figure 6.6 shows a 4-panel IR image, and Figure 6.7 shows the various cooling rates during the 1.5 hour period from 2030 - 2157 UTC. In this case, the rapidly growing convective cell has a maximum cooling rate of 2.6 K per minute using the 1-minute sampling rate, and only 1.1 K per minute using the 5-minute data and 0.75 K per minute using the 15-minute data.

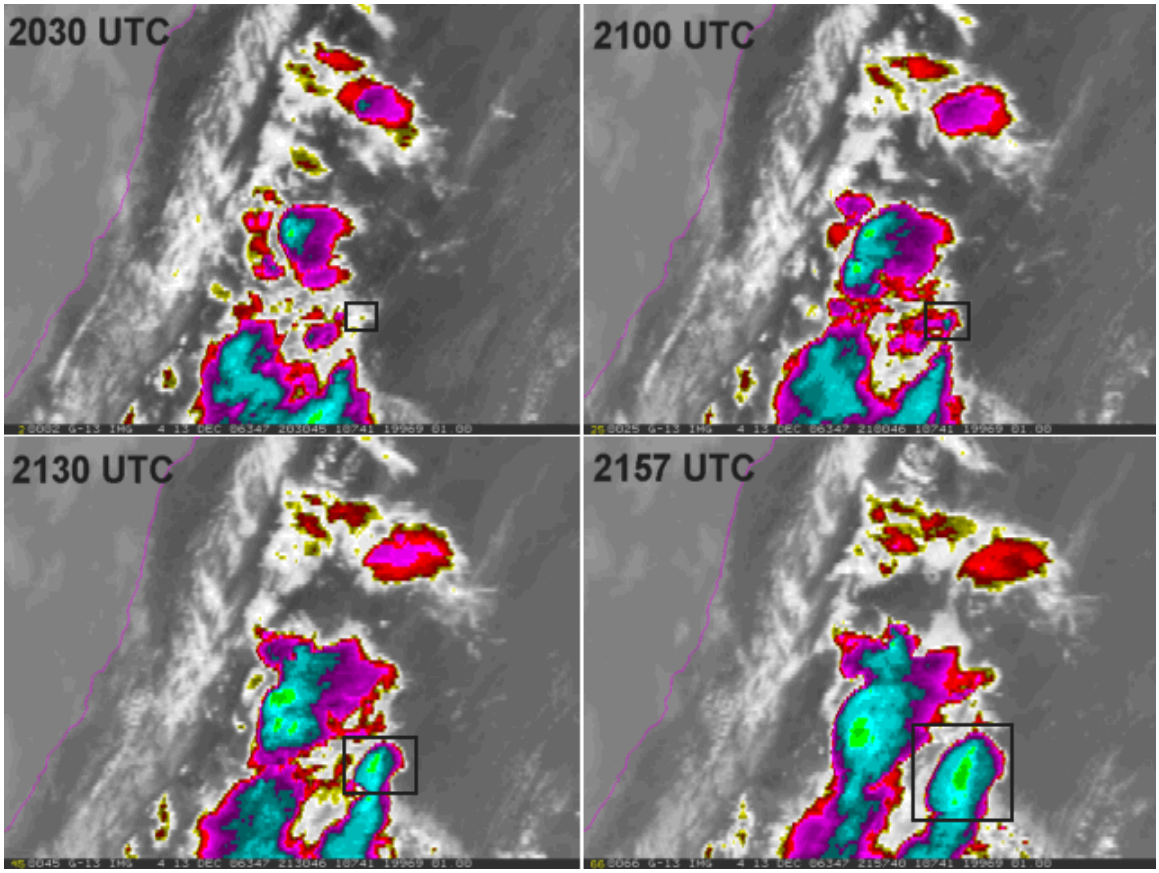

Figure 6.6: Same as Figure 6.4, except over central Argentina on 13 December 2006.

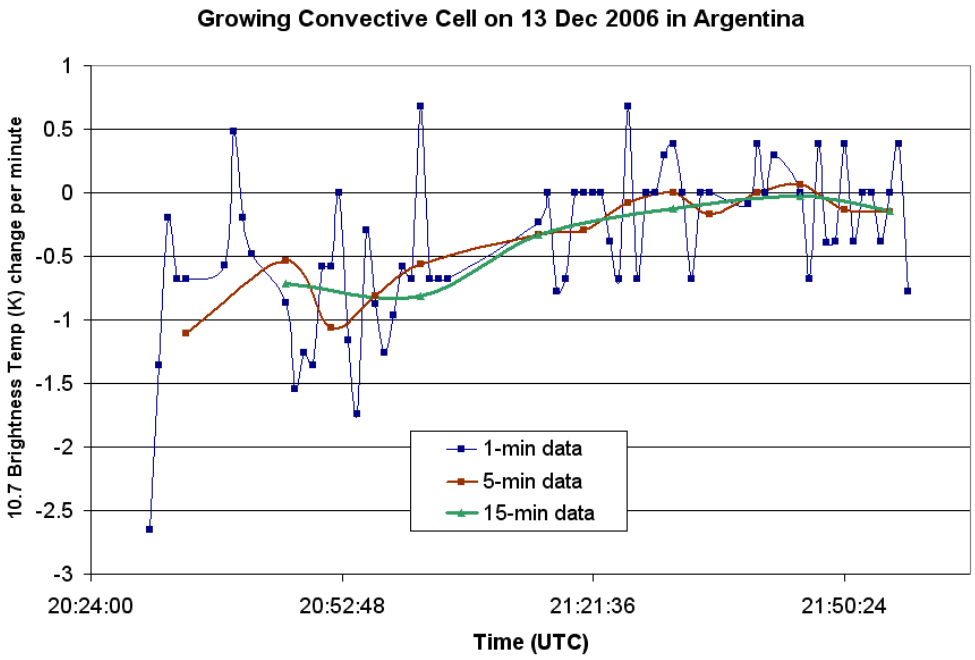

Figure 6.7: Same as Figure 6.5, except for the storm indicated in Figure 6.6.

The analysis above shows that active convection, both severe and non-severe, changes on time scales shorter than every 5 minutes, and in some cases shorter than every minute. Our current series of satellites collect routine 15-minute data, but sample more rapidly during Rapid Scan Operation (one image every 5-8 minutes). The GOES-R series, scheduled for launch in 2014, will routinely capture 5-minute data, and its RSO will be able to obtain 30-second data. Cooling rates observed with GOES-R will likely be even greater than the examples above since improved spatial resolution allows the detection of smaller-scale overshooting tops. This analysis has shown that such high resolution satellite data is necessary to adequately calculate the IR cooling rate of thunderstorms.

6.5. Coordination with University of Alabama/Huntsville

Throughout the GOES-13 Science Test in December 2006, NOAA Science Team members coordinated with researchers from the NASA-MSFC SPoRT Center and the University of Alabama/Huntsville (UAH) THOR Center/Hazardous Weather Testbed. The goal was to capture high resolution satellite imagery (30-seconds) to compare with ground-based polarimetric radar and VHF total lightning data from Huntsville. Since the Science Test occurred in December 2006, widespread convection was barely observed in the U.S., but on 12 December 2006, there was a threat for some weak convection in the Southeast associated with an approaching cold front. After speaking with UAH/NASA researchers, we decided to call for 30-second imagery centered over Huntsville, in hopes that thunderstorms would indeed develop over the area.

Figure 6.8 shows a 10.7 µm satellite image from 2057 UTC on 12 December 2006. There was active convection, but most of it was confined to the southern half of Alabama. No lightning was observed within the coverage area of the 3-D VHF Lightning Mapping Array.

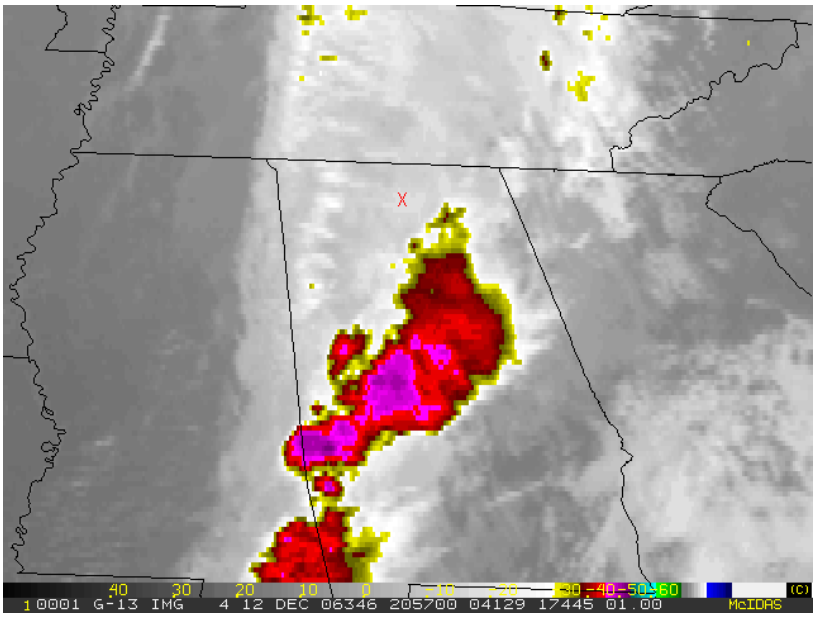

Figure 6.8: GOES-13 10.7 µm image from 2057 UTC on 12 December 2006. The red "X" in northern Alabama denotes the location of Huntsville.

However, coincident with the rapid scanning, another very interesting feature was captured by the UAH ARMOR polarimetric radar. Figure 6.9 shows the radar reflectivity (top) and radial velocity (bottom) at 2058 UTC. It is believed that the northeast/southwest oriented line of enhanced reflectivity and with large gradients in radial velocity was caused by an undular bore. Figure 6.10 shows a radar cross-section of differential reflectivity (ZDR). The radar bright band (melting level) shows up as a zone of increased positive ZDR value, and is located at approximately the same height, except for an abrupt change in elevation at the location of the bore. Close examination of the 30-second satellite data did not reveal any indication of the bore or its attendant influence on the precipitation bands. There appeared to be two decks of clouds, the topmost layer possibly obscuring a cloud-top bore signature in the lower deck.

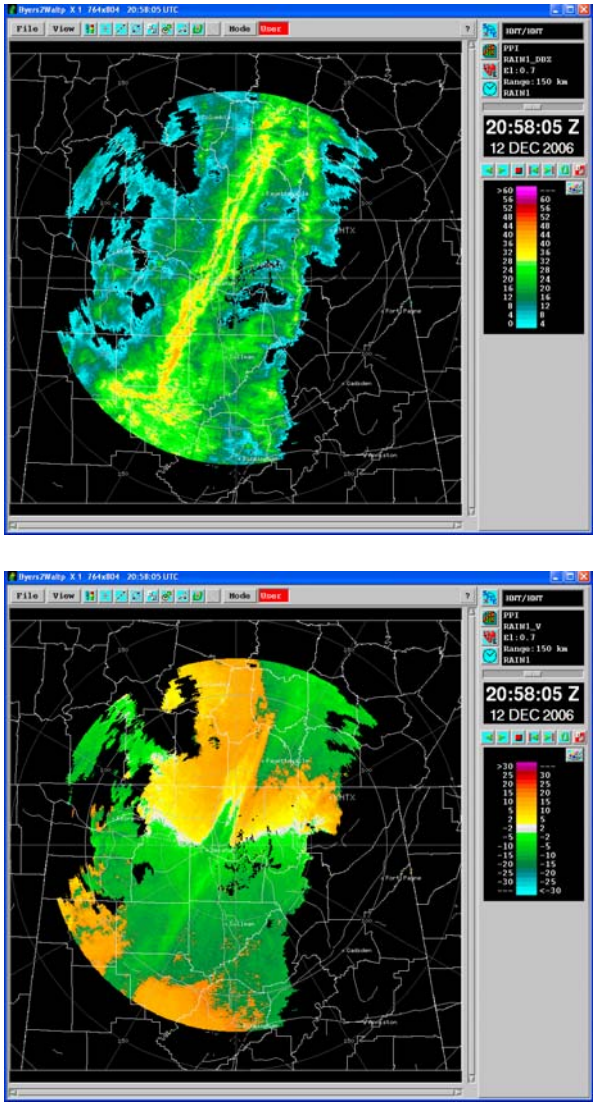

Figure 6.9: Reflectivity (top) and radial velocity (bottom) from the HNT radar on 12 December 2007 at 2058 UTC.

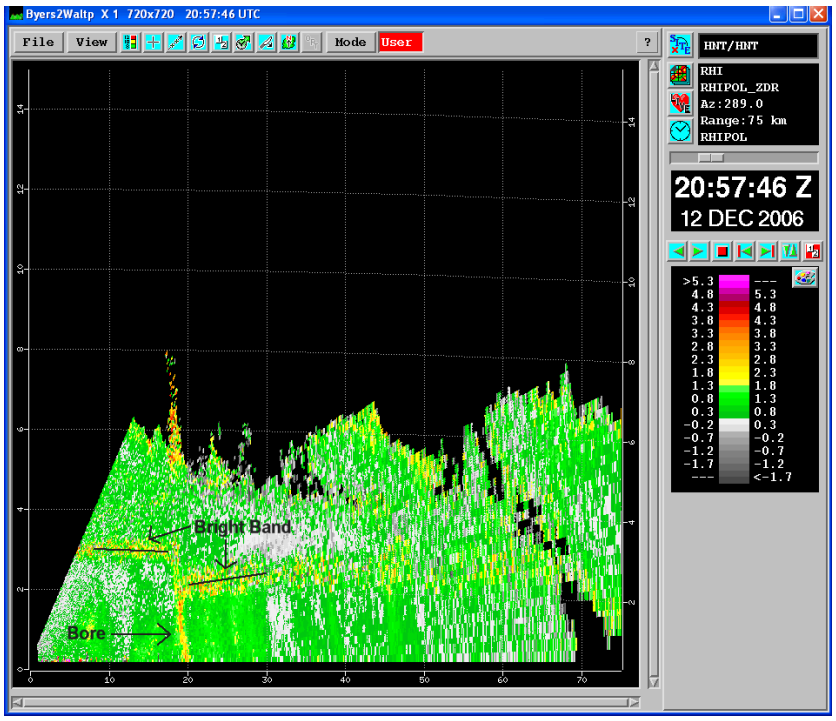

Figure 6.10: RHI scan of differential reflectivity (ZDR) from the HNT radar on 12 December 2007 at 2058 UTC. Location of an undular bore and the radar bright band is indicated.

6.6. VISITview

A GOES-N pre-launch overview VISITview training module has been developed and posted at: ftp://ftp.ssec.wisc.edu/visit/goes_n_audio_2006.zip This module contains audio as well.

6.7. Improved Image Registrations

6.7.1. Wildfire in Upper Peninsula of Michigan

An animation (http://cimss.ssec.wisc.edu/goes/blog/2007/08/03/wildfire-in-the-upper-peninsula-of-michigan/) of GOES-12 (upper two panels) and GOES-13 (lower two panels) visible channel and 3.9 μm IR images shows a smoke plume *(drifting southeastward)* and "hot spots" *(black IR pixels)* associated with a large wildfire burning in the eastern Upper Peninsula of Michigan on 3 August 2007. Note the improvement in image navigation and registration (INR) that is evident with the GOES-13 satellite: the coastline features and the fire hot spots remain fairly steady from image to image, compared to the GOES-12 images which exhibit a good deal of "wobble" in the animation.

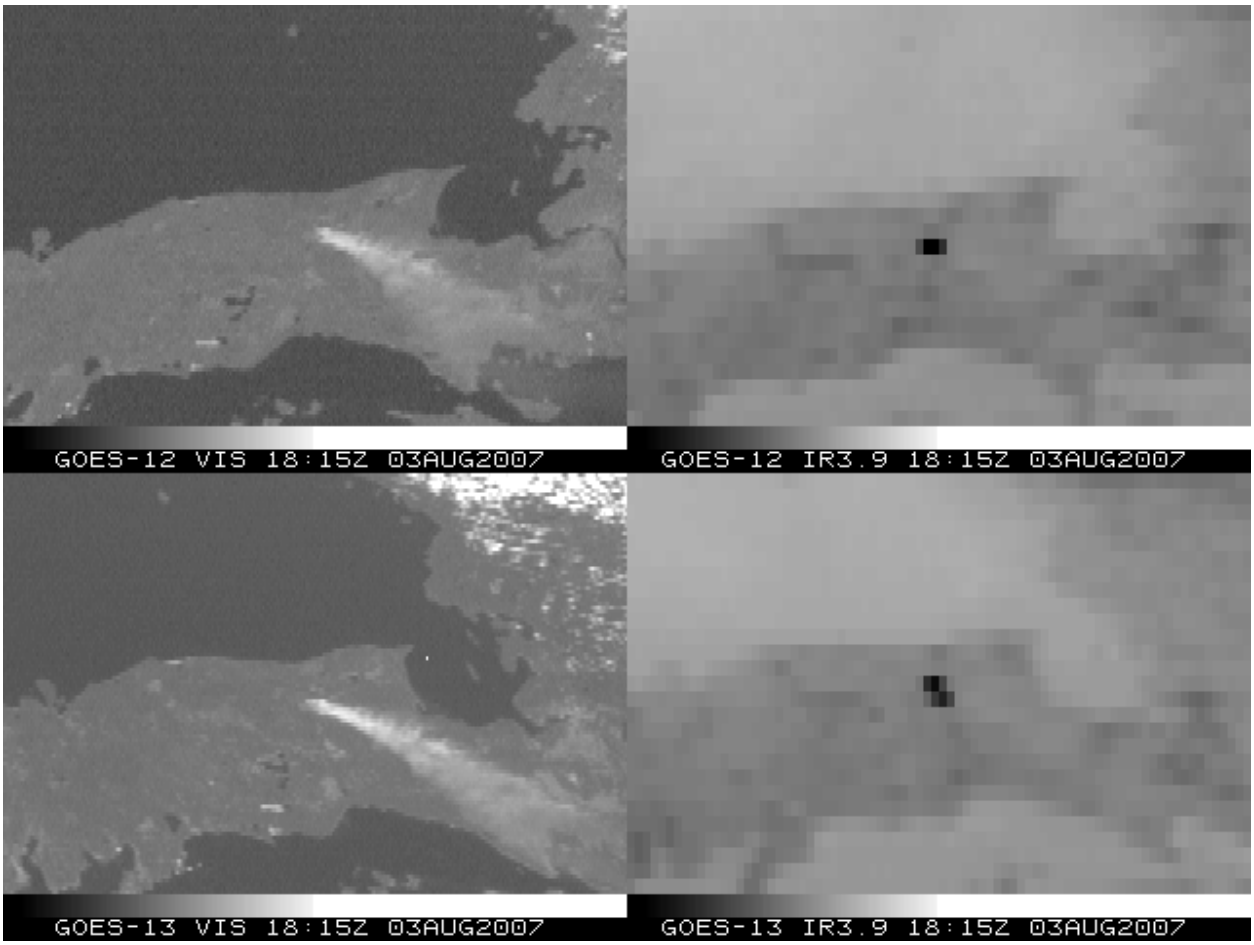

Figure 6.11: GOES-12 (upper two panels) and GOES-13 (lower two panels) visible channel and 3.9 μm IR images shows a smoke plume (drifting to the southeast) and "hot spots" (black IR pixels) associated with a large wildfire burning in the eastern Upper Peninsula of Michigan on 3 August 2007.

6.7.2. Ice floes in Hudson Bay

A comparison of GOES-13 and GOES-12 visible channel images (http://cimss.ssec.wisc.edu/goes/blog/2007/07/30/cold-water-eddies-in-hudson-bay/) better showed the motion of these ice floes during the 6-hour period from 1402-2015 UTC. Note the improved image navigation and registration (INR) evident with the GOES-13 satellite: the coastline and island features remain fairly steady from image to image, in contrast with the GOES-12 images which exhibit a notable amount of "wobble" in the animation.

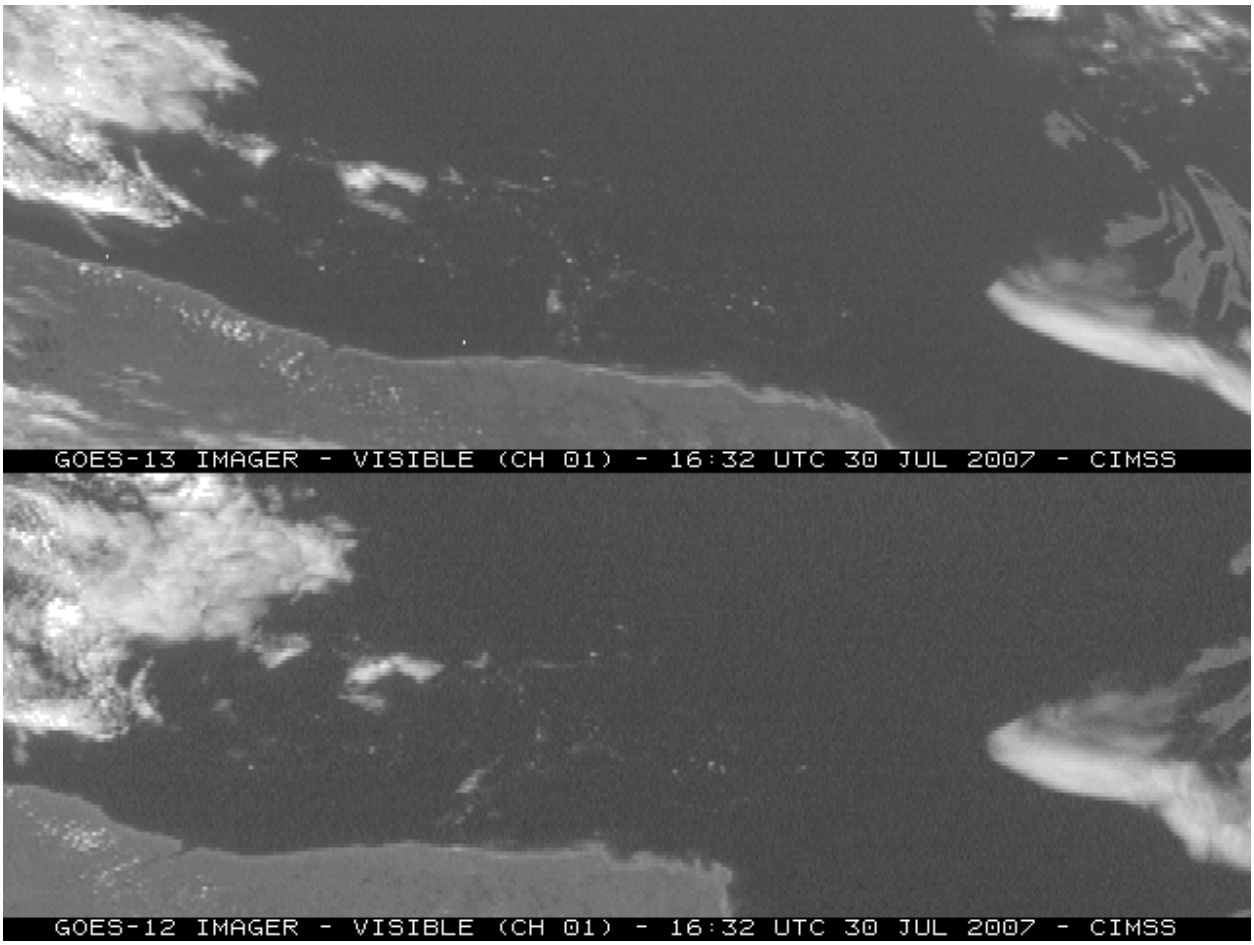

Figure 6.12: GOES-13 and GOES-12 visible channel images shows several small ice floes that were moving slowly west/northwestward across the southern portion of Hudson Bay, Canada on 30 July 2007.

7. Recommendations for Future Science Tests

The following conclusions and recommendations were drawn during the GOES-13 Science Test:

- Science Tests should continue as a vital aspect of the checkout of each GOES satellite, as this was found to be a way to detect problems both in the data and in the ground system.

- Science Test duration should be at least 4 weeks and ideally should be in times of the year with active convention over the continental U.S.

- An additional aspect to the Science Test would involve yearly checkout of GOES data when individual spacecraft are taken out of storage and turned on.

- While the GOES-13 GVAR data stream are captured and saved by a number of research groups, these unique and important pre-operational data should find there way into the official GOES archive.

Acknowledgments

A large number of people played important roles in the success of the GOES-13 Science Test. The contributors listed on the front cover of this report provided analysis of GOES-13 data and Imager and Sounder products. Dan Lindsey and John Knaff (StAR/RAMMB), Gary Wade (StAR/ASPB), and Scott Bachmeier (UW/CIMSS) are specially thanked for their participation in the daily coordination where decisions were made to determine which GOES-13 schedule would be implemented in order to capture the weather event(s) of the day. In addition, thanks to Kevin Ludlum (GOES Scheduling Lead), John Tusi (GOES Engineering) and the rest of the GOES-13 Team at NOAA/NESDIS/OSO (Office of Satellite Operations), for coordinating and establishing the numerous GOES-13 schedules and sectors used during the Science Test. These various schedules provided the capability to capture a variety of different weather events with different time and spatial scales.

This project funded by the NOAA/NESDIS Office of Systems Development (OSD).

The views, opinions, and findings contained in this article are those of the authors and should not be construed as an official National Oceanic and Atmospheric Administration or U.S. Government position, policy, or decision.

References

Daniels, J.M., T.J. Schmit, and D.W. Hillger, 2001: Imager and Sounder Radiance and Product Validations for the GOES-11 Science Test, *NOAA Technical Report NESDIS 103*, (August), 49 pp.

Daniels, J., R. Scofield, G. Ellrod, R. Kuligowski, D.W. Hillger, T.J. Schmit, W. Bresky, J.C. Davenport, and A.J. Schreiner, 2006: Validation of GOES-N Imager data and products during the GOES-N Science Test, *14th Conf. Sat. Meteor. Ocean.*, AMS, 29 January – 3 February, Atlanta GA, 5 pp.

Gunshor, M.M.; T.J. Schmit, W.P. Menzel, and D.C. Tobin, 2006: Intercalibration of the newest geostationary imagers via high spectral resolution AIRS data. *14th Conf. Sat. Meteor. Ocean.*, AMS, Atlanta, GA, 29 January-2 February 2006 (preprints). AMS, Atlanta GA, Paper P6.13.

Hillger, D.W., T.J. Schmit, and J.M. Daniels, 2003: Imager and Sounder Radiance and Product Validation for the GOES-12 Science Test. *NOAA Technical Report, NESDIS 115*, (September), 70 p.

Hillger, D.W., and T.H. Vonder Haar, 1988: Estimating Noise Levels of Remotely Sensed Measurements from Satellites Using Spatial Structure Analysis. *J. Atmos. Oceanic Technol.*, **5**, 206-214.

Hillger, D.W., T.J. Schmit, D. Lindsey, J. Knaff, and J. Daniels, 2006: An overview of the GOES-N Science Test, *14th Conf. Sat. Meteor. Ocean.*, AMS, 29 January – 3 February, Atlanta GA, 6 pp.

Hillger, D.W., and T.J. Schmit, 2007: An overview of the GOES-13 Science Test, *Third Symposium on Future National Operational Environmental Satellites*, AMS, 14-18 January, San Antonio TX, 17 pp. On-line: http://rammb.cira.colostate.edu/projects/goes_n/GOES-13_Overview_AMS_2007.pdf

Ma, X. L., T. Schmit, and W.L. Smith, 1999: A non-linear physical retrieval algorithm - its application to the GOES-8/9 sounder. *J. Appl. Meteor.*, **38**, 501-513.

Menzel, W.P., F.C. Holt, T.J. Schmit, R.M. Aune, G.S. Wade, D.G. Gray, and A.J. Schreiner, 1998: Application of GOES-8/9 Soundings to weather forecasting and nowcasting. *Bull. Amer. Meteor. Soc.*, **79**, 2059-2078.

Merchant, C.J., A.R. Harris, E. Maturi, and S. MacCallum, 2005, Probabilistic physically-based cloud-screening of satellite infrared imagery for operational sea surface temperature retrieval. *Quart. J. Roy. Meteorol. Soc.*, **131**(611), 2735-2755.

Schmit, T.J., E.M. Prins, A.J. Schreiner, and J.J. Gurka, 2002a: Introducing the GOES-M imager. *Nat. Wea. Assoc. Digest*, **25**, 2-10.

Schmit, T.J., W.F. Feltz, W.P. Menzel, J. Jung, A.P. Noel, J.N. Heil, J.P. Nelson III, G.S. Wade, 2002b: Validation and Use of GOES Sounder Moisture Information. *Wea. Forecasting,* **17**, 139-154.

Schmit, T.J., G.S. Wade, M.M. Gunshor, J.P. Nelson III, A.J. Schreiner, J. Li, J. Daniels, and D.W. Hillger, 2006: The GOES-N Sounder Data and Products, *14th Conf. Sat. Meteor. Ocean.*, AMS, 29 January – 3 February, Atlanta GA, 6 pp.

Weinreb, M.P., M. Jamison, N. Fulton, Y. Chen, J.X. Johnson, J. Bremer, C. Smith, and J. Baucom, 1997: Operational calibration of Geostationary Operational Environmental Satellite-8 and -9 Imagers and Sounders. *Appl. Opt.*, **36**, 6895-6904.

Appendix A: Web Sites Related to the GOES-13 Science Test

GOES-13 NOAA/Science Post Launch Test page:
http://rammb.cira.colostate.edu/projects/goes_n/

GOES-13 RAMSDIS Online: http://rammb.cira.colostate.edu/ramsdis/online/goes-13.asp
(contained realtime GOES-13 imagery and product during the Science Test)

CIMSS Satellite Blog: Archive for the 'GOES-13' Category:
http://cimss.ssec.wisc.edu/goes/blog/category/goes-13/

CIMSS GOES Realtime Derived Products: http://cimss.ssec.wisc.edu/goes/rt/ (included GOES-13 products during the Science Test)

CIMSS: GOES-13 Science Test: http://cimss.ssec.wisc.edu/goes/g13_report/

CIMSS-derived Planck Coefficients for the Band-averaged Imager and Sounder:
http://cimss.ssec.wisc.edu/goes/calibration/PFC/sndimg13.pfc

NESDIS/StAR: GOES-13 Post Launch Test:
http://www.orbit.nesdis.noaa.gov/smcd/spb/fwu/solar_cal/GOES13_PLT/index.html

NASA GSFC: GOES N DataBook: http://goes.gsfc.nasa.gov/text/goes.databookn.html or http://goes.gsfc.nasa.gov/text/GOES-N_Databook/databook.pdf (Dated: 2006 April 26)

NASA/GSFC, NOAA/NESDIS booklet: GOES-N,O,P - The Next Generation:
http://www.osd.noaa.gov/GOES/GOES_NQBooklet.pdf (Dated: 2005 April)

Boeing: GOES N, O, P: http://www.boeing.com/defense-space/space/bss/factsheets/601/goes_nopq/goes_nopq.html (Dated: 2005 May)

Appendix B: Acronyms Used in this Report

ABI	Advanced Baseline Imager (GOES-R)
AIRS	Atmospheric InfraRed Sounder
AMV	Atmospheric Motion Vector
ASPB	Advanced Satellite Products Branch
CICS	Cooperative Institute for Climate Studies
CIMSS	Cooperative Institute for Meteorological Satellite Studies
CIRA	Cooperative Institute for Research in the Atmosphere
CONUS	Continental United States
CRTM	Community Radiative Transfer Model
CSBT	Clear Sky Brightness Temperature
CSU	Colorado State University
DPI	Derived Product Image
FOV	Field Of View
GOES	Geostationary Operational Environmental Satellite
GOES-R	Next generation GOES, starting with GOES-R
GVAR	GOES Variable (data format)
hPa	Hectopascals (equivalent to *millibars* in non-SI terminology)
INR	Image Navigation and Registration
IR	InfraRed
KOZ	Keep Out Zone
LI	Lifted Index
LW	Longwave
LWIR	LongWave InfraRed
McIDAS	Man-Computer Interactive Data Access System
MSFC	Marshall Space Flight Center
NASA	National Aeronautics and Space Administration
NEdR	Noise Equivalent delta Radiance
NESDIS	National Environmental Satellite, Data, and Information Service
NSSTC	National Space Science and Technology Center
NOAA	National Oceanic and Atmospheric Administration
OPDB	Operational Products Development Branch

ORA	Office of Research and Applications (now StAR)
OSDPD	Office of Satellite Data Processing and Distribution
OSO	Office of Satellite Operations
PLT	Post Launch Test
PW	Precipitable Water
RAMMB	Regional and Mesoscale Meteorology Branch
RAMSDIS	RAMM Advanced Meteorological Satellite Demonstration and Interpretation System
RAOB	Radiosonde Observation
RMS	Root Mean Square
RSO	Rapid Scan Operations
RT	Real Time
RTM	Radiative Transfer Model
SAB	Satellite Analysis Branch
SPB	Sensor Physics Branch
SOCC	Satellite Operations Control Center
SPEC	Specifications
SPoRT	Short-term Predication Research and Transition center
SRF	Spectral Response Function
SRSO	Super Rapid Scan Operations
SSEC	Space Science and Engineering Center
SST	Sea Surface Temperature
StAR	SaTellite Applications and Research (formerly ORA)
SW	Shortwave
SWIR	Split-Window InfraRed
THOR	Tornado and Hazardous weather Observations Research center
TPW	Total Precipitable Water
UAH	University of Alabama, Huntsville
UTC	Coordinated Universal Time
UW	University of Wisconsin (Madison)
WV	Water Vapor
μm	Micrometers (*micron* was officially declared obsolete in 1968)

NESDIS 105 Validation of SSM/I and AMSU Derived Tropical Rainfall Potential (TRaP) During the 2001 Atlantic Hurricane Season. Ralph Ferraro, Paul Pellegrino, Sheldon Kusselson, Michael Turk, and Stan Kidder, August 2002.

NESDIS 106 Calibration of the Advanced Microwave Sounding Unit-A Radiometers for NOAA-N and NOAA-N=. Tsan Mo, September 2002.

NESDIS 107 NOAA Operational Sounding Products for Advanced-TOVS: 2002. Anthony L. Reale, Micheal W. Chalfant, Americo S. Allergrino, Franklin H. Tilley, Michael P. Ferguson, and Michael E. Pettey, December 2002.

NESDIS 108 Analytic Formulas for the Aliasing of Sea Level Sampled by a Single Exact-Repeat Altimetric Satellite or a Coordinated Constellation of Satellites. Chang-Kou Tai, November 2002.

NESDIS 109 Description of the System to Nowcast Salinity, Temperature and Sea nettle (*Chrysaora quinquecirrha*) Presence in Chesapeake Bay Using the Curvilinear Hydrodynamics in 3-Dimensions (CH3D) Model. Zhen Li, Thomas F. Gross, and Christopher W. Brown, December 2002.

NESDIS 110 An Algorithm for Correction of Navigation Errors in AMSU-A Data. Seiichiro Kigawa and Michael P. Weinreb, December 2002.

NESDIS 111 An Algorithm for Correction of Lunar Contamination in AMSU-A Data. Seiichiro Kigawa and Tsan Mo, December 2002.

NESDIS 112 Sampling Errors of the Global Mean Sea Level Derived from Topex/Poseidon Altimetry. Chang-Kou Tai and Carl Wagner, December 2002.

NESDIS 113 Proceedings of the International GODAR Review Meeting: Abstracts. Sponsors: Intergovernmental Oceanographic Commission, U.S. National Oceanic and Atmospheric Administration, and the European Community, May 2003.

NESDIS 114 Satellite Rainfall Estimation Over South America: Evaluation of Two Major Events. Daniel A. Vila, Roderick A. Scofield, Robert J. Kuligowski, and J. Clay Davenport, May 2003.

NESDIS 115 Imager and Sounder Radiance and Product Validations for the GOES-12 Science Test. Donald W. Hillger, Timothy J. Schmit, and Jamie M. Daniels, September 2003.

NESDIS 116 Microwave Humidity Sounder Calibration Algorithm. Tsan Mo and Kenneth Jarva, October 2004.

NESDIS 117 Building Profile Plankton Databases for Climate and EcoSystem Research. Sydney Levitus, Satoshi Sato, Catherine Maillard, Nick Mikhailov, Pat Cadwell, Harry Dooley, June 2005.

NESDIS 118 Simultaneous Nadir Overpasses for NOAA-6 to NOAA-17 Satellites from 1980 and 2003 for the Intersatellite Calibration of Radiometers. Changyong Cao, Pubu Ciren, August 2005.

NESDIS 119 Calibration and Validation of NOAA 18 Instruments. Fuzhong Wang and Tsan Mo, December 2005.

NESDIS 120 The NOAA/NESDIS/ORA Windsat Calibration/Validation Collocation Database. Laurence Connor, February 2006.

NESDIS 121 Calibration of the Advanced Microwave Sounding Unit-A Radiometer for METOP-A. Tsan Mo, August 2006.

NESDIS 122 JCSDA Community Radiative Transfer Model (CRTM). Yong Han, Paul van Delst, Quanhua Liu, Fuzhong Weng, Banghua Yan, Russ Treadon, and John Derber, December 2005.

NESDIS 123 Comparing Two Sets of Noisy Measurements. Lawrence E. Flynn, November 2006.

NESDIS 124 Sounding Unit-A for NOAA-N Prime. Tsan Mo, September 2007.

NOAA SCIENTIFIC AND TECHNICAL PUBLICATIONS

The National Oceanic and Atmospheric Administration **was established as part of the Department of Commerce on October 3, 1970. The mission responsibilities of NOAA are to assess the socioeconomic impact of natural and technological changes in the environment and to monitor and predict the state of the solid Earth, the oceans and their living resources, the atmosphere, and the space environment of the Earth.**

The major components of NOAA regularly produce various types of scientific and technical information in the following types of publications:

PROFESSIONAL PAPERS - Important definitive research results, major techniques, and special investigations.

CONTRACT AND GRANT REPORTS - Reports prepared by contractors or grantees under NOAA sponsorship.

ATLAS - Presentation of analyzed data generally in the form of maps showing distribution of rainfall, chemical and physical conditions of oceans and atmosphere, distribution of fishes and marine mammals, ionospheric conditions, etc.

TECHNICAL SERVICE PUBLICATIONS - Reports containing data, observations, instructions, etc. A partial listing includes data serials; prediction and outlook periodicals; technical manuals, training papers, planning reports, and information serials; and miscellaneous technical publications.

TECHNICAL REPORTS - Journal quality with extensive details, mathematical developments, or data listings.

TECHNICAL MEMORANDUMS - Reports of preliminary, partial, or negative research or technology results, interim instructions, and the like.

U.S. DEPARTMENT OF COMMERCE
National Oceanic and Atmospheric Administration
National Environmental Satellite, Data, and Information Service
Washington, D.C. 20233